

# **Molecular definition of paratuberculosis pathologies by functional genomics**

Jennifer Smeed



PhD Thesis  
The University of Edinburgh  
2008



## **Declaration**

I declare that all work included in this thesis is my own work except where otherwise stated. No part of this work has been, or will be, submitted for any other degree of professional qualification.

Jennifer Smeed  
2008

Veterinary Biomedical Sciences  
University of Edinburgh  
Summerhall  
Edinburgh  
EH9 1QH

## **Acknowledgements**

I would first like to thank my supervisors John Hopkins and Craig Watkins. John has shown me unending support and enthusiasm and encouraged me to become a better scientist. Craig taught me so much and has kept me going through all of the setbacks and difficult times in my research. Thanks also to Anton Gossner and Sofia Roupaka, for their help, support and advice, and for making the lab a fun place to be. Thanks to my summer student Danielle Muscat for the IGFBP-6 cloning and sequencing work, to Jill Sales for the microarray analysis and to Susan Rhind and the histopathology groups at MRI and Easter Bush for the preparation and staining of the tissue sections. Thanks to Karen Stevenson and the rest of the Mycobacteria group at MRI for their help, advice, criticism and friendship over the past three years.

My family have supported my every step of the way and I thank them all for this. Finally, I want to thank Tim, for putting up with my bad moods, stressed out days and without whom I could not have done this.

## Abstract

Paratuberculosis (Johne's disease) is a chronic intestinal disease of ruminants caused by *Mycobacterium avium* subspecies *paratuberculosis* (MAP). Three forms have been described in sheep – multibacillary, paucibacillary and asymptomatic. Real-time RT-PCR (qPCR) and microarray analyses were used to compare gene expression in ileal tissue from sheep with the three forms of the disease in order to understand the immune responses underpinning these three defined pathologies. All animals from the infected flocks were IS900 positive by qPCR and therefore infected with MAP. Asymptomatic sheep had no clinical signs of disease, showed no evidence of acid-fast bacteria (ZN<sup>-</sup>), exhibited normal histology of the terminal ileum and were seronegative. Paucibacillary sheep were ZN<sup>-</sup> and showed lymphocyte/eosinophil infiltrate into the lamina propria. 2/6 of the paucibacillary animals were seropositive. Multibacillary sheep had high numbers of ZN<sup>+</sup> bacteria associated with infiltrating sheets of epithelioid macrophages and were seropositive. Control sheep were IS900 negative and thus uninfected with MAP.

qPCR experiments compared the expression of the following genes - IL-1 $\alpha$ , IL-1 $\beta$ , IL-3, IL-6, IL-8, IL-10, IL-12p40, IL-18, CD34, CXCR4, GM-CSF, IFN $\gamma$ , IGFBP-2, IGFBP-6, TGF $\beta$ , TIRAP, TNF $\alpha$ , TRAF-1 and TRAM. The results confirmed that pauci- and multibacillary forms are linked to the differential expression of IFN $\gamma$  and IL-10 respectively, but imply that polarisation is incomplete, with upregulation of both proinflammatory IL-18 and anti-inflammatory TGF $\beta$  in both disease forms. Increased levels of the proinflammatory cytokines IL-1 $\beta$ , IL-8, TNF $\alpha$  and TRAF-1, indicative of persistent inflammatory lesions, were observed in clinical tissues. IL-3 was detected at low levels in all infected animals but never in uninfected control samples. IGFBP-6 was up-regulated and CXCR4 down-regulated in paucibacillary samples

compared to multibacillary samples. SNP analysis was carried out on these genes, identifying three novel SNPs in each gene, but none were linked to disease pathology.

Microarray experiments discovered 63 differentially expressed genes. Four genes were found to be differentially expressed in infected tissue compared to uninfected controls, and a further eight in clinical tissues compared to uninfected controls. Eight genes were differentially expressed in clinical tissue compared to asymptomatic tissue. Seven genes were quantified by qPCR and validated the microarray data well. Pathway analysis of the microarray data identified several immune pathways that are involved in pathogenesis. Infected tissues displayed up-regulation of the genes involved in complement activation, and down-regulation of TCR signalling and MHC class II genes. In addition, clinical tissues displayed up-regulation of genes involved in the JAK-STAT and TLR2 signalling pathways, NK cell cytotoxicity and antibody production. Multibacillary tissues also displayed up-regulation of genes involved in leukocyte migration.

Overall, these data confirm that multibacillary pathology is linked to type 2 and paucibacillary pathology is linked to type 1 immune responses, and identify novel genes and gene pathways for future analyses.

## Contents

	<b>Page</b>
Title	i
Declaration	ii
Acknowledgements	iii
Abstract	iv
Contents	vi
List of Figures	xi
List of Tables	xii
Abbreviations	xiii
<b>Chapter 1: Introduction</b>	<b>1</b>
<b>1.1 Paratuberculosis</b>	<b>2</b>
1.1.1 Symptoms and pathology	2
1.1.2 Prevalence and costs	4
1.1.3 Detection and diagnosis	5
1.1.4 Control and treatment	8
<b>1.2 <i>Mycobacterium avium</i> subspecies <i>paratuberculosis</i></b>	<b>9</b>
1.2.1 The <i>M. avium</i> clade	9
1.2.2 Transmission of MAP	11
1.2.3 Attachment and invasion	13
<b>1.3 Immune response to MAP infection</b>	<b>15</b>
1.3.1 Macrophage responses	15
1.3.2 Antibody response	17
1.3.3 T cell responses	18
<b>1.4 Host gene expression in MAP infection</b>	<b>21</b>
<b>1.5 Crohn's disease</b>	<b>24</b>
<b>1.6 Aims and objectives</b>	<b>26</b>
<b>Chapter 2: Materials and methods</b>	<b>27</b>

<b>2.1 Experimental animals and disease diagnosis</b>	28
2.1.1 Experimental animals	28
2.1.2 Diagnosis of paratuberculosis and definition of pathological forms	28
<b>2.2 Tissue selection and removal</b>	29
<b>2.3 Isolation of RNA from ileum tissue</b>	31
2.3.1 Homogenisation of tissues	31
2.3.2 RNA extraction from tissues	31
2.3.3 Measurement of RNA/DNA concentration	31
<b>2.4 Reverse transcriptase-polymerase chain reaction</b>	32
2.4.1 Reverse transcription of RNA into cDNA	32
2.4.2 Primer design	33
2.4.3 Amplification	33
<b>2.5 Agarose gel electrophoresis</b>	36
2.5.1 Preparation of agarose gels	36
2.5.2 Running agarose gels	36
<b>2.6 Cloning of the PCR product</b>	36
2.6.1 Ligation into pGEM®-T easy vector	36
2.6.2 Transformation into JM109 cells	37
2.6.3 Plasmid DNA purification	37
2.6.4 Restriction enzyme digest	37
<b>2.7 DNA sequencing</b>	37
<b>2.8 Real-time reverse-transcriptase polymerase chain reaction</b>	38
2.8.1 Overview	38
2.8.2 Linearization of plasmids	38
2.8.3 Generation of standard curves from cloned pDNA template	38
2.8.4 Reaction mix and cycling conditions	39
2.8.5 Variability assay	40
2.8.6 Real-time RT-PCR for genes of interest	40

2.8.7 Normalisation of real-time data	41
<b>2.9 SNP analysis of CXCR4 and IGFBP-6</b>	<b>42</b>
2.9.1 Overview	42
2.9.2 Genomic DNA extraction from tissues	42
2.9.3 Primer design	42
2.9.4 Cloning and sequencing of gene fragments	43
2.9.5 SNP analysis of sequences	43
<b>2.10 Microarray analysis</b>	<b>45</b>
2.10.1 Overview	45
2.10.2 cDNA generation	45
2.10.3 cDNA purification	45
2.10.4 cDNA dye-coupling reaction	46
2.10.5 Dye-coupled cDNA purification	46
2.10.6 Analysis of fluorescence labelled cDNA	47
2.10.7 Pre-soak and pre-hybridisation of microarray slides	47
2.10.8 Microarray hybridisation	48
2.10.9 Post-hybridisation treatment	48
2.10.10 Microarray slide scanning	49
2.10.11 Bluefuse analysis of microarray results	49
2.10.12 Bioconductor normalisation of microarray data	50
2.10.13 Data filtering	50
2.10.14 Pathway analysis	51
<b>2.11 Real-time RT-PCR validation of microarray results</b>	<b>51</b>
2.11.1 Reverse transcription of RNA into cDNA	51
2.11.2 Primer design and cloning	51
2.11.3 Primer optimisation and generation of standard curves	52
2.11.4 Selection of reference genes	52
2.11.5 Reaction mix and cycling conditions	52
2.11.6 Real-time PCR for genes of interest	53

2.11.7 Normalisation of real-time RT-PCR results	53
<b>Chapter 3: Definition of pathological forms</b>	<b>56</b>
3.1 Introduction	57
3.2 Definition of pathological forms	58
3.3 Discussion	71
<b>Chapter 4: Differential cytokine gene expression</b>	<b>72</b>
4.1 Introduction	73
4.2 RNA extraction from ileum	74
4.3 Sequences of cloned PCR products	74
4.4 Gene Expression analysis in ileal tissues	74
4.4.1 Generation of standard curves	74
4.4.2 Real-time PCR analysis of mRNA expression	77
4.5 Discussion	82
<b>Chapter 5: Differential expression and SNP analysis of non-cytokine genes</b>	<b>86</b>
5.1 Introduction	87
5.2 Real-time RT-PCR analysis of gene expression	88
5.3 Extraction of genomic DNA from paratuberculosis tissue	92
5.4 CXCR4 sequence and PCR fragments	92
5.5 IGFBP-6 sequence and PCR fragments	93
5.6 Production of PCR products	93
5.7 Cloning and sequencing of PCR products	96
5.8 SNP analysis of CXCR4	96
5.9 SNP analysis of IGFBP-6	100
5.10 Discussion	103

## List of Figures

	Page
1.1: Anatomy of the ovine intestinal tract	3
3.1: Results of IS900 real-time RT-PCR	59
3.2: Histopathology of the terminal ileum from asymptomatic sheep	60
3.3: Histopathology of the terminal ileum from asymptomatic sheep	61
3.4: Histopathology of the terminal ileum from asymptomatic sheep	62
3.5: Histopathology of the terminal ileum from paucibacillary sheep	63
3.6: Histopathology of the terminal ileum from paucibacillary sheep	64
3.7: Histopathology of the terminal ileum from paucibacillary sheep	65
3.8: Histopathology of the terminal ileum from multibacillary sheep	66
3.9: Histopathology of the terminal ileum from multibacillary sheep	67
3.10: Histopathology of the terminal ileum from multibacillary sheep	68
4.1: Generation of linearised plasmid DNA standard curves for real-time PCR	76
4.2: Statistically significant fold-changes in genes in infected animals compared to uninfected control groups	80
4.3: Statistically significant fold-changes in genes in the three infected groups	81
5.1: Statistically significant fold-changes in genes in infected animals compared to uninfected control groups	90
5.2: Statistically significant fold-changes in genes in the three infected groups	91
5.3: Schematic diagram of the structure of the ovine CXCR4 gene	95
5.4: Schematic diagram of the structure of the ovine IGFBP-6 gene	95
5.5: Position of SNPs in the CXCR4 gene	98
5.6: Position of SNPs in the IGFBP-6 gene	101
5.7: CXCR4 signalling pathways	105
6.1: Heat map of channel 2 on 3P vs. 2C chip	114
6.2: MA plots of 3P vs. 2C chip	115
6.3: Boxplot of one set of microarrays	116
6.4: Generation of cDNA standard curves for real-time PCR	123
6.5: Mean fold-change of genes compared to calibrator sample	124

## List of Tables

	<b>Page</b>
2.1: Breed, age, sex and FEC of experimental animals	30
2.2: Accession numbers and primer sequences	34
2.3: Copy numbers of SDHA in variability assay	40
2.4: Example of normalisation, taking into account the 75 <sup>th</sup> percentile	41
2.5: Primer sets used to sequence CXCR4 and IGFBP-6	44
2.6: Accession numbers and primer sequences for microarray validation	54
2.7: Accession numbers and primer sequences of reference genes	55
3.1: PPD ELISA Results	69
3.2: Definition of pathological forms	70
4.1: RNA concentration and RIN	75
4.2: Copy numbers of all genes of interest in all groups normalised to reference gene expression	79
5.1: Copy numbers of all genes of interest in all groups normalised to reference gene expression	89
5.2: DNA sample concentrations	94
5.3: Number of correct sequences for each sample	97
5.4: Samples and disease groups containing the three CXCR4 SNPs	99
5.5: Samples and disease groups containing the three IGFBP-6 SNPs	102
6.1: Samples and comparisons used for microarray analysis	118
6.2: Mean fold-changes of significantly differentially expressed genes	119
6.3: Relative fold-changes of genes analysed in real-time RT-PCR	122

## Abbreviations

A	Adenine
AILC	Afferent intestinal lymph cell
Amp	Ampicillin
C	Cytosine
CD	Crohn's Disease
cDNA	Complementary deoxyribonucleic acid
CMI	Cell-mediated immunity
CWD	Cell wall deficient
DEPC	Diethylpyrocarbonate
DMSO	Dimethyl sulfoxide
DNA	Deoxyribonucleic acid
dNTP	Deoxynucleotide triphosphate
DTT	Dithiothreitol
dUTP	Deoxyuridine triphosphate
EB	Elution buffer
ELISA	Enzyme linked immunosorbent assay
FACS	Fluorescence-activated cell sorting
FEC	Faecal egg count
FN	Fibronectin
G	Guanine
GAL	GenePix Array List
GC	Guanine or cytosine
H&E	Hematoxylin and eosin
HSC	Haematopoietic stem cell
HSP	Heat shock protein
HUGO	Human genome organisation
IPTG	Isopropyl $\beta$ -D-1-thiogalactopyranoside
IS	Insertion sequence
KEGG	Kyoto Encyclopaedia of Genes and Genomes
LAM	Lipoarabinomannan
LPS	Lipopolysaccharide
MA	Average log intensity versus log ratio
MAP	<i>Mycobacterium avium</i> subspecies <i>paratuberculosis</i>
MGIT	Mycobacterial Growth Indicator Tube
MHC	Major histocompatibility complex
MIAME	Minimum Information About a Microarray Experiment
MLN	Mesenteric lymph node
MMLV	Moloney murine leukaemia virus
MOI	Multiplicity of infection
MRI	Moredun Research Institute

ND	Not done
NK	Natural killer
NO	Nitric oxide
NTC	Non-template control
PBMC	Peripheral blood mononuclear cell
PCR	Polymerase chain reaction
pDNA	Plasmid deoxyribonucleic acid
PFGE	Pulsed field gel electrophoresis
PI	Post infection
PMT	Photo multiplier tube
PPD	Purified protein derivative
RFLP	Restriction fragment length polymorphism
RIGUA	Ruminant immunoinflammatory gene universal array
RIN	Ribonucleic acid integrity number
RNA	Ribonucleic acid
ROX	6-Carboxyl-X-Rhodamine
RT	Reverse transcriptase
RT-PCR	Reverse transcriptase-polymerase chain reaction
SDF	Stroma derived factor
SNP	Single nucleotide polymorphism
SYBR	Synergy Brands
T	Thymine
TACO	Tryptophan-aspartate containing coat protein
Th1	T helper 1
Th2	T helper 2
UDG	Uracil Deoxyribonucleic acid glycosylase
UV	Ultra-violet
XGAL	5-bromo-4-chloro-3-indolyl- beta-D-galactopyranoside
ZN	Ziehl-Neelsen

<b>Gene symbol</b>	<b>Gene name</b>	<b>HUGO symbol (where different)</b>
ABC	Adenosine triphosphate binding cassette	
$\beta$ 2M	$\beta$ 2Microglobulin	B2M
BCAR1	Breast cancer anti-oestrogen resistance 1	
BCR	B cell receptor	CD79A
C2a	Complement component 2a	
C3	Complement component 3	
C3b	Complement component 3b	
C7	Complement component 7	

C9	Complement component 9	
CAV1	Caveolin-1	
CCR5	Chemokine (C-C motif) receptor 5	
CCR7	Chemokine (C-C motif) receptor 7	
CD11a	LFA-1 alpha chain	ITGAL
CD11b	Integrin, alpha M	ITGAM
CD13	Alanyl (membrane) aminopeptidase	ANPEP
CD18	Integrin, beta 2	ITGB2
CD21	Complement receptor 2	CR2
CD29	Integrin, beta 1	ITGB1
CD34	Haematopoietic progenitor cell antigen	
CD3 $\gamma$	T-cell receptor T3 gamma chain	CD3G
CD3 $\delta$	T-cell receptor T3 delta chain	CD3D
CD3 $\epsilon$	T-cell receptor T3 epsilon chain	CD3E
CD3 $\zeta$	T-cell receptor T3 zeta chain	CD247
CD4	T-cell surface glycoprotein CD4	
CD40	TNF receptor superfamily member 5	
CD40L	TNF receptor superfamily member 5 ligand	CD40LG
CD45	Protein tyrosine phosphatase, receptor type, C	PTPRC
CD49d	Integrin, alpha 4	ITGA4
CD54	ICAM-1	ICAM1
CD55	Decay accelerating factor for complement	
CD62L	L-selectin	SELL
CD63	CD63 molecule	
CD71	Transferrin receptor	TFRC
CD74	Major histocompatibility complex, class II invariant chain	
CD8	Cell surface glycoprotein CD8	
CD80	CD80 antigen	
CFB	Complement Factor B	
CFH	Complement Factor H	
CLIC5	Chloride channel p64	
CP	Ceruloplasmin	
CRK	Sarcoma virus CT10 oncogene homolog	
CXCL12	Stromal cell-derived factor 1	
CXCR3	Chemokine (CXC motif) receptor 3	
CXCR4	Chemokine (CXC motif) receptor 4	
DAP12	TYRO protein tyrosine kinase binding protein	TYROBP
DEFB1	Beta defensin 1	
ELK1	ELK1, member of ETS oncogene family	
FcER $\gamma$	Fc receptor, IgE, high affinity I, gamma polypeptide	FCER1G
GAPDH	Glyceraldehyde 3 phosphate dehydrogenase	

GATA 3	GATA binding protein 3	GATA3
GM-CSF	Granulocyte macrophage colony stimulating factor	CSF2
GNAI1	Guanine nucleotide binding protein, alpha inhibiting activity polypeptide 1	
GNB1	Guanine nucleotide binding protein, beta polypeptide 1	
GNGTI	Guanine nucleotide binding protein, gamma transducing activity polypeptide 1	
HRAS	Harvey rat sarcoma viral oncogene homolog	
Hsp70	Heat shock protein 70	
IFN $\gamma$	Interferon gamma	IFNG
IgA	Immunoglobulin A	IGHA1
IgE	Immunoglobulin E	IGHE
IGF2R	Insulin-like growth factor 2 receptor	
IGFBP-2	Insulin-like growth factor binding protein 2	IGFBP2
IGFBP-3	Insulin-like growth factor binding protein 3	IGFBP3
IGFBP-6	Insulin-like growth factor binding protein 6	IGFBP6
IGF-I	Insulin-like growth factor 1	IGF1
IGF-II	Insulin-like growth factor	IGF2
IgG	Immunoglobulin G	IGHG
IgM	Immunoglobulin M	IGHM
IL-1 $\alpha$	Interleukin 1 alpha	IL1A
IL-2	Interleukin 2	IL2
IL-3	Interleukin 3	IL3
IL-4	Interleukin 4	IL4
IL-5	Interleukin 5	IL5
IL-6	Interleukin 6	IL6
IL-8	Interleukin 8	IL8
IL-10	Interleukin 10	IL10
IL-12p40	Interleukin 12 p40	IL12B
IL-16	Interleukin 16	IL16
IL-18	Interleukin 18	IL18
IL18RAP	Interleukin 18 receptor activating protein	IL18RAP
J chain	J chain	IGJ
MAPKK	Mitogen-activated protein kinase kinase	MAP2K
MAPKp38	Mitogen-activated protein kinase p38	
MCP-1	Monocyte chemoattractant protein-1	CCL2
MCP-2	Monocyte chemoattractant protein-2	CCL8
MMP14	Matrix metalloproteinase 14	
MMP3	Matrix metalloproteinase 3	
MMP7	Matrilysin	
MMP9	Matrix metalloproteinase 9	
Myd-1	Signal-regulatory protein alpha	SIRPA
NADH	Nicotinamide adenine dinucleotide dehydrogenase	

N-cadherin	Cadherin 2, type 1	CDH2
NF $\kappa$ B	Nuclear factor of kappa light polypeptide gene enhancer in B-cells	NFKB
NOD2/CARD15	Nucleotide-binding oligomerization domain containing 2	NOD2
NPYR3	Neuropeptide $\gamma$ receptor 3	CXCR4
NRAMP1	Natural resistance-associated macrophage protein 1	SLC11A1
NRP	Nucleolin-related protein	NRP
OXT	Oxytocin	OXT
PI3	Trappin 2	
PIGR	Secretory component / poly Ig receptor	
PTK2	Protein tyrosine kinase 2	
PTK2B	Protein tyrosine kinase 2 beta	
PXN	Paxillin	
RAF1	Murine leukaemia viral oncogene homolog 1	
RANTES	Regulated upon activation, normal T-cell expressed, and secreted	CCL5
RAP1	Telomeric repeat binding factor 2, interacting protein	TERF2IP
RASSF5	Ras association (RalGDS/AF-6) domain family 5	
SCYB10	Interferon-gamma-inducible protein 10	CXCL10
SDHA	Succinate dehydrogenase complex subunit A	
SOCS	Suppressor of cytokine signalling proteins	
STAT1	Signal transducer and activator of transcription 1	
STAT3	Signal transducer and activator of transcription 3	
STS	Steroid sulfatase	
TCR Cd	T cell receptor Cd	TRDC
TGF $\beta$	Transforming growth factor beta	TGFB
TIMP1	Tissue inhibitor of metalloproteinase 1	
TIMP2	Tissue inhibitor of metalloproteinase 2	
TIRAP	Toll-interleukin 1 receptor domain containing adaptor protein	
TLR2	Toll-like receptor 2	
TNFR2	Tumour necrosis factor receptor 2	TNFRSF1B
TNF $\alpha$	Tumour necrosis factor alpha	TNF
TRAF1	Tumour necrosis factor receptor associated factor 1	
TRAM	Translocating chain-associating membrane protein	
VIM	Vimentin	
YWHAZ	tyrosine 3-monooxygenase/tryptophan 5-monooxygenase activation protein, zeta	

## Chapter 1: Introduction

## 1.1 Paratuberculosis

### 1.1.1 Symptoms and Pathology

Paratuberculosis (Johne's disease) is a chronic inflammatory disease of the gut of ruminants, caused by infection with *Mycobacterium avium* subspecies *paratuberculosis* (MAP). It is characterised by granulomatous enterocolitis, lymphangitis and lymphadenitis (52). After infection, sheep display a long asymptomatic phase of up to two years (6) after which clinical symptoms may develop. These symptoms are wasting, diarrhoea, loss of condition and eventual death, caused by inflammation of the intestine leading to lower absorbance of water and nutrients (6,231). The main site of infection and pathogenesis is the ileum, and several forms of the disease have been previously described (41,231) based on gross pathology of the gut (Figure 1.1). These forms are similar to the pathologies of human leprosy (55) and can be unambiguously differentiated into paucibacillary (tuberculoid), multibacillary (lepromatous) and asymptomatic (infected but no pathology) (53). What determines which of these three forms of the disease develops is unknown, but it may be related to the genetic background of the host (35).

Asymptomatic individuals come from flocks with endemic paratuberculosis and are infected with the mycobacteria, but have no clinical symptoms and no signs of intestinal pathology (224).

On examination of the gut of paucibacillary animals, a slight thickening of the intestine can be observed. Histopathological examination reveals a large lymphocytic infiltrate and the presence of multinucleated giant cells. Few mycobacteria can be seen in Ziehl-Neelsen (ZN) stained tissue. The mucosal surface is flattened, and normal villus architecture interrupted. Paucibacillary lesions contain many lymphocytes, with very few macrophages or visible mycobacteria (56,90,231,249).

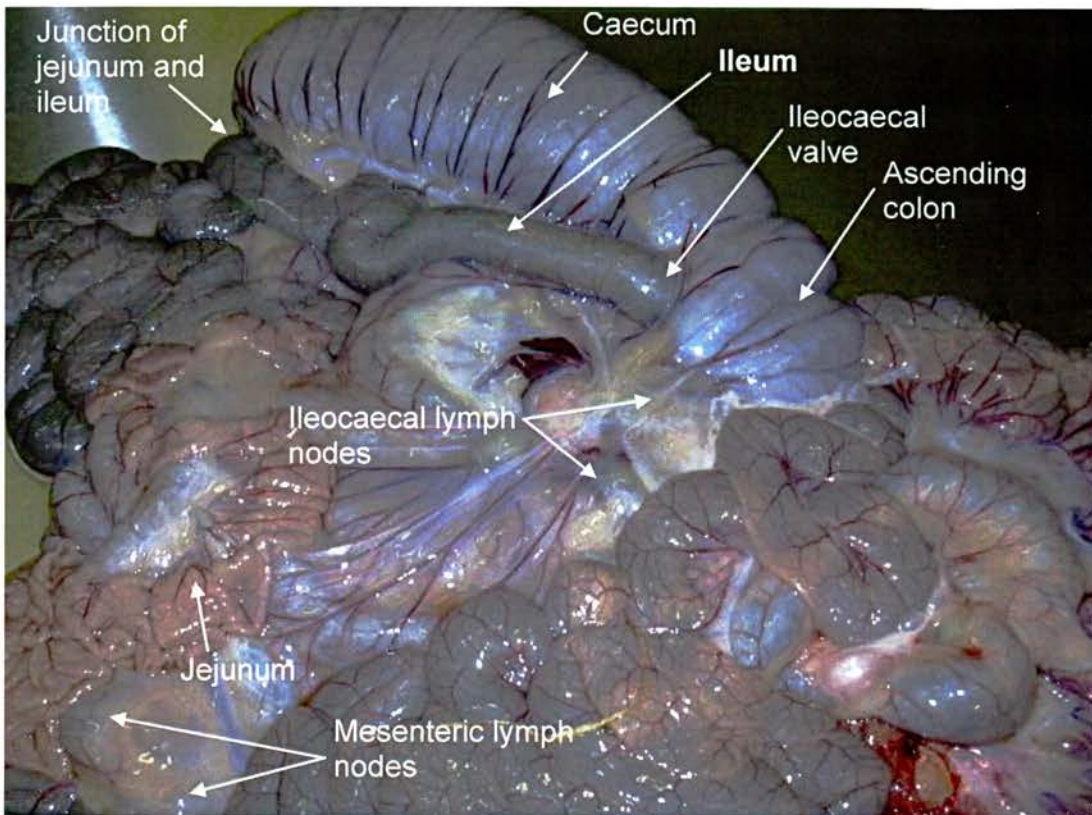


Figure 1.1: Anatomy of the ovine intestinal tract, showing the position of the ileum where the majority of paratuberculosis pathology is found.

When the gut of multibacillary animals is examined, the small intestine is thickened and may be pigmented. Histopathological examination reveals a large macrophage infiltrate, with few or no giant cells. Large numbers of bacteria can be seen in ZN stained tissue. Again, the mucosal surface is flattened, and normal villus architecture interrupted (56,90,231,249).

### **1.1.2 Prevalence and costs**

The worldwide prevalence of paratuberculosis is a subject that attracts much attention and research, but there is as yet very little solid information available. The information can be split into two different types – herd or flock level prevalence i.e. the percentage of herds or flocks with any level of paratuberculosis, and the prevalence of infection in individual animals. A recent study in cattle concluded that worldwide, the herd level prevalence in cattle ranged from 0% to 71% (155). In the USA, herd level prevalence in cattle ranges from 20-40%, depending on herd size and geographical location (10,88,95,142). Across Europe, estimates of herd level prevalence vary widely. In the UK, prevalence ranges from 3.5-17%, depending on detection method (95,225). In other European countries, the herd level prevalence estimates are as follows: The Netherlands 31-71%; Denmark 47-70%; Germany 20%; Belgium 8-27%; Spain 12-18%; Italy 11-13%, Switzerland 8%; Austria 7% and The Czech Republic 12% (69,95,142,225). The herd level prevalence in New Zealand is 60% (95). In Australia, the overall herd level prevalence is 15% (95), but there is a great deal of variation between states – from 9% in New South Wales to 22% in Victoria (10).

Prevalence estimates based on individual animals are even more variable than herd based estimates, due to the asymptomatic nature of the disease and the low sensitivity of some detection methods. In cattle estimates range from 1.6-10% in the USA (230) to 30% in Brazil (189) and 11-84%

in India (29,214). In sheep, prevalence has been estimated at 1.28% in India (29); 2.83% in Galicia in Spain (69); 14-20% in Greece (134); 45% in Italy (168) and less than 50% in Australia (1). However, many of these studies focused on single flocks, or solely on asymptomatic sheep, and thus may not be entirely reliable.

Based on these prevalence estimates, several studies have attempted to calculate the actual cost of paratuberculosis. It is estimated to cost the USA dairy industry \$200-250 million per year (146,175). This is mainly due to increased culling - Canadian cattle infected with MAP have 1.38 times the risk of being culled compared to non-infected cattle (246) and lower milk, fat and protein yields (104). Studies have shown that cows with clinical paratuberculosis produce 19.5% less milk and cows with sub-clinical paratuberculosis produce 16% less milk (24).

In Scotland in 1993-2002, there were 465 recorded cases of paratuberculosis in all species (234). However, this figure only reflects cases reported to Health Protection Scotland by veterinary laboratories, which is not commonly done as paratuberculosis is not a notifiable disease. A study taking into account herd sizes, milk prices, replacement costs and average milk yields concluded that the cost of paratuberculosis in the UK is about £26 per cow per year (238), although this increases with milk prices. There is very little information as to the incidence or cost of paratuberculosis in sheep.

### **1.1.3 Detection and diagnosis**

Detecting infection with MAP before the onset of clinical symptoms with associated bacterial shedding is problematic. If MAP infection could be detected before the onset of faecal shedding and the infected animal removed from the flock, this would prevent much of the spread of the disease. Faecal culture is considered the 'gold standard' in detection, with

high levels of sensitivity and specificity. This is, however, expensive and can take up to twelve weeks (232). Culture of MAP also requires specific conditions, including the addition of mycobactin J to the media, and extensive decontamination of faecal samples (177). An alternative to faecal culture is faecal smears, where the samples are smeared and stained with a ZN stain to detect acid-fast bacteria. However, this method is not as sensitive as culture due to the very low numbers of mycobacteria present in the faeces of asymptomatic and paucibacillary animals (259). Culture of intestinal tissue can also be used post-mortem to detect MAP infection (240). Recent advances in faecal culture include the introduction of BACTEC and MGIT rapid mycobacterial culture systems. The BACTEC system is a radiometric culture system which involves culturing MAP in a media containing a  $^{14}\text{C}$  substrate which is broken down into radio-labelled carbon, which can be detected in the gas phase of the culture vessel and allows 'real-time' measurement of MAP growth (272). The MGIT system works on a similar principle, but uses a fluorescent substrate. Although these systems significantly reduce the time required to culture MAP, the sensitivity can be as low as 13% compared to traditional culture, and the contamination rate higher (99).

In Australia and New Zealand, animals slaughtered in abattoirs are inspected for gross signs of paratuberculosis. This is a cheap and easy way of detecting MAP infection within a flock. However, it has low sensitivity for detecting flocks which have been recently infected, or that have low levels of infection (1).

Several commercial ELISA based tests are currently available as a method of detecting antibodies to MAP surface proteins in serum. The sensitivity of these tests compared to faecal culture varies widely, from 13.7% where the animals would be classed as low shedders to 100% of high shedders (75,151,248,255). However, as most animals would be

classed as low shedders, current ELISA tests perform poorly overall compared to faecal culture. Much work is currently being done to identify new proteins in MAP to improve the ELISA tests (15,26,49,142), with several having higher sensitivities than the currently available tests.

Other MAP detection methods available include an IFN $\gamma$  ELISA (Bovigam, CSL) (187,237) which detects the increase in IFN $\gamma$  production which occurs in preclinical animals infected with MAP. It is also possible to carry out IFN $\gamma$  and proliferation assays by exposing PBMCs from infected animals to PPD (162,165). However, a major drawback to these kinds of tests is that the responses are time dependent. The IFN $\gamma$  response, especially in sheep, is short-lived, and may not be detectable after the initial peak at the time of infection. In goats, lymphocyte proliferation tests can work from around day 60 post infection, whereas ELISA tests may not work until 180 days post infection (162).

PCR-based tests are also becoming more widespread. The most common PCR assays detect the presence of IS900 (50,90,232), and can be more sensitive than faecal culture (116). It may also be possible to use PCR based tests to detect MAP in samples infected with mixed *M.avium* species (154). A recent study described a new method of DNA extraction from faeces for PCR, giving a test with similar detection limits to culture but higher sensitivity (258). However, PCR based tests simply detect the presence of mycobacterial DNA in a sample, not the presence of viable mycobacteria, and as such have to be used in conjunction with other detection methods. This lack of agreement between tests for MAP infection is a problem (8,152) which can only be overcome by using various combinations of testing methods, with the associated increase in cost and time taken for diagnosis. A second major problem with all tests is that the age of the animal being tested can have an impact on the

sensitivity of the test, with younger animals more likely to give false negative results (171).

#### 1.1.4 Control and treatment

The treatment of paratuberculosis is also difficult. Animals can be cleared of MAP infection by prolonged chemotherapy, but this is too expensive and time-consuming for widespread use (78). The cost of MAP in the UK, especially when milk prices are low, is not high enough to provide an incentive for dairy farmers to control or treat the disease (238). Other therapies, such as mycophage therapy, have been proposed but have not proven to be effective (78). Currently, the majority of animals displaying symptoms of paratuberculosis are culled.

The most cost-effective way of preventing paratuberculosis is by vaccination. The current Gudair™ vaccine is a whole cell preparation of heat-killed MAP (114). The vaccine elicits both humoral and cellular immune responses (57), and studies in Australia have shown that vaccination reduces mortality, faecal shedding and the numbers of mycobacteria shed by up to 90% (185,274). There are, however, several drawbacks to this vaccine. Approximately 50% of vaccinated animals will develop a granulomatous lesion at the site of injection, which reduces with age. A recent study concluded that this was a minor problem, as the value of the carcass was not reduced by the presence of a lesion (82,114,274). The vaccine induces the production of antibodies, which prevents the differentiation of vaccinated and unvaccinated animals (161). Vaccinated animals can also react with *M.bovis* skin tests, which can lead to an increase in culling (148,169). Perhaps more seriously, of the few vaccinated sheep that do go on to develop paratuberculosis, all have the multibacillary form of the disease(185,274). The vaccine is also expensive and thus not economical on farms with low levels of the disease. A study carried out in goats in India showed that vaccines

containing local strains of MAP were more efficacious and economical than commercially available vaccines (221).

Due to these drawbacks with the currently available vaccine, there are many studies underway looking to develop a new, improved vaccine. A live modified vaccine has been shown to elicit a strong cellular immune response, lasting over two years, along with a transient antibody response. However, administration of this vaccine did lead to false positive results in an *Mycobacterium bovis* screen (132,153). Other groups have developed DNA plasmid vaccines expressing MAP proteins which stimulate an appropriate immune response, and in one case has been shown to protect against MAP infection in sheep (34,114,206). A recombinant MAP Hsp70 vaccine has also been shown to reduce faecal shedding in vaccinated cattle (130).

In flocks where the incidence of paratuberculosis is low, other control strategies can be effective. Purchasing animals from uninfected flocks, decontaminating lambing and weaning pastures by grazing management and culling infected animals can be as effective as vaccination in reducing MAP prevalence in flocks with low levels of infection (68).

## **1.2 *Mycobacterium avium* subspecies *paratuberculosis***

### **1.2.1 The *M.avium* clade**

The genus mycobacterium consists of 71 species, many of which are important pathogens of both humans and animals. All mycobacteria are gram positive, although this stain does not work well. Mycobacteria can easily be identified by staining with basic fuchsin – they are acid-fast and thus will resist decolourisation by weak acids. This is due to the presence of a thick cell wall, separated from the cell membrane by the periplasmic space. This cell wall is made up of four layers – lipids, mycolic acid,

arabinogalactan and peptidoglycan. The various types of these molecules can be used to differentiate mycobacterial species. The morphology of mycobacteria is variable from short, round cells to long filaments. Several species, including strains of MAP, produce yellow-orange scotochromogens, leading to pigmented cultures (93).

Culturing mycobacteria can be difficult, and for some species, including *M.leprae*, has never been achieved. In culture, all species require the presence of oxygen, carbon and nitrogen sources, and metal ions including iron. Some species have more specific requirements – MAP cannot be grown without the addition of mycobactin to the media, for example. The metabolic pathways in most mycobacteria were thought to be similar to those in other bacterial species (93). However, new insights from genomic and proteomic studies have shown that there are pathways unique to mycobacteria, and that there is a great deal of variation in pathway use between species (149).

The first division of mycobacterial isolates is into fast and slow growers – fast growers, for example *M.abscessus*, produce visible growth in culture within 7 days, whereas slow growers, for example *M.tuberculosis*, take at least 7 days (91,93). Fast and slow growers can be differentiated by staining with neutral red and then treating with alkali – slow growers tend to resist decolourisation. 16s rRNA sequence can then be used to classify isolates into the various species (91). All species, except *M.tuberculosis*, have environmental strains (93). These environmental strains tend to have more variable DNA sequences than pathogenic strains (86).

The *M.avium* clade is composed of four species of slow growing mycobacteria - MAP, *M.avium* subspecies *avium*, *M.intracellulare* and *M.silvaticum* - which are 90% similar at the nucleotide level (94,159).

These species differ in host species, pathogenicity and disease phenotype (159). MAP was first cultured in 1912 on a modified egg media containing heat killed *M.tuberculosis* to provide mycobactin (249). MAP takes 5-14 weeks to produce visible growth in culture and is differentiated from other species in the clade by this mycobactin dependence (94,244). One strain of MAP has been sequenced and revealed to have a single circular chromosome of 4 million base pairs, encoding 4350 predicted open reading frames. Further analysis revealed that MAP has 4300 genes homologous to genes in *M.tuberculosis*, with a truncation in the mycobactin gene cluster (225). Strains of MAP are differentiated by restriction fragment length polymorphism (RFLP) analysis of IS900, a specific insertion sequence (178) or pulsed field gel electrophoresis (PFGE) of total genomic DNA (225). Strains of MAP can be divided into type I, comprising pigmented ovine strains, and types II and III, comprising strains from a wide range of hosts based on PFGE (66,233) and RFLP (178) profiles. Type I and type II strains can be easily distinguished by genetic means (71) and recently a PCR based test has been developed to discriminate type II and type III strains (42). However, MAP strains not dependent on mycobactin and non-MAP mycobacteria containing IS900 have been identified recently, so new methods of characterisation may be required (58,80,213).

### **1.2.2 Transmission of MAP**

MAP must be passed from animal to animal within a group in order to cause paratuberculosis. The experimental infectious dose for MAP is around  $10^7$  to  $10^8$  mycobacteria, although the natural infectious dose is likely to be lower than this (187). It is thought to be spread mainly by the faecal-oral route via contaminated feed (218,252), as most infected animals will shed the bacteria in their faeces at some point during the infection (232). High shedders will, of course, be responsible for higher rates of transmission (256). As young animals can be readily infected by

their mothers (8,254), it is accepted that most animals are infected as neonates by this route. Studies have shown that red deer can be infected through vertical infection, and are most susceptible to infection below the age of 8 months (147). Sheep have been implicated in spreading MAP to cattle on the same farm (163) although the reverse of this may also be true. However, recent studies have suggested that between herd transmission of MAP is mainly via the trade in livestock (264). Faecal-oral spread does not require direct contact with faeces - a recent survey in Northern Ireland found MAP contamination in 8% of untreated water samples (271). A second recent study also found that environmental water samples taken from a dairy were more likely to test positive for MAP by culture than manure samples taken from a cattle pen (27). This may, however, be due to lower levels of inhibitors in the water samples.

There are several other proposed routes of infection for MAP. Studies have suggested that MAP can be transmitted vertically in milk from apparently healthy mothers, and this route of infection may be common under normal breeding practises (168). MAP can be cultured from around 2% of milk samples taken from infected herds, 1.6% of milk samples taken from pasteurised retail milk and 3.6% of cheese samples from the Czech Republic (11,115), although a recent inter-laboratory study has found that detection rates can vary widely depending on the method used. PCR methods had the highest sensitivity, and the BACTEC the lowest, detecting none of the contaminated samples (72). A study into the persistence of MAP in cheddar cheese showed that MAP could be cultured from ripening cheese for up to 27 weeks (73).

MAP can be cultured from the semen of some infected rams and bulls, leading to the proposal that MAP could be spread during breeding (10,81). Viable mycobacteria can be isolated from the reproductive organs of infected animals, and from foetuses of infected cattle (252). However,

studies in Holstein cattle have suggested that intrauterine transmission is not an important route of transmission in these animals (155).

There is no evidence of any seasonal effect on MAP transmission (239) although environmental factors play a part. High rainfall and temperate climates which encourage higher densities of livestock can lead to higher rates of transmission. These factors can also lead to annual variations in transmission rates due, for example, to lower rainfall leading to clustering of livestock around water sources (1). Soil with a low pH and calcium and high iron, zinc and manganese content is more likely to harbour infectious MAP (172). MAP can also be cultured from a range of environmental nematodes and amoebae, suggesting that ingestion of these organisms by livestock may aid MAP transmission (192).

Transmission of MAP can occur between livestock species and wild species which share their habitat – a recent survey in the United States found only eight different MAP subtypes in thirty-three diverse species of wild and domestic animals across a wide area of the USA (157). Rabbits can carry MAP, and tend to share grazing ground with domesticated animals, allowing contamination of ruminant feed with rabbit faeces (65,122,259).

### **1.2.3 Attachment and invasion**

How MAP binds to and translocates the intestinal wall is a matter of much debate and research. The major hypothesis states that binding of fibronectin by the mycobacteria is key. MAP expresses a fibronectin attachment protein homologue which mediates the binding of fibronectin (FN) to the surface of the mycobacteria as it passes through the gut (209). *In vitro*, this attachment is optimised by acid pre-treatment, as would occur in natural infection as the bacteria pass through the stomach. This bound fibronectin can then bind to integrins on the surface of M cells in the follicle-associated epithelium of the Peyer's patches of the ovine gut

(210). M cells are proposed as the target cell of MAP because they express integrins on their surface, unlike other cells of the intestinal epithelium (211,217). The mycobacteria are then internalised by the M cells and translocate to the basolateral surface of the Peyer's patches. Invasion of the Peyer's patches is increased 2.6 fold by the binding of FN (211). This invasion is rapid, with MAP transversing the intestinal wall and infecting distal organs within one hour of initial infection (277).

More recent studies have shown, however, that MAP is able to attach to the intestinal epithelium in areas without Peyer's patches, suggesting that the mycobacteria can also bind to enterocytes (216). This in turn suggests that other receptors are necessary, as enterocytes do not express the integrins required for FN binding. As the ability of MAP to attach to the epithelium is consistent no matter which area of the gut is studied, this further suggests that M cells cannot be the only cell able to bind the mycobacteria (199). A recent hypothesis suggested that MAP can bind  $\alpha$ -dystroglycan and exploit a host recycling mechanism to allow invasion of the host cell. This method of invasion is seen in *Mycobacteria tuberculosis* invasion of Schwann cells (262), although there is no evidence as yet of the method playing a role in MAP infection. However, a second study has shown that MAP can attach to and infect enteric glial cells in culture (208).

After crossing the intestinal epithelium, MAP is phagocytosed by intestinal macrophages (218). MAP can be opsonised by the complement component C3b or antibody at this stage, which greatly increases uptake by macrophages (110,278). CD11/CD18 seems to be the main receptor involved in phagocytosis of MAP, although mannose receptors and CD14 can also be used (226). Once within macrophages, MAP can establish a persistent infection by preventing acidification of the phagolysosome.

### 1.3 Immune response to MAP infection

#### 1.3.1 Macrophage responses

In a typical bacterial infection, the bacteria are phagocytosed by macrophages, neutrophils or dendritic cells and held in the cell in phagosomes. This phagocytosis can be mediated by bacterial attachment to a number of receptors, including Fc receptors that bind to antibodies, and complement receptors. Phagocytosis via these receptors leads to macrophage activation. The cellular bacteria lysosomes bind to the phagosome to form a phagolysosome, which becomes gradually acidified, leading to bacterial death and digestion. This then leads to bacterial peptide presentation on the cell surface via MHC class II and activation of the acquired immune system (181,218).

Once within the macrophage, MAP can prevent the maturation of the phagosome. *In vitro* studies have shown that MAP can survive in phagosomes for several weeks, and *in vivo* studies have reported finding intact mycobacteria within ileal macrophages (12,230,252). Compared to infection with *M.smegmatis*, a less pathogenic mycobacteria, phagosomes containing MAP had higher levels of Transferring Receptor, an early phagosome marker, and lower levels of Lysosome Associated Membrane Protein 1, a late maturation marker (110). Similarly, a study comparing MAP infection with *Mycobacterium avium* found that macrophages were twice as efficient at killing *M.avium* as they were at killing MAP (266). This difference may be mediated by differential activation of the MAPKp38 pathway (228). This situation is similar in *M.tuberculosis* infection, with mycobacteria-containing macrophages displaying a lack of maturation (54). Although some studies have shown that the bacteria may be able to grow and multiply within the phagosome, the number of viable MAP remains constant, suggesting that the macrophage is capable of killing a limited number of mycobacteria. This killing may depend on

the multiplicity of infection (MOI) (16,276), and the activation state of the macrophage (109). A recent study suggested that this survival is due to the infecting strain of MAP, indicating that some strains may be more efficient than others at interrupting host immune responses (87).

The mycobacteria prevent bacterial killing through several mechanisms, including preventing or reducing phagosome and lysosome fusion and preventing oxygen radical production (230). Studies have shown that MAP enters the cell via binding to the C3 receptor (181,218). This is mediated by the association of complement cleavage product C2a. This can cleave C3, leading to opsonisation of the mycobacteria by C3b and macrophage recognition (201). This allows the mycobacteria to avoid the initial anti-microbial activities of the macrophages, as internalisation via the complement receptors avoids triggering the oxidative burst (181,218). Mycobacteria are known to recruit a host protein – tryptophan-aspartate containing coat protein (TACO) – and retain it on their surface. TACO is a normal component of the phagosome coat that is lost before acidification, so bacteria retention of TACO prevents phagosome-lysosome fusion (133,181). Other host genes involved in this lack of phagolysosome formation include the rab family of GTPases (133) and coronin-1. Coronin-1 is a leukocyte specific protein, which blocks lysosomal delivery (119). Two further genes, nucleolin-related protein (NRP) and nicotinamide adenine dinucleotide dehydrogenase (NADH) were not up-regulated in macrophage responses to MAP infection, unlike in macrophages infected with *E.coli* (247), suggesting these genes may play a role in phagosome maturation. Mycobacterial genes are also involved directly in negating the host immune response. MAP has been found to secrete a tyrosine phosphatase upon entry into macrophages, which may act to dephosphorylate signalling and adaptor molecules (12,227). MAP can also secrete superoxide dismutase, which can inactivate reactive oxygen species (218). Interaction of MAP with TLR2 induces MAPKp38

signalling and thus an increase in IL-10 expression, reducing anti-microbial responses further (229).

This lack of bacterial killing and macrophage activation can prevent the activation of the acquired immune response. Infected macrophages are able to produce cytokines, including IL-1, IL-6, IL-12 and TNF $\alpha$ , and macrophage cultures pre-incubated with IFN $\gamma$  do show increased bacterial killing (218,227,278). However, infected macrophages do show a reduction in T-cell activation capacity. This reduction seems to be time dependent, with normal levels of T-cell activation being observed immediately after infection, and poor activation being observed one week after infection (230,278). Infection of monocytes with MAP also leads to increased levels of apoptosis, although this is not observed in infected macrophages (4).

### **1.3.2 Antibody response**

Antibodies to MAP are produced early in infection, but never offer protection. Studies of MAP infection in cattle have shown antibodies to two unidentified proteins appearing between 7 and 14 days post infection (133) and antibodies to lipoarabinomannan (LAM) appearing around 134 days post infection (133,263). Studies using MAP vaccines, again in cattle, have shown different production times of antibodies, with antibodies first observed at 56-112 days post infection, peaking at 250 days post infection and undetectable by 420 day post infection (132). Some studies in sheep have shown antibody detection from 90 days post infection (136), whereas others have observed a reduction in circulating IgG upon infection with MAP (23). This early antibody response can be influenced by several external factors. The age of the animal at infection or vaccination can have an effect on antibody production and detection. A study in sheep and goats showed that the size and persistence of the antibody response to a MAP vaccine is directly related to the age of the

goats (57). A study in cattle showed that the commercial ELISA test cannot be used to detect antibody until the animal is over 3 years old (113). Indeed, in some studies, the ELISA test was not able to detect antibody responses in cattle shown to be MAP positive through different tests (263). The infecting strain can also influence antibody production in sheep. A study comparing five strains found that antibodies were produced at different levels and at different times in the five groups (260).

Later in infection, antibody levels correlate with bacterial load and severity of the disease (36), similar to the situation in tuberculosis in humans (170). In both cattle and deer, there is a strong correlation between antibody persistence and disease severity (147,174,237). However, in goats and sheep the association is less straight forward. A study of MAP challenged goats found only one of three seropositive animals developed faecal shedding, a sign of disease progression (236). A similar study in sheep found that no clinically infected sheep developed an antibody response, despite persistent faecal shedding (235), whereas other studies have found high levels of antibody production in all clinically infected sheep (35). This discrepancy seems to be a function of the different pathologies observed in ovine pathology – studies that group the sheep by type of pathology found that all animals with multibacillary disease produce antibodies, whereas only some animals with paucibacillary disease do (35,136). A recent study has also shown that sheep can produce autoantibodies in response to MAP heat-shock proteins, which may lead to complications in these sheep, including anti-neutrophil cytoplasmic antibodies -associated vasculitis (26).

### **1.3.3 T cell responses**

T cell responses are central to the control of all mycobacterial diseases. CD4+, CD8+ and  $\gamma\delta$  T cells are thought to be the main cells involved in protection, producing IFN $\gamma$ , which can activate macrophages and lead to

killing of mycobacteria. Antigens presented to CD4+ helper cells are associated with MHC class II, whereas antigens associated with MHC class I are presented to CD8+ cytotoxic T cells (218). CD8+ T cells tend to be associated with anti-viral immune responses and CD4+ T cells are associated with anti-bacterial and anti-parasitic responses (118). CD4+ T cells can be classified as Th1 or Th2 depending on their function and cytokine profiles (156). Th1 cells produce IFN $\gamma$  and act to promote mycobacterial killing through the activation of macrophages. Th2 cells produce IL-4 and IL-10 and act to promote the production of antibodies. Th2 cells are ineffective against intracellular mycobacteria (131,218).

In tuberculosis infections in humans, CD4+ T cells are critical to control, and CD8+ T cells contribute to this control by producing IFN $\gamma$  (173,184). This response can lead to long term immunity and control of infection by the formation of granulomatous lesions which control bacterial growth (196). This successful response is a Th1 response, characterised by the production of IFN $\gamma$  (173) and can in some types of tubercular disease clear the bacteria (17).

The T-cell response in bovine paratuberculosis is largely similar, with CD4+ Th1 cells thought to be central to control through the production of IFN $\gamma$  (19,242,252), although there is some evidence that in calves, IFN $\gamma$  production in response to new antigens may be by NK cells, rather than CD4+ T cells (8). In both human and bovine tuberculosis, NK cells produce IFN $\gamma$ , increasing macrophage activation and mycobacterial killing (67,84). In early, sub-clinical MAP infections,  $\gamma\delta$  T cells are increased, along with MHC class II expressing B cells (127). This suggests a role for  $\gamma\delta$  T cells in the control of MAP infection, although this is still to be elucidated, as they do not produce IFN $\gamma$  or increase nitric oxide (NO) production (19,131,219). The number of CD8+ cells in these cattle is similar to uninfected and clinically infected cattle (127,131). Some studies

have shown a decrease in the number of CD4+ cells at this stage of infection (131) whereas others have found that the number of CD4+ cells does not change (60,127). It seems that early in infection, the IFN $\gamma$  produced by these CD4+ and CD8+ cells is sufficient to activate macrophages and control bacterial growth (219). This does not prevent disease progression, because of a reduction in the ability of infected macrophages to produce NO and express MHC class II (219,266,267). Additionally, studies in macrophage cell lines have shown that, although infected macrophages can produce inflammatory cytokines capable of activating Th1 cells, the second, antigen specific activation step is inhibited by MAP infection (278). Later in infection, these controlling CD4+ and CD8+T cells are lost through apoptosis (131) leading to a loss of macrophage activation and thus an increase in bacterial load (242). The expression of IFN $\gamma$  is reduced, and Th2 cytokines dominate.

The T cells response in ovine paratuberculosis is initially similar to that in bovine paratuberculosis.  $\gamma\delta$  T cells are increased early at the site of infection (21,23,144), suggesting that these cells may play a role in early immunological events. CD4+ and CD8+ cells are increased later in infection (144,186). However, in sheep, the T cell response later in infection is polarised, and leads to the observed differences in pathology. Higher numbers of CD4+ and  $\gamma\delta$  T cells are observed in paucibacillary lesions, with a corresponding increase in the expression of IL-2 and IFN $\gamma$  (36,144). Conversely, multibacillary lesions contains fewer CD4+ cells and an increased number of CD8+ cells, with the related decrease in the release of proinflammatory cytokines, such as IFN $\gamma$  and TNF $\alpha$  (36,144). However, in both cases this constitutes a terminal disease state, and there is no switch from a Th1 to a Th2 type response (224).

T regulatory cells (Tregs) have a CD4+CD25+FoxP3+ phenotype, and are capable of inducing anergy to self and foreign antigens and preventing

migration of immune cells to the site of infection (273). In both human tuberculosis and mouse models of tuberculosis, these cells are increased in number and accumulate at the site of infection. In mice with no Treg cells, the number of mycobacteria is reduced compared to wild type mice, and in mice and humans Tregs can prevent the production of both IL-10 and IFN $\gamma$  in response to *M.tuberculosis* infection (46,111,137,203). This evidence suggests that Treg cells have a vital role to play in tuberculosis pathogenesis. It is therefore likely, although little is currently known about Treg cells in paratuberculosis, that these cells are also involved in the response to paratuberculosis.

#### **1.4 Host gene expression in MAP infection**

The profiling of the host gene expression response in MAP infection and clinical paratuberculosis is ongoing, and reveals much about the immune response and immune pathways involved in this disease. Most studies so far have analysed gene expression in cattle, concentrating mainly on expression in peripheral blood mononuclear cells (PBMCs), using both microarray and PCR technologies, and several have used non-ruminant cell lines. One recent study using a murine macrophage cell line described decreased expression of immunoresponsive gene 1 (IFG1) in MAP infected cells compared to LPS stimulated cells (18). A second study used a human monocyte cell line to assess the response to different types of MAP. When the cells were infected with sheep isolates, up-regulation of several proinflammatory genes was observed. This up-regulation was not observed in the cells after infection with cattle or human strains (158)

A series of microarray experiments by Coussens *et al* have comprehensively characterised gene expression in bovine PBMCs taken from MAP infected cattle. PBMCs from clinically infected cows displayed down-regulation of 83 genes when stimulated with MAP, including fibroblast growth factor and Lyn B protein kinase. Eight genes were up-

regulated in these cattle, including CD40L, IFN $\gamma$  and IL-10. Conversely, stimulation of PBMCs from sub-clinically infected cattle with Map induced the up-regulation of 71 genes, including CD40L and several matrix metalloproteases (MMPs), and the down-regulation of a further 16 genes (61). A second study found that stimulation with MAP was not needed to produce a difference in gene expression in PBMCs, with 86 genes being differentially expressed in unstimulated PBMCs from infected cattle compared with similar cells from control cattle (60). A further experiment showed that stimulation of PBMCs from infected cattle produced a gene expression response within 4 hours of exposure, although many of the changes were no longer appreciable by 8 hours post exposure (62). Further studies to characterise these differentially expressed genes found that IL-5, GATA 3, TIMP1, TIMP2, IL-10, IFN- $\gamma$ , TGF $\beta$  and IL-8 were up-regulated and MMP14 was down-regulated (59). Studies carried out by other groups on PBMCs from infected cattle have identified several more differentially expressed genes. Urocortin, a neuropeptide of the corticotrophin-releasing hormone family, is up-regulated (261) and TNF $\alpha$ , RANTES and MCP-1 are down-regulated in infected bovine PBMCs (37).

A second set of studies into host gene expression in paratuberculosis have concentrated on differential expression in bovine macrophages. Two recent microarray studies identified 52 and 47 genes that are differentially expressed in macrophages from infected cattle compared to uninfected controls (223,266). Exposure to MAP lead to the up-regulation of IL-1 $\alpha$ , IL-10, GM-CSF, IL-18, TNF $\alpha$  and TRAF1, and down-regulation of IL-12, IFN $\gamma$ , nucleolin related protein (NRP), nicotinamide dinucleotide adenine dehydrogenase (NADH) and MHC class I and II genes in bovine macrophages compared to unexposed controls (48,227,247,267,269). Similar studies on MAP infected bovine dendritic cells described up-regulation of CCR7, CCR5, CD40, CD80 and IL-10 and down-regulation

of MHC class II genes, IL-12, IL-18 and IL-6 (138,141). A recent study, however, has shown that the genes differentially expressed in infected macrophages may depend on the bacterial strain. The study showed significantly different expression of several genes, including IL-10, TNF $\alpha$ , MMP3 and TIMP1, when the expression patterns of cells infected with sheep and cattle strains were compared (117).

A third group of studies has analysed gene expression in tissues taken from the ileum of infected cattle. In such tissues, up-regulation of IFN $\gamma$ , TGF $\beta$ , IL-5, IL-8, IL-10, TRAF-1, IL-1 $\alpha$ , MCP-2, N-cadherin and CD29 and down-regulation of IL-16 was observed (3,63,128), although this varied depending on the stage of the disease. Cattle with late, lepromatous lesions have up-regulated IL-4, IL-10 and IL-2 and down-regulated IL-18 compared to cattle with early, tuberculoid lesions and uninfected controls (242).

Far fewer studies have been carried out on the expression profiles of sheep infected with MAP, perhaps assuming that the profiles would be similar to those seen in cattle. A study comparing stimulated blood lymphocytes taken from sheep with both clinical forms of the disease showed that lymphocytes from multibacillary sheep have down-regulated IFN $\gamma$  and IL-2 compared to lymphocytes from paucibacillary sheep (36). Afferent intestinal lymph cells (AILCs) from sheep with clinical paratuberculosis have decreased IL-4, IL-5 and IL-13 and increased IFN $\gamma$  and TNF $\alpha$  compared to AILCs from sheep with a parasitic infection (102). A study on infected ovine ileum found increased TNF $\alpha$ , IL-18 and IL-6 compared to uninfected controls (6). Overall, little is known about gene expression in ovine paratuberculosis, and there have been no extensive microarray studies done in this area.

### 1.5 Crohn's disease

Crohn's disease (CD) is a chronic inflammatory intestinal disease of humans, first described in 1932 (44). The symptoms and gross pathology are similar to Johne's disease in ruminants (222). It can affect any part of the intestinal tract, and may also affect the liver and pancreas (44). There are two competing theories as the cause of CD – the first assumes an autoimmune cause, with no specific infectious agent, leading to an uncontrolled inflammatory response. The second states that infection with MAP leads to immune dysregulation and again an uncontrolled inflammatory response, similar to that seen in ruminant paratuberculosis (45). In both cases, breakdown of the intestinal barrier and invasion by gut bacteria are seen as essential to the continuation of the disease (101).

The evidence for the role of MAP in CD is wide ranging and often contradictory. Many Crohn's disease patients are infected with MAP. Two studies of Sardinian patients showed that 83-87% were IS900 positive in blood, compared to 10% of control patients. In addition, MAP could be cultured from the blood of 63% of CD patients compared to 10% of controls (197,207). A study in Germany found that 52% of CD tissues were IS900 positive compared to 5% of controls. The IS900 positive tissues included small bowel and colon (9). A USA study detected MAP DNA in the buffy coat fragment of blood from 46% of CD patients, compared to 20% of controls. MAP could also be cultured from the blood of 50% of CD patients (167). An Indian study detected MAP antibodies in 100% of CD patients compared to 38% of controls (220). A wide ranging review of such studies concluded that the association of MAP with CD was specific, but not necessarily causal (83). Although MAP cannot be visualised in CD tissues by ZN staining, this is thought to be due to the presence of cell wall deficient bacteria, which do not stain (97,105). MAP infection can alter the immune response to CD, perhaps worsening the disease. Increased concentrations of TNF $\alpha$  are found in tissues from MAP

positive CD patients, compared to CD patients without MAP infection, non-CD patients with MAP infection and non-infected controls (50).

Transmission of MAP from ruminants to humans is thought to happen through the consumption of milk and dairy products, or through faecal contaminated water. A study of dairy farmers found no connection between contact with dairy cattle infected with MAP and incidence of CD (120). Viable MAP can be detected by IS900 PCR in raw or pasteurised milk (11,97), river water destined for domestic water supplies (180) and commercial cheese samples (51). A recent study found a significant link between consumption of hand-made cheese and MAP infection in Sardinia (197). However, an epidemiological study found that consumption of milk is associated with a reduced risk of CD, and that there was no link between consumption of contaminated water and CD (2).

Susceptibility to CD is associated with polymorphisms in the NOD2/CARD15 and NRAMP1 genes (74,205). Susceptibility to MAP in cattle is also associated with polymorphism in these genes, suggesting a common disease pathway (182,193). However, in CD an association could not be found between NOD2/CARD15 mutations and MAP infection (28).

These observations have lead to suggestions that anti-MAP therapy could be an efficient treatment for CD. However, a recent study of the efficacy of combined anti-microbial agents in the treatment of CD did not find any long-term benefit (212). Sulfasalazine is commonly used as an anti-inflammatory drug to treat CD, and has recently been shown to inhibit MAP growth in culture, leading to the study author suggesting that the anti-inflammatory nature of this drug is due to the inhibition of MAP (96).

Taking all of this evidence together, a recent epidemiological study concluded that four of six epidemiological causal criteria (strength of association, consistency of effect, temporality and biological plausibility) were satisfied and thus that the evidence strongly supports the causal relationship between MAP and CD (251).

### **1.6 Aims and objectives**

This study tested the hypothesis that expression of immunoinflammatory genes differs in the three forms of paratuberculosis.

This PhD had four major aims:-

- To define comprehensively the three types of pathology, through gross pathology, histopathology and molecular approaches, in order to provide robust definitions for the rest of the study.
- To quantify expression of specific cytokine genes in order to confirm the polarisation of the immune response in sheep with the two clinical forms of the disease, and to explore the cytokine responses in asymptomatic sheep.
- To quantify the expression of a range of immunoinflammatory genes using microarray technology to produce a comprehensive molecular signature of the different pathologies.
- To explore the presence of SNPs in genes found to be differentially expressed in the two clinical forms of the disease, in order to assess whether genetic changes are responsible for the observed differences.

The results of the studies provide a robust molecular definition of the forms of ovine paratuberculosis, and provide a framework for further analysis of the pathways involved in immune response to this disease.

## 2. Materials and Methods

## 2.1 Experimental animals and disease diagnosis

### 2.1.1 Experimental animals

Animals with and without clinical paratuberculosis were out bred sheep from one of three farms. Sheep suffering from wasting, loss of condition and diarrhoea were delivered to the Moredun Research Institute (MRI) suspected of having of paratuberculosis. Thirty infected sheep were used – ten multibacillary, ten paucibacillary and ten asymptomatic. All sheep were euthanized at MRI and ileum and lymph node tissue and blood samples taken. Faecal samples were taken and faecal egg counts made (Table 2.1). All experimental procedures involving animals were performed under licence as required by the UK Animals (Scientific Procedures) Act 1986. Control sheep were from a flock that had never had a clinical case of paratuberculosis (n=9).

### 2.1.2 Diagnosis of paratuberculosis and definition of pathological forms

All experimental animals were diagnosed on the basis of histopathology of the terminal ileum and IS900 real-time RT-PCR. The age, sex and breed of these sheep are given in Table 2.1. Terminal ileum samples for histopathology were fixed in 10% formal-saline. Sections 4µm thick were cut from paraffin wax-embedded tissue and stained with haematoxylin and eosin (H&E) (143) or Ziehl-Neelsen (ZN) (126).

Ileum derived RNA samples from all experimental sheep and mesenteric lymph node RNA samples from asymptomatic sheep were tested for the presence of MAP by real-time RT-PCR for IS900, a MAP specific insertion sequence (29,232). Primers and probes were designed by Eishi *et al* (76), and the reactions were carried out in an ABI prism 7000 real-time PCR machine. Each reaction contained 12.5µl Platinum® Quantitative PCR SuperMix-UDG with ROX (Invitrogen), 50nM each primer, 100nM probe and 5µl cDNA, generated from 2.5µg RNA, made up to 25µl with

deionised water. The reactions were cycled as follows: 50°C for 2 minutes, 95°C for 10 minutes and 40 cycles of 95°C for 15 seconds, then 60°C for 1 minute. (Addresses of all suppliers listed in appendix 1).

A commercial antibody ELISA (Institut Pourquier) was used to detect the level of MAP specific antibody in the blood of the experimental animals. This ELISA has a sensitivity of 34.9% and a specificity of 98.8% in sheep (98). The assays were carried out by Biobest Laboratories Ltd. Briefly, the ELISA tested for antibodies towards a protoplasmic extract of MAP. Each sample was tested in duplicate. The results were expressed as a percentage of the reaction in a standardised positive control. A result of less than 60% was considered to be negative, a result of 60-70% was considered doubtful and repeated, and a result of more than 70% was considered positive.

## **2.2 Tissue selection and removal**

Terminal ileum tissue was chosen, as this area of the intestine is known to be the main focus of pathology in MAP infection (211,218).

Approximately 0.5g of ileum tissue was removed post-mortem, placed in five volumes of *RNAlater*<sup>TM</sup> (Ambion) and left overnight at 4°C. The ends were then trimmed and the tissue archived at -80°C.

Table 2.1: Breed, age, sex and FEC of experimental sheep

Sample	Breed	Age (years)	Sex	FEC*	Type of Infection
3	Blackface X Bleu du Maine	4.5	F	-	Paucibacillary
4	Texel	5.5	F	225	Paucibacillary
5	Blackface x Bleu du Maine X Lley n x Roussin	2.5	F	252	Paucibacillary
6	Lley n X Roussin	3.5	F	36	Paucibacillary
7	Bleu du Maine	4	F	423	Paucibacillary
8	Blackface x Bleu du Maine	6	F	180	Paucibacillary
9	Texel	2.5	F	378	Paucibacillary
10	Blackface	2.5	F	0	Paucibacillary
32	Blackface X Bleu du Maine	4.5	F	252	Paucibacillary
34	Blackface X Bleu du Maine	4.5	F	117	Paucibacillary
11	Blackface	3	F	2171	Multibacillary
12	Blackface	2	F	1188	Multibacillary
13	Blackface	4	F	5058	Multibacillary
14	Blackface	4	F	3210	Multibacillary
16	Blackface	3	F	2358	Multibacillary
17	Blackface	3	F	-	Multibacillary
27	Blackface	5	F	2124	Multibacillary
28	Blackface	5	F	3150	Multibacillary
29	Blackface X Bleu du Maine	4.5	F	-	Multibacillary
30	Blackface X Bleu du Maine	4.5	F	-	Multibacillary
19	Blackface X Bleu du Maine	7	F	189	Asymptomatic
20	Blackface X Bleu du Maine	7	F	1116	Asymptomatic
21	Greyface	2-4	F	3	Asymptomatic
22	Greyface	2-4	F	108	Asymptomatic
23	Texel	1	F	13	Asymptomatic
24	Blackface	2.5	F	1731	Asymptomatic
25	Greyface	2-4	F	4	Asymptomatic
26	Greyface	2-4	F	1197	Asymptomatic
31	Blackface X Bleu du Maine	4.5	F	1305	Asymptomatic
33	Blackface X Bleu du Maine	4.5	F	135	Asymptomatic

\*There were no statistically significant differences in FEC between the three groups of samples.

## 2.3 Isolation of RNA from Ileum tissue

### 2.3.1 Homogenisation of tissues

Tissue samples were removed from  $-80^{\circ}\text{C}$  storage and thawed on the bench. 250mg was weighed out into a sterile Petri dish, and chopped into small pieces using a sterile scalpel. Shredded tissue was placed in a sterile Lysing Matrix D ribolyser tube (Q-Biogene) containing 1.4mm ceramic spheres. This tissue was disrupted and homogenised in lysis buffer containing guanidine isothiocyanate (RNeasy from Qiagen) using a ribolyser and then spun at 13,000xg for ten minutes to pellet the cell debris. Lysate was removed and placed in a sterile 15ml Falcon™ tube (BD Biosciences). A second aliquot of buffer was added to the ribolyser tube, and the homogenisation was repeated to maximise RNA concentration. The second aliquot was added to the Falcon™ tube, and the total volume made up to 15ml with the lysis buffer.

### 2.3.2 RNA extraction from tissues

The lysate was centrifuged for 10 minutes at room temperature, and then the supernatant placed in an RNeasy Maxi column, taken from the Qiagen RNeasy® Maxi Kit. Further steps were carried out according to manufacturer's instructions. The RNA was eluted into 0.8ml of RNase-free water. The RNA was concentrated by ethanol precipitation and resuspended in 0.3ml of RNase-free water. The samples were DNase treated using the Ambion DNase I kit, according to manufacturer's instructions. Samples were checked for genomic DNA contamination by the presence or absence of a GAPDH PCR product (For primers see Table 2.2).

### 2.3.3 Measurement of RNA/DNA concentration

The concentration of nucleic acid in a sample is directly proportional to the absorption of UV radiation at 260nm by the sample. The

concentration of nucleic acid in a sample was determined by spectrophotometry. The absorbance was measured at 260nm and 280nm. The ratio of these absorbances was used as a measure of the quality of the sample – a ratio of 2:1 was considered optimal.

RNA concentration =  $A_{260} \times 40 \times$  dilution factor

DNA concentration =  $A_{260} \times 50 \times$  dilution factor

The RNA samples were also quantified using an Agilent Bioanalyser 2100, which uses LabOnChip technology to determine RNA quantity and quality. The RNA integrity number (RIN) is a value provided by the Agilent Bioanalyser software (2100 expert), giving a measure of RNA fragmentation – samples with a RIN of less than 6 were excluded from the experiment (202). RIN values were not available for samples 29-34 or the control samples as they were analysed on an earlier version of the Agilent Bioanalyser software. These samples had previously been used successfully in real-time RT-PCR and were therefore judged to be of sufficient quality. RNA of control sheep was kindly provided by Dr K. Nalubamba.

## **2.4 Reverse transcriptase-polymerase chain reaction**

### **2.4.1 Reverse transcription of RNA into cDNA**

2.5µg of RNA was suspended in a final volume of 16.25µl in nuclease free water, giving a final RNA concentration of 0.1µg/µl. 500ng of Oligo(dT) (Promega) was added, and incubated for five minutes at 70°C, followed by five minutes on ice. To this 5µl of 5x MMLV buffer, 1.25µl of 100mM dNTPs and 1µl of MMLV RT enzyme (Promega) were added, and the mixture was incubated at 42°C for 60 minutes, followed by 15 minutes at 70°C to inactivate the enzyme.

### 2.4.2 Primer design

Primer sequences and accession numbers are given in Table 2.2. Primer sets marked with \* were kindly provided by other members of the research group. Primers were designed for the rest of the genes of interest using published ovine or bovine sequences with Primer3 ([http://frodo.wi.mit.edu/cgi-bin/primer3/primer3\\_www.cgi](http://frodo.wi.mit.edu/cgi-bin/primer3/primer3_www.cgi)) and NetPrimer (<http://www.premierbiosoft.com/netprimer/netprlaunch/netprlaunch.html>) software. Ideally, primers would have a GC content of between 40-60%; be 18 to 25 bases long; produce a fragment of between 100-250bp in length and have minimal secondary structure and self-complementarity. Primers were designed to be as close to this ideal as possible.

### 2.4.3 Amplification

Amplification was carried out in a Hybaid Sprint Thermocycler, in a final volume of 50µl. 2µl of cDNA synthesised from 2.5µg of RNA was added to the following reagents: 5µl of 10x *Taq* DNA Polymerase buffer (Promega); dNTPs to a final concentration of 800µM; forward and reverse primers to a final concentration of 500µM; and 1.25U of *Taq* DNA Polymerase (Promega), made up to 50 µl with nuclease free water. Optimisation of annealing temperature for each primer set was carried out. The reactions were cycled as follows:-

95°C	2 minutes	
95°C	30 seconds	} 30-40 cycles
*°C	45 seconds	
72°C	1 minutes	
72°C	5 minutes	

\*The annealing temperature was optimised for individual primer sets

Table 2.2: Accession numbers and primer sequences

Gene	Species	Accession Number	Primers	Tm (°C)	Annealing temp (°C)	Product size (bp)
IL-1a	Bovine	NM_174092.1	F - TTGGTGCACATGGCAAAGTG R - GCACAGTCAAGGCTATTTTTCC	58.64 58.88	50	72
TRAF1	Bovine	XM_589090.1	F - AGCAGAGGGTGTGGAGTTG R - CTGGGGAGAGAGGCTGAC	60.3 59.93	60	186
IGFBP-6	Bovine	XM_614379.1	F - AAGGAGAGTAAGCCCCAAGC R - CGGGAAGGAGTGTAGAGGT	59.85 60.5	60	95
TRAM	Bovine	U19578.1	F - CACATTTCCCGCCTATTTTAC R - TCTGGTTCTCTGCTCTTGCT	58.51 57.9	55	148
CD34*	Bovine	ABO21662	F - CCGTCCCTCTTGCCCTCATT R - ATCCCTTTTCACCCCTTCTGG	57.15 58.07	57	210
IL-3*	Ovine	Z18897	F - ACCTCCTTCTGCTCCTGCTT R - TATTTCCCAAGTCCCCATCTT	58.06 56.05	57	193
CXCR4*	Bovine	AF399642	F - ACCTCCTGTTTGTCTCCTAGG R - AATGTCCACCTCGCTTGC	51.94 56.17	62	163
IGFBP-2	Ovine	S44612.1	F - GCACCTCTATTCCCTACACATC R - GTTACACACACCAAGCACTCC	57.69 57.52	58	109
TIRAP	Bovine	XM_609564.1	F - TGTCGTGTCTGTGTCTTCATCC R - CTTTCTCCTGACGCCCTGCT	61.18 60.68	58	167
IL-1 $\beta$ *	Ovine	X56972	F - CCTTGGGTATCAGGGACAA R - TGGGTATGGCTTCTTTAGG	55.24 56.65	57	317
IL-6*	Ovine	X68723	F - TCCAGAACGAGTTTGAGG R - CATCCGAATAGCTCTCAG	50.52 47.72	52	236

Table 2.2 cont

Gene	Species	Accession Number	Primers	T <sub>m</sub> (°C)	Annealing temp (°C)	Product size (bp)
IL-8*	Ovine	X78306	F - ATGAGTACAGAACTTCGA R - TCATGGATCTTGCTTCTC	40.91 47.27	55	222
IL-12p40*	Ovine	AF004024	F - TCAGACCAGAGCAGTGAGGT R - GCAGGTGAAGTGTCCAGAAT	54.75 54.47	57	243
TNF $\alpha$	Ovine	X56756	F - GAATACCTGGACTATGCCGA R - CCTCACTTCCCTACATCCCT	55.08 55.46	57	238
TGF $\beta$ *	Ovine	X76916	F - GAACTGCTGTGTCGTCAGC R - GGTGTGCTGGTTGTACAGG	56.16 55.94	55	169
IL-18*	Ovine	AJ401033	F - GAGCACAGGCATAAAGATGG R - TGAACAGTCAGAAATCAGGCATA	55.61 55.77	55	241
GM-CSF*	Ovine	X53561	F - GATGGATGAAACAGTAGAAGTCG R - CAGCAGTCAAAGGGAATGAT	56.04 54.88	57	261
IFN- $\gamma$ *	Ovine	NM_001009803	F - CTAAGGGTGGGCCTCTTTTC R - CATCCACCGGAAATTTGAATC	58.19 57.57	55	237
IL-10*	Ovine	U11421	F - CTGTTGACCCAGTCTCTGCT R - ACCGCCCTTTGCTCTTTGTTT	54.57 57.45	52	223
GAPDH*	Ovine	AF030943.1	F - GGTGATGCTGGTGCTGAGTA R - TCATAAAGTCCCTCCACGATG	59.86 58.52	58	265
SDHA*	Bovine	NM_174178.2	F - ACCTGATGCTTTGTGCTCTGC R - CCTGGATGGGCTTGGAGTAA	62.84 62.20	58	126

## **2.5 Agarose gel electrophoresis**

### **2.5.1 Preparation of agarose gels**

Agarose gels were prepared at different concentrations depending on the size of the DNA fragments to be visualised. PCR products were visualised on a 2% agarose gel, linearised plasmids were visualised on a 1% agarose gel. Gels were prepared by adding the correct weight of agarose (Qualex Gold Agarose, Thermo-Hybaid) to 1x Bionic buffer (Sigma) and heating until the agarose was fully dissolved. This was then cooled, and 1µl of 10mM ethidium bromide or 1µl/ml GelRed nucleic acid gel stain (Cambridge Bioscience Ltd) was added. The gel was poured into a tray and allowed to set.

### **2.5.2 Running agarose gels**

The gel was submerged in 1x Bionic buffer. Samples were mixed with 6x loading dye (Promega) and loaded into wells. 1Kb and 100bp DNA ladders (Promega) were used. Electrophoresis was carried out at a constant 150V until sufficient DNA separation was achieved. Gels were examined in an ultraviolet transilluminator (Ultraviolet Products) and captured using Labworks™ software.

## **2.6 Cloning of the PCR product**

### **2.6.1 Ligation into pGEM®-T easy vector**

PCR products were purified using the Qiagen QIAquick PCR purification kit according to manufacturer's instructions. The PCR products were eluted into 50µl of EB (10mM Tris ·Cl, pH 8.5). 3µl of the PCR product was ligated into the pGEM®-T easy vector (Promega) according to manufacturer's instructions.

### 2.6.2 Transformation into JM109 cells

The ligated pGEM®-T easy vector reactions were transformed into 20µl of JM109 High Efficiency Competent cells, according to the Promega pGEM®-T easy vector protocol. The cells were plated onto Amp/XGAL/IPTG plates to allow blue/white selection of colonies. Only white colonies contained the vector and insert.

### 2.6.3 Plasmid DNA purification

An overnight culture of bacteria picked from white colonies on the agar plates was lysed and spun to pellet the insoluble fraction. The supernatant was then applied to a QIAprep column. The pDNA from cloned JM109 cells containing the Promega pGEM®-T easy vector was purified using the Qiagen QIAprep spin miniprep kit, following the manufacturer's instructions and the concentration determined.

### 2.6.4 Restriction enzyme digest

To check the size of the insert, pDNA was digested using *EcoRI* restriction enzyme (New England Biolabs). 500ng – 1µg of DNA was diluted to a final volume of 17µl in nuclease free water. 2µl of 10x *EcoRI* buffer and 1µl of *EcoRI* enzyme were added, and the reaction incubated at 37°C for two hours. The insert was separated on a 2% agarose gel.

### 2.7 DNA sequencing

DNA sequencing was carried out according to instructions received from Zoology Sequencing Stores, Oxford. 1µl of template DNA was mixed with 0.5µl BigDye, 1.75µl 5x sequencing buffer, 3.2µl of 1µM T7 or Sp6 primer and 3.55µl nuclease free water. The reaction mixtures were cycled in Hybaid Sprint Thermocycler as follows:-

96°C	10 seconds	} 30 cycles
50°C	5 seconds	
60°C	2 minutes	

The DNA was ethanol precipitated and excess ethanol removed by drying under a vacuum. The reactions were sent to Zoology Sequencing Stores, Oxford for sequencing.

## 2.8 Real-time reverse-transcriptase polymerase chain reaction

### 2.8.1 Overview

Briefly, samples were reverse transcribed and run in real-time RT-PCR alongside a standard curve of known template concentration. Comparison with the standard curve allowed absolute quantitation of the copy number of a gene of interest, and thus allowed the levels of mRNA of genes in different samples to be compared.

### 2.8.2 Linearization of plasmids

Purified pDNA was linearised using either *NcoI* or *NdeI* restriction enzymes (New England Biolabs). 1µg of pDNA was diluted in nuclease free water to a total volume of 17µl. 2µl of 10x buffer and 1µl of the restriction enzyme were added, and the reaction mixture incubated overnight at 37°C. A 2µl aliquot of the linearised plasmid was run on a 1% agarose gel to check the linearization was complete.

### 2.8.3 Generation of standard curves from cloned pDNA template

Linearised plasmid DNA was purified using a Qiagen MinElute PCR purification kit and eluted into 10µl of EB. The concentration of each cloned pDNA was then determined. A one in ten serial dilution ( $10^{-1}$  to  $10^{-10}$ ) of the linearised plasmid was produced and used to construct a standard curve in a Rotorgene 6™ real-time PCR machine (Corbett Life

Science). Duplicates of 2µl of each dilution were run along with a negative control (nuclease free water), and a positive control (cDNA generated from ileum derived RNA).

A melt curve was run for each standard curve. SYBR Green binds to any double stranded DNA in the sample, and thus if primer-dimers are produced this can affect the reported concentration of the gene of interest. The melt curve contains a peak for every different size of DNA fragment produced during the amplification. A good amplification should have one peak in the melt curve, whereas an amplification containing primer-dimers has two or more peaks. Therefore using a melt curve allowed runs where primer-dimers were present to be excluded.

#### 2.8.4 Reaction mix and cycling conditions

For each real-time RT-PCR reaction, 2µl of template cDNA were added to 18µl of reaction mix. The mix contained 2µl of 10x buffer, 200µM of dNTPs, 250nM of each primer, MgCl<sub>2</sub> to an optimum concentration, 0.7µl of a 1/1000 dilution of SYBR green master mix and 0.75U FastStart *Taq* DNA Polymerase (Roche), made up to a final volume of 18µl with nuclease free water. The cycling conditions were as follows:-

94°C	5 minutes	
94°C	20 seconds	} 45 cycles
60°C*	20 seconds	
72°C	20 seconds	

Melt curve: 65°C rising to 94°C at 0.3°C per second

\*For all genes except CD34 which was 57°C

### 2.8.5 Variability assay

To determine the level of variability inherent in the real-time RT-PCR reactions, a variability assay was carried out. A single sample was reverse transcribed in three simultaneous reactions. The cDNA produced was then amplified ten times each in an SDHA real-time PCR reaction. The resulting copy numbers were then compared to give a value for the variability inherent within the reactions (Table 2.3).

Table 2.3: Copy numbers of SDHA in variability assay

RT reaction	Maximum copy number of SDHA	Minimum copy number of SDHA	Mean copy number of SDHA	Fold change (max/min)
1	349,426	256,928	299,159	1.4
2	335,181	214,713	289,186	1.6
3	240,399	161,965	195,420	1.5
<b>Mean</b>	308,335	211,202	256,655	<b>1.5</b>
<b>Range</b>	349,426	161,965	-	<b>2.2</b>

The overall inherent variability of the assay was 2.2 fold. This was taken as the threshold value for the analysis of the genes of interest.

### 2.8.6 Real-time RT-PCR for genes of interest

Genes of interest for the real-time RT-PCR analysis were selected from published sources and preliminary microarray data. RNA was extracted from ileum samples and reverse transcribed. The cDNA was diluted 1:4 in nuclease free water. GAPDH PCR was run on each sample to make sure that amplifiable material was present. 2µl of each sample was run in triplicate against both the gene of interest and a reference gene. Each run included five dilutions from the standard curve and a negative control (nuclease free water) for both the gene of interest and the reference gene. Four assays were run for each gene, each containing a different group of samples (paucibacillary, multibacillary, asymptomatic or control).

### 2.8.7 Normalisation of real-time data

The copy number of each gene of interest was normalised to allow for variation in the starting material and technical error. Copy numbers of reference genes were divided by the 75<sup>th</sup> percentile of the reference gene copy numbers and then the mean was calculated to give the normalisation coefficient. Each value for copy number of the gene of interest was then divided by the normalisation coefficient. The mean of the three values of copy number for each sample was given as the overall copy number for that sample. An example is given in Table 2.4.

Table 2.4: Example of normalisation, taking into account the 75<sup>th</sup> percentile

Sample	SDHA copy number	Normalisation coefficient	IL-10 copy number	Normalised IL-10 copy number
1	5	1.05	10	8.3
	6		7	
	4		9	
2	6	0.98	10	10.2
	4		11	
	4		9	
3	2	0.56	4	7.1
	3		3	
	3		5	

Samples with a normalisation coefficient of less than 0.45 or greater than 2.2 were excluded from the analysis, as this was outside the acceptable level of variation of the assay (see 2.8.5).

## 2.9 SNP analysis of CXCR4 and IGFBP-6

### 2.9.1 Overview

From the results of the real-time RT-PCR analysis the two candidate genes that demonstrated differential expression between paucibacillary and multibacillary samples - CXCR4 and IGFBP-6 - were chosen to be further studied using single nucleotide polymorphism (SNP) analysis. Briefly, primers were designed to amplify the coding regions of these genes. These regions were then cloned and sequenced in all

multibacillary, paucibacillary and asymptomatic samples, and compared to identify SNPs.

### 2.9.2 Genomic DNA extraction from tissues

Genomic DNA was extracted from ileum samples from all paucibacillary, multibacillary and asymptomatic sheep of interest using either the Qiagen DNEasy Blood and Tissue kit or the Qbiogene FastDNA kit according to manufacturer's instruction. Using the DNeasy Kit, 25mg of *RNAlater*<sup>TM</sup> treated ileum tissue was thawed and cut up into small pieces. The tissue placed in a salt buffer containing proteinase K and incubated at 56°C until the tissue was fully lysed. The samples were then RNase A treated and the pH adjusted using buffers supplied in the kit. This mixture was placed into a DNeasy mini spin column and spun to bind the DNA to the membrane. The column was washed twice and the DNA eluted into 200µl of AE buffer. Using the FastDNA kit, 25mg of *RNAlater*<sup>TM</sup> treated ileum tissue was placed in a tube containing garnet beads and a ¼ inch ceramic sphere, along with a specific tissue cell lysis buffer. This was homogenised in a FastPrep instrument until the tissue was fully lysed, and centrifuged to collect the cell debris. The supernatant was placed in a fresh tube with a DNA binding matrix. The sample was then spun again to pellet the binding matrix, and the supernatant removed. The binding matrix was washed and re-suspended in 100µl DES. The sample was again spun, and the supernatant containing the genomic DNA removed and placed in a fresh tube.

After extraction, all samples were quantified in the Nanodrop 1000 spectrometer (Nanodrop Technologies).

### 2.9.3 Primer design

Full length mRNA sequence was obtained for both genes, and aligned to bovine genomic sequence to identify the coding regions for both genes in

the genomic sequence. Primers were then designed as described in section 2.4.3 to amplify the whole coding region and the intron / exon boundaries where possible. The primers are given in Table 2.5 below.

#### **2.9.4 Cloning and sequencing of gene fragments**

Three PCR reactions using each set of primers were carried out on all paucibacillary, multibacillary and asymptomatic samples. The PCR products were mixed, purified, ligated, cloned into the PGEM-T easy vector as described in section 2.6 and sequenced as described in section 2.7. Three minipreps of each of the amplified fragments, giving three independent sequences, were produced for each sample.

#### **2.9.5 SNP analysis of sequences**

Three clones of each gene fragment were sequenced in the forward direction for each sample. All sequences were first checked to ensure that they contained the intended insert – those that did not were discarded. The three correct sequences were entered into VectorNTI AlignX software and aligned to produce a consensus sequence for each sample. The consensus sequences were then aligned. Differences between the genomic sequences were considered to be SNPs when the same change was found consistently in two or more of the consensus sequences.

Table 2.5: Primer sets used to sequence CXCR4 and IGFBP-6

Gene	Species	Accession Number	Primer Sequence	T <sub>m</sub> (°C)	Fragment size (bp)
CXCR4	Bovine	NM_174301.3	F1 - GAAACTTCAGTGTGTTGGCT	52.23	186
			R1 - CCACTCAGAGAGCGGTTG	53.78	
			F2 - ATTCCCTTGCCTGTTTTTCA	57.35	561
			R2 - GTACCTCTCATCCACCTCCCTTG	57.78	
			F3 - GTCTGGCTACCTGCTGTCCT	56.57	536
			R3 - GAATGTCCACCTCGCTTGC	58.50	
			F4 - CCCATCCTCTATGCTTCCT	58.17	398
			R4 - CGGTCTTACAATGACACACAGC	60.36	
			F5 - GAAATCTTCAAAGTTTTTCACTCCAG	55.5	593
			R5 - GCCAAAGGAATGCCAATAG	55.75	
IGFBP-6	Bovine	NM_001040495.1	F1 - CTGGGAAGGGAGGAGGTAGAG	59.47	456
			R1 - CGCAGTTGGGAGTGTAGACC	57.78	
			F2 - CTTGCGGCTGTAGGAGAGAATC	60.9	255
			R2 - CAGGACTGGGATGGGAGACTT	60.23	
			F3 - AAGTCTCCCATCCCAGTCCT	60.31	296
			R3 - GAAAGGCAGCGTCTCATTTA	60.35	
			F4 - GAGTCCCTTGCTGGTGTG	53.25	306
			R4 - GAACACAGAGACATAAACCCAGAG	53.53	

## 2.10 Microarray Analysis

### 2.10.1 Overview

Briefly, six RNA samples of each type were reverse-transcribed in the presence of amino allyl dUTP to produce amino allyl modified cDNA. A fluorescent dye was then chemically coupled to the modified cDNA. Two samples, labelled with either red (Cy5) or green (Cy3) fluorescent dyes, were then mixed and hybridised to a RIGUA Microarray slide in a competitive hybridisation assay. The slides were then scanned and the relative intensities of each dye calculated. This was then used to compare the relative concentrations of specific mRNA in each sample, and thus compare gene expression under different conditions.

### 2.10.2 cDNA generation

cDNA generation was carried out using the Fairplay III Microarray Labelling Kit (Stratagene) according to manufacturer's protocol. 10µg of total RNA was re-suspended in 12µl diethylpyrocarbonate (DEPC) treated water. 1µl of 500ng/µl oligonucleotide d(T)<sub>12-18</sub> primer was added to the RNA and the sample was incubated at 70°C for ten minutes and cooled on ice. 2µl of 10x AffinityScript RT buffer; 1µl of 20x dNTP mix; 1.5µl of 0.1M dithiothreitol (DTT); 0.5µl of RNase block and 3µl AffinityScript reverse transcriptase were then added to the sample. The sample was incubated at 42°C for 60 minutes. 10µl of 1M sodium hydroxide was added to hydrolyze the RNA and the mix heated to 70°C for 10 minutes. The sample was then cooled to room temperature and 10µl of 1M hydrochloric acid added to neutralize the reaction.

### 2.10.3 cDNA purification

cDNA was purified following the RT reaction to remove unincorporated nucleotides and hydrolyzed RNA, which may interfere with the cDNA labeling and hybridisation steps. 4µl of 3M sodium acetate; 1µl 20mg/ml

glycogen and 100µl of 95% ethanol were added to the sample. The samples were then placed at -20°C for up to two months.

After storage at -20°C, samples were placed in a centrifuge and spun at 13500xg for 15 minutes at 4°C. The supernatant was removed from the samples and the resultant pellet washed with 500µl ice-cold 70% ethanol. The samples were spun at 13500xg for 15 minutes at 4°C, the supernatant removed and the pellet dried.

#### **2.10.4 cDNA dye-coupling reaction**

Before the cDNA dye-coupling reaction, one vial of either Cy3 or Cy5 mono-reactive dye (GE Healthcare) was resuspended in 45µl of DMSO. The purified cDNA pellet was then re-suspended in 5µl of 2x coupling buffer (supplied with Fairplay III kit). To the resuspended cDNA 5µl of either Cy3 or Cy5 dye was added, and the sample incubated for 30 minutes in the dark at room temperature.

#### **2.10.5 Dye-coupled cDNA purification**

The DyeEx spin 2.0 kit (Qiagen) was used to remove unincorporated dye from the labelled cDNA according to the manufacturer's instructions. Briefly, a column containing hydrated gel-filtration resin was spun to remove excess liquid. The dye-coupling reactions were then placed onto the top of the column. The column was centrifuged at 2100rpm for three minutes. The eluate from the column containing the purified labelled cDNA was retained.

### 2.10.6 Analysis of fluorescence labelled cDNA

Labelled cDNA was analysed using a Nanodrop 1000 instrument. The absorbance spectrum at 240-800nm was collected and the concentration of dye in each sample calculated using the Beer-Lambert Equation (Absorbance = extinction co-efficient x path length x concentration) as follows:-

$$\text{Cy3 concentration} = A_{550} / (150000 \times \text{path length})$$

$$\text{Cy5 concentration} = A_{650} / (250000 \times \text{path length})$$

Concentrations were calculated by the Nanodrop 1000 software and expressed as pmol/ $\mu$ l of dye.

### 2.10.7 Pre-soak and pre-hybridisation of microarray slides

Pre-hybridisation treatment, hybridisation and post-hybridisation washes of the microarray slides were carried out using the Pronto!<sup>TM</sup> Universal Hybridisation Kit (Corning). Before commencing pre-hybridisation treatment, wash solutions were prepared using kit reagents as follows:-

Wash solution 1: 447.5ml of water  
50ml of wash reagent A  
2.5ml of wash reagent B

Wash solution 2: 1425ml of water  
75ml of wash reagent A

Wash solution 3: 300ml of wash solution 2  
1200ml of water

The slides were first placed in pre-heated (42°C) pre-soak solution containing a 1:100 dilution of liquid borohydride and incubated at 42°C for 20 minutes. They were washed twice for thirty seconds in wash solution 2, and then immersed in pre-heated (42°C) pre-hybridisation

solution for 15 minutes. The slides were then washed once in wash solution 2 for 60 seconds, twice in wash solution 3 for 30 seconds and once in nuclease-free water for 30 seconds. The slides were then dried by centrifugation at 1600 x g for two minutes.

### **2.10.8 Microarray hybridisation**

Prepared Microarray slides were placed in the hybridisation chambers of a Slidebooster™ hybridisation station (Implen). A coupling buffer (Advason™, Implen) was placed between the slide and the agitation chips on the slide booster to improve sample agitation, and a humidifying buffer (Advahum™, Implen) was pipetted into the wells in the slidebooster to prevent sample drying. A 22x22mm lifterslip (VWR) was then placed over the array and the slide pre-heated to 42°C.

Equal dye concentrations from two samples coupled with each dye were mixed and dried. The samples were re-suspended in 20µl cDNA hybridisation solution and incubated at 95°C for two minutes and then centrifuged at 13500 x g for two minutes. The samples were introduced to the array by pipetting the solution under one corner of the lifter slip and allowing the solution to spread over the array by capillary action. The hybridisation chamber was then closed and the slide incubated for 16-20 hours at 42°C with agitation every 7 seconds.

### **2.10.9 Post-hybridisation treatment**

After hybridisation, the slides were removed from the hybridisation chambers and the lifter slip removed by rinsing with pre-heated (42°C) wash solution 1. The slides were then immersed in wash solution 1 at 42°C for 5 minutes. They were removed from wash solution 1, placed into an Advawash™ (Implen) slide washing station and washed five times for two minutes in wash solution 2, and three times for 3 minutes in wash

solution 3. The slides were dried by centrifugation at 1600rpm for 2 minutes.

#### **2.10.10 Microarray slide scanning**

The slides were scanned in an Axon Autoloader 4200AL scanner (Molecular Devices), controlled by Genepix Pro software. A preliminary scan was done to automatically set the photo multiplier tube (PMT) gain, followed by a data scan at a resolution of 10nm. Images were saved as .tiff files.

#### **2.10.11 Bluefuse analysis of microarray results**

Images obtained in Genepix were loaded into Bluefuse™ software version 3.3 (BlueGnome Ltd). The Cy5 images were set to channel one (CH1), and the Cy3 images set to channel two (CH2). Bluefuse software was then used to align a GAL file with the image. The GAL file contains information on the position and identity of each spot on the array, and is used by Bluefuse to align a grid with the image. The image was then quantified. Integral to this program is the subtraction of background noise and the quantification of the intensity of each channel for each spot, producing ratios of the two channels. Each quantified spot was then examined visually for spots that were smeared or disrupted by dust particles. These were deemed invalid and were manually excluded from further analysis. Quality control checks were carried out on each array by examining heat plots of spot intensity, graphs of channel one amplitude versus channel two amplitude, average log intensity versus log ratio (MA plot) and box plots of inter array variation. Heat plots of spot intensity were quantified by calculating the correlation of the intensity of one spot and that of its four neighbours. This is expressed as an R value, where acceptable arrays have an R value of <0.4 (188).

### **2.10.12 Bioconductor normalisation of microarray data**

Data generated by Bluefuse was entered into Bioconductor, an open source statistical package using R programming language and limma (linear models for microarray data) packages. All Bioconductor-based analysis was carried out by Mrs Jill Sales (Senior Statistician, Bioinformatics and Statistics Scotland). Normalisation was carried out using a weighted print-tip Loess method. Briefly, microarray normalisation involves the assumption that there should be no difference in the expression of most genes, thus the expected MA plot is horizontal and centred on zero. Print tip loess fits a linear regression model to each subgrid on the array, and adjusts this to fit the expected curve. Spots were weighted by the confidence given in Bluefuse; in addition the blanks (unknown), buffer spots and Calf Thymus DNA were given a weight of zero and hence were ignored in the normalisation process. Manually excluded spots had been assigned a confidence of zero in the data files so these were also automatically ignored. Although spot weights were used in the normalisation, no spots were removed from the data set so normalised values were available for all spots, including those that had been assigned a weight of zero. To combine the data from all replicates, the software averaged the estimates over the sets. P values were calculated by a t-test, and adjusted to account for the false discovery rate, as described by Benjamini and Hochberg (25).

### **2.10.13 Data filtering**

The raw normalised data was filtered first by fold-change, discarding data with a fold-change of less than 1.5. The remaining data was then filtered by statistical significance, discarding data with an adjusted p value greater than 0.05. Next, data for the two independent oligos for each gene were compared, and where the trends for each oligo disagreed, the data was discarded. Finally, an average fold-change across of the

oligos for each gene was calculated, and a list of significantly different genes produced.

#### **2.10.14 Pathway Analysis**

The gene list generated as described in section 2.10.13 was first altered so all of the gene names were consistent with HUGO gene nomenclature committee names ([www.genenames.org](http://www.genenames.org)). The gene list was then entered into freely available bioinformatics software (<http://david.abcc.ncifcrf.gov/home.jsp>) and pathways of interest identified. These pathways were visualised using KEGG pathways (<http://www.genome.ad.jp/kegg/pathway.html>) and Biocarta pathways (<http://www.biocarta.com/index.asp>).

### **2.11 Real-time RT-PCR validation of microarray results**

#### **2.11.1 Reverse transcription of RNA into cDNA**

All RNA samples were diluted to a final concentration of 100µg/µl in nuclease free water. 5µl of each RNA sample was mixed with 11µl nuclease free water, 500ng of Oligo(dT) and 1µl of 100mM dNTPs (Promega) and incubated for 5 minutes at 70°C, followed by 5 minutes on ice. To this 5µl of 5x First Strand buffer, 1µl 0.1M DTT and 1µl of Superscript™ III RT enzyme (Invitrogen) were added, and the mixture was incubated at 50°C for 30 minutes, followed by 15 minutes at 70°C to inactivate the enzyme. This was done in triplicate for all RNA samples. GAPDH real-time RT-PCR was run on each sample to make sure that amplifiable material was present.

#### **2.11.2 Primer design and cloning**

Primers were designed and the fragments cloned as described in section 2.4.3. The primers are shown in Table 2.6 below.

### 2.11.3 Primer optimisation and generation of standard curves

Primers were optimised for annealing temperature and primer concentration using a standard curve generated from linearised pDNA as described in section 2.7. All serial dilutions were generated by the CAS-1200 automated PCR setup machine (Corbett Robotics). Standard curves used to determine the efficiency of the PCR assays were generated from serial dilutions of a pool of all cDNA samples. These standard curves were also used to determine the optimum cDNA concentration for the assays.

### 2.11.4 Selection of reference genes

Reference genes were selected using GeNorm software. Briefly, a panel of reference genes were assayed against all of the samples in real-time RT-PCR, and the results entered into the GeNorm software. A list of these genes and their primers are given in Table 2.7. The software determined which gene was the most stably expressed in the given sample set by taking account of the average pairwise variation. The two most stably expressed genes, SDHA and YWHAZ, were chosen to normalise the real-time RT-PCR assays.

### 2.11.5 Reaction mix and cycling conditions

All real-time PCR reactions were set-up by the CAS-1200 machine. 4µl of cDNA at the optimum dilution was added to a mix containing 5µl 2x FastStart SYBR Green Master mix (Roche) and 0.5µl of each primer at the optimum concentration and cycled as follows.

94°C	5 minutes	
94°C	20 seconds	} 45 cycles
60°C	20 seconds	
72°C	20 seconds	

Melt curve: 65°C rising to 94°C at 0.3°C per second

### **2.11.6 Real-time RT-PCR for genes of interest**

Each run assayed one gene of interest and contained all samples in duplicate, a cDNA standard curve and a non-template control. This was then repeated twice using a cDNA from the second and third RT reactions.

### **2.11.7 Normalisation of real-time PCR results**

The real-time data was normalised using QBase software (103). The software first calculated the average Ct value for each sample and then converted this into relative quantities, taking account of the efficiency of the reaction, using a pre-determined calibrator sample – for most comparisons this was one of the control samples. The reference genes were then used to calculate a normalisation factor as per Vandesompele *et al* 2002 (257). The relative quantities were then divided by the normalisation factor to give normalised relative quantities. A 2-sample t-test was then performed on each of the six comparisons.

Table 2.6: Accession numbers and primer sequences for microarray validation

Gene	Species	Accession Number	Primers	T <sub>m</sub> (°C)	Product size (bp)
MMP9	Bovine	X78324.1	F - GAGGGTAAGGTGCTGCTGTTC R - AAGATGTCGTGCGTGCTAATG	58.94 58.85	133
ICAM1	Ovine	NM_001009731.1	F - GCTGTGACCCCTCATCTTGG R - GGCGTGGATTTCAGTTTC	55.45 53.07	125
CD63	Bovine	BC151412.1	F - GGGCTGTGTGGAGAAAGATTG R - GATGAGGGGGCTGAAGAGAC	60.66 61.14	178
ITGB2	Ovine	NM_001009485.1	F - CTCACCGACAACCTCCAAAACA R - AAAAGTGGAACCCATCGTCTG	56.34 57.16	180
TYROBP	Ovine	AJ419228.1	F - GACCTGATGCTGACCCCTCC R - CTGTCTCCGTGATGTGCTGT	56.94 56.06	112
IGF2R	Ovine	AF353513.1	F - GACGACCTGAAGACCCCTGAA R - GCAAATGAAGCGGATGATG	60.24 60.17	150
MMP7	Bovine	NM_001075130.1	F - CAGCAAAAACACACCTTCATTTC R - GGAGAGACATAAAAACCAACCA	58.27 58.10	132
OXT	Ovine	NM_001009801.1	F - GCTGCCGAGAGGAGAACTAC R - GTGCTCCGATGGTGTCAAG	56.54 58.90	189
TLR2	Ovine	AM183218	F - GCACCTCAACCCCTCCCTTTTA R - TCTCCGAAAAGCACAAAGATG	58.73 56.15	125

Table 2.7: Accession numbers and primer sequences of reference genes

Gene	Species	Accession Number	Primers	T <sub>m</sub> (°C)	Product size (bp)
B2M	Ovine	AY549962.1	F - ACTCAAGACACCCGCCAGAA R - ACTCAGCGTGGACAGAAAGG	60.18 59.87	177
SDHA	Bovine	NM_174178.2	F - ACCTGATGCTTTGTGCTCTGC R - CCTGGATGGGCTTGGAGTAA	62.84 62.2	126
YWHAZ	Bovine	BC102382	F - TGTAGGAGCCCGTAGGTCATC R - TCTCTCTGTATTCTCGAGCCAT	59.15 55.99	101

## Chapter 3: Definition of pathological forms of paratuberculosis

### 3.1 Introduction

In sheep, MAP infection can give rise to three different forms of disease with only about 30% of animals in an infected flock becoming clinically affected. The majority of animals are asymptomatic; they are infected but show no pathology and do not develop clinical disease. The remaining clinically affected sheep show two distinct forms of the disease.

Approximately 30% of cases are affected by the paucibacillary form of paratuberculosis; they have very few bacteria and show a T cell infiltration into the gut. About 70% of cases have the multibacillary form, which is characterized by a high level of bacterial infection and a macrophage and B cell infiltration into the gut lamina propria. Both the pauci- and multibacillary forms are equally fatal but there is no evidence that the asymptomatic animals ever succumb to disease (52).

Paratuberculosis pathogenesis in cattle may differ from that in sheep as it is presumed that there is disease progression from the asymptomatic to paucibacillary and then to the fatal multibacillary form (230). In cattle, it is estimated that 4-11% of animals in an affected herd are infected, with 2-4% of animals in such herds going on to develop clinical disease (43,275). The paucibacillary cases tend to have a strong cell-mediated immunity (CMI), high levels of IFN $\gamma$  and IL-2 and low levels of antibody (6,35,36); the multibacillary cases have high antibody and pro-inflammatory cytokine levels and weak CMI (6,35). Little is known about the asymptomatic form in cattle although they are positive for bacterial growth, IS900 and specific antibody (41).

There have, as yet, been no studies giving a definitive description of the three forms of paratuberculosis in sheep. Several studies have described the difference between the paucibacillary and multibacillary forms (41,183,231), mainly in terms of gross pathology, but all of these studies ignored the presence of asymptomatic sheep. This short study aimed to

generate a definition of the three pathologies in both histopathological and molecular terms.

### 3.2 Definition of pathological forms

All animals from the Johne's disease infected flocks were identified as IS900 positive in the ileum by real-time RT-PCR analysis and therefore infected with MAP (Figure 3.1). The asymptomatic group were also IS900 positive in the mesenteric lymph node (MLN) confirming that the ileum IS900 positive results were not due to surface bacteria. Three groups of IS900+ animals could be discriminated on the basis of gross pathology, ZN staining and histopathology. The asymptomatic group had no clinical signs of paratuberculosis, on post-mortem showed no evidence of the presence of acid-fast bacteria (ZN-) and exhibited normal histology of the terminal ileum (Figures 3.2, 3.3, 3.4). All other sheep showed clinical signs of paratuberculosis and could be differentiated into two groups on the basis of ZN staining. The paucibacillary sheep had no detectable ZN+ bacteria (Figure 3.5) and showed a mixed inflammatory infiltrate into the lamina propria (Figure 3.6) comprising lymphocytes, eosinophils (Figure 3.7, small arrows) and multinucleate giant cells (Figure 3.7, large arrow) but few macrophages. The multibacillary sheep had high numbers of ZN+ acid-fast bacteria (Figure 3.8) associated with infiltrating sheets of epithelioid macrophages, which distend the lamina propria and flattened the surface mucosa (Figure 3.9 & 3.10). A fourth group of unrelated, control sheep was IS900 negative and therefore defined as uninfected with MAP. All of the multibacillary animals, 2/6 of the paucibacillary animals and none of the asymptomatic animals tested positive for MAP specific antibodies by antibody ELISA (Table 3.1). These results are summarised in Table 3.2. CMI responses were not analysed as they have been previously described in sheep (35) and the intention of the study was to quantify the expression of IFN $\gamma$  as part of the gene expression studies.

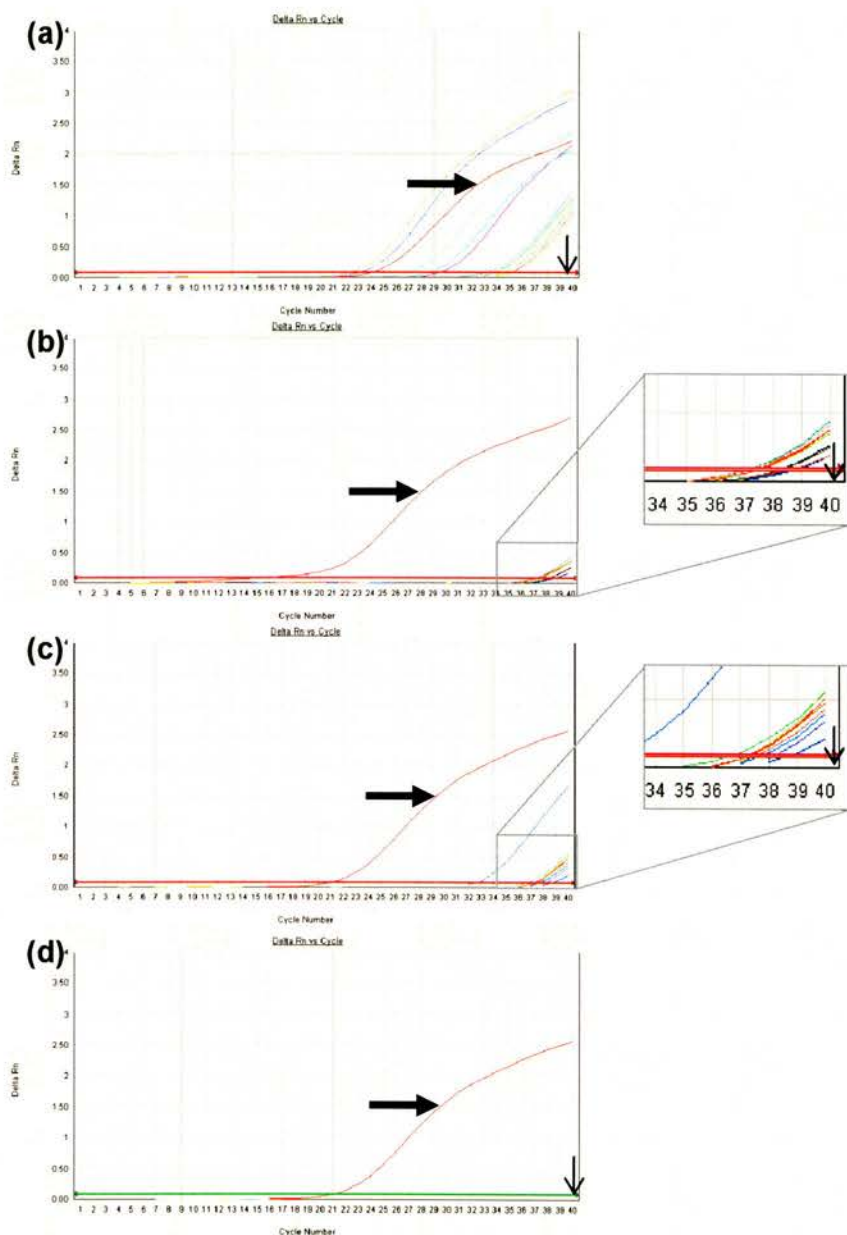


**Figure 3.1: Results of IS900 real-time RT-PCR** Graphs show fluorescence versus cycle number. Large arrows indicate positive control, small arrows indicate negative control. Each line represents one sample – a line curving upward and crossing the threshold value is considered positive. (a) depicts results for multibacillary samples, (b) depicts results for paucibacillary samples, (c) depicts results for asymptomatic samples and (d) depicts results for control sheep samples.

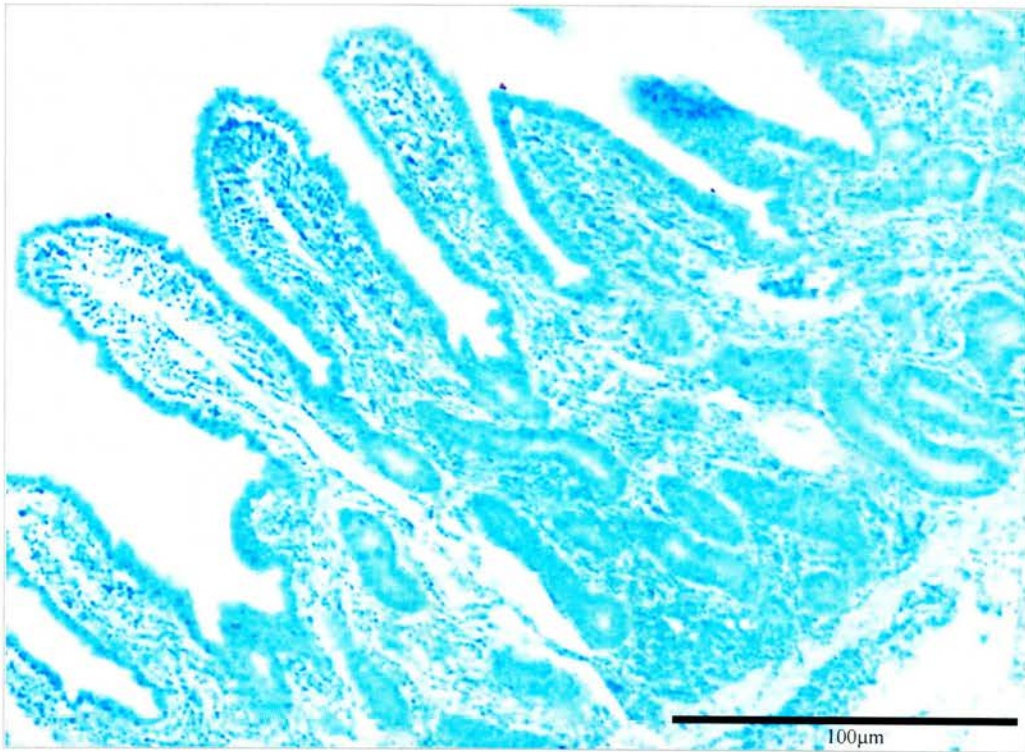


**Figure 3.2: Histopathology of the terminal ileum from asymptomatic sheep**  
Ziehl-Neelsen stain for acid-fast bacteria (x 250) showing the absence of mycobacteria.

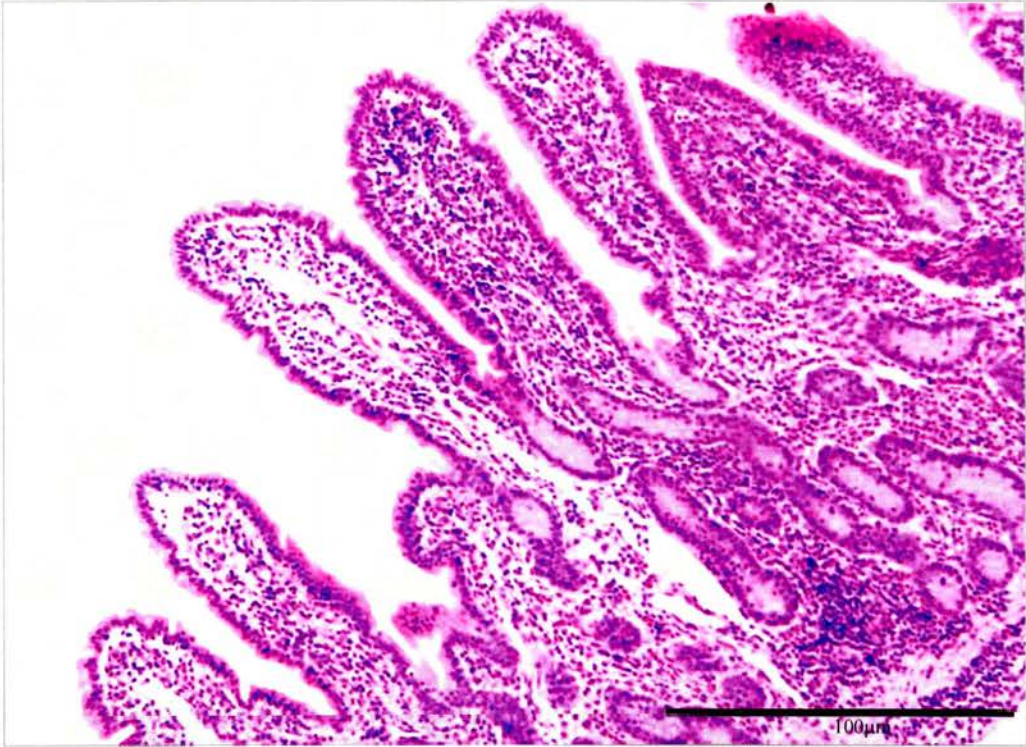


**Figure 3.3: Histopathology of the terminal ileum from asymptomatic sheep**  
H&E stained low power (250x) showing normal histology.

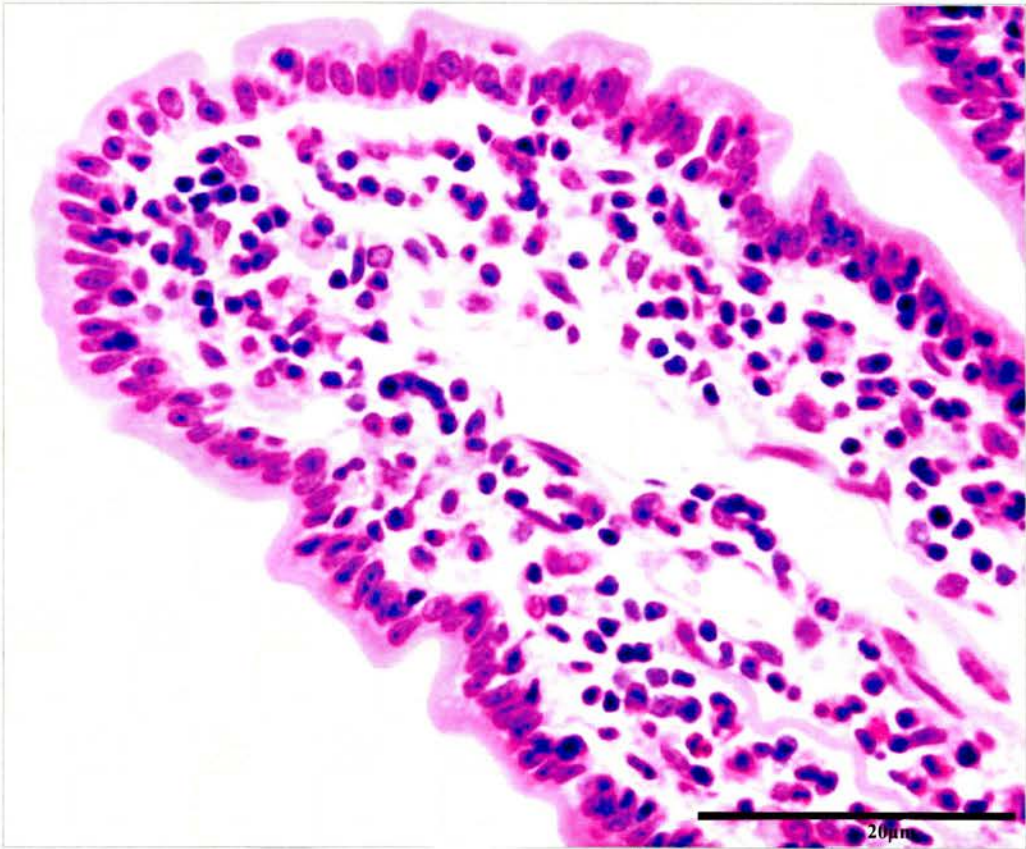


**Figure 3.4: Histopathology of the terminal ileum from asymptomatic sheep**  
H&E stained high power (x400) showing normal histology.

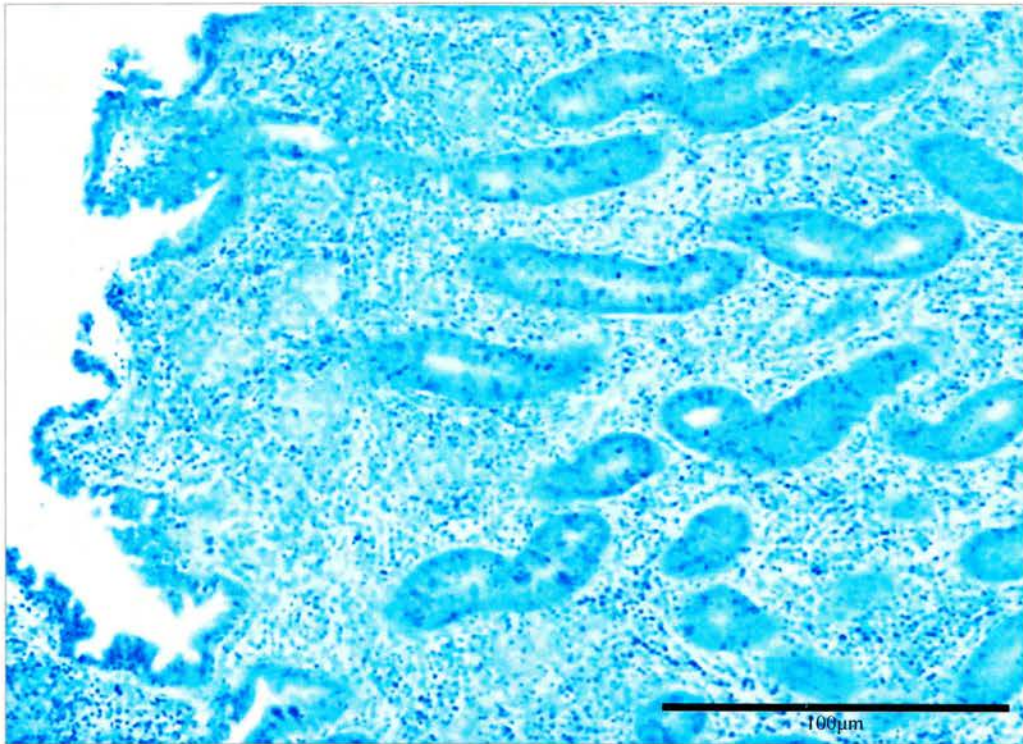


**Figure 3.5: Histopathology of the terminal ileum from paucibacillary sheep**  
Ziehl-Neelsen stain (x250) showing the absence of mycobacteria.

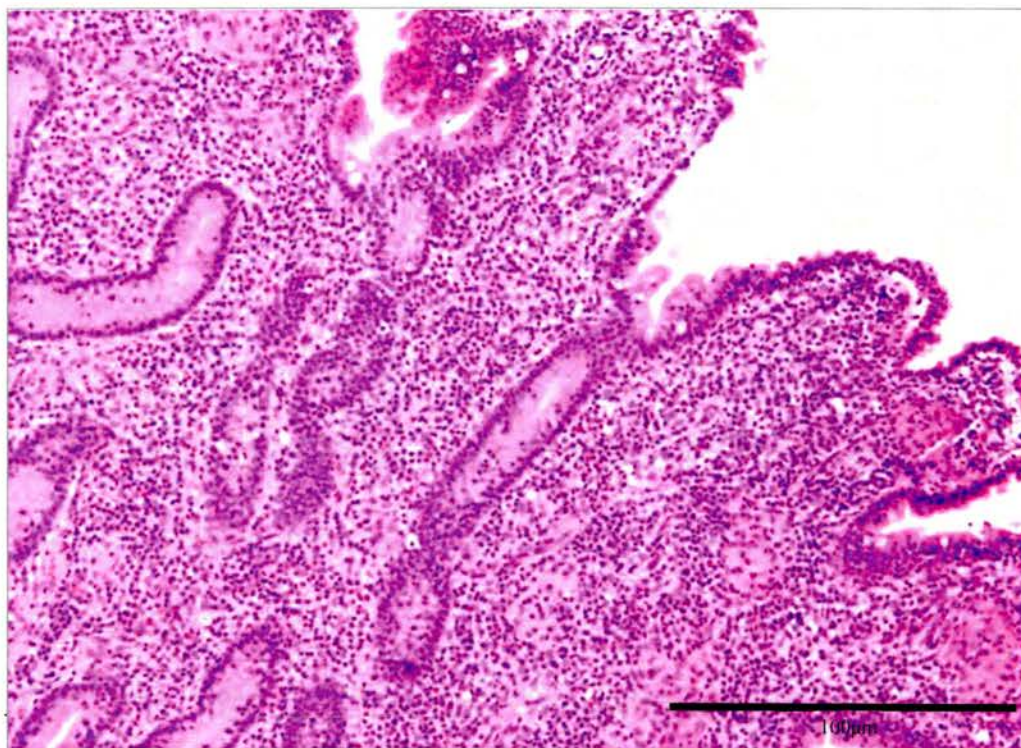


**Figure 3.6: Histopathology of the terminal ileum from paucibacillary sheep**  
H&E stained low power (x250) showing mixed inflammatory infiltrate into lamina propria comprising lymphocytes, eosinophils, macrophages and multinucleate giant cells.

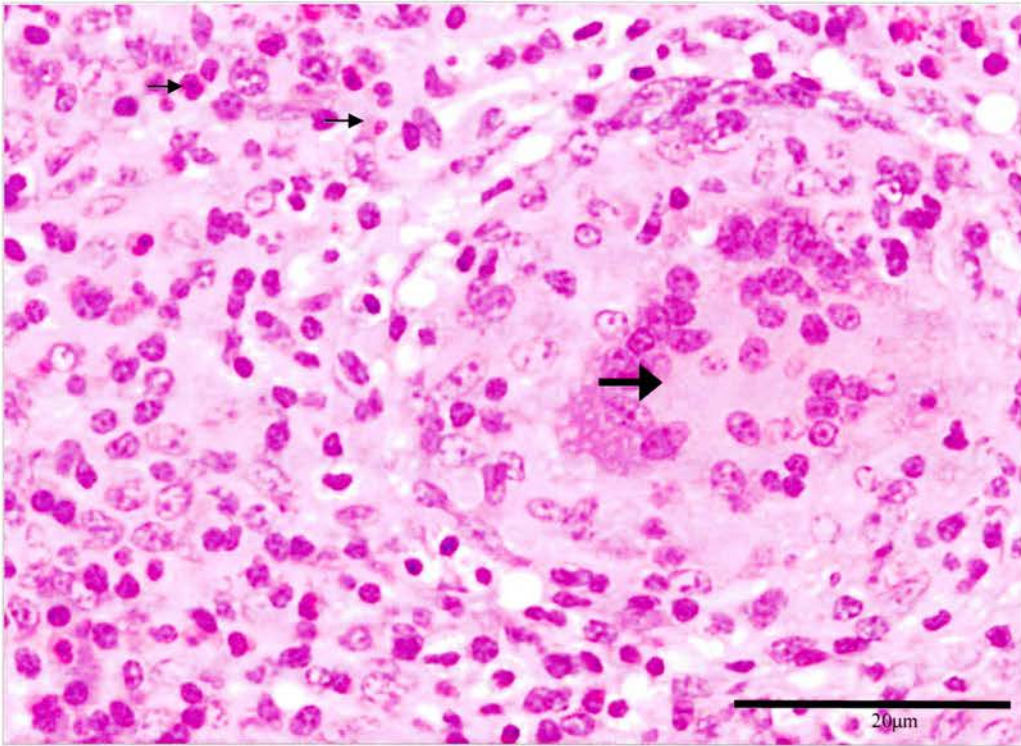


**Figure 3.7: Histopathology of the terminal ileum from paucibacillary sheep**

H&E stained high power (x400) showing multinucleate giant cells (large arrow). There is an associated proprial inflammatory reaction dominated by lymphocytes and eosinophils (small arrows).

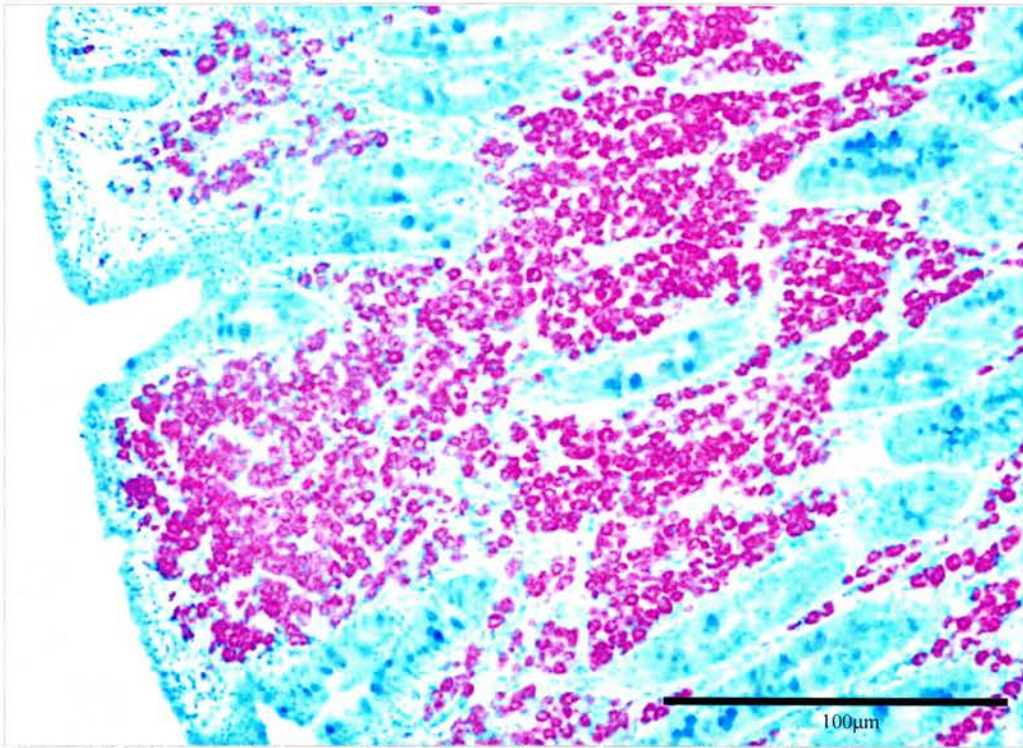


**Figure 3.8: Histopathology of the terminal ileum from multibacillary sheep**  
Ziehl-Neelsen stain (x 250) showing the presence of many intracellular mycobacteria associated with the infiltrating macrophages.

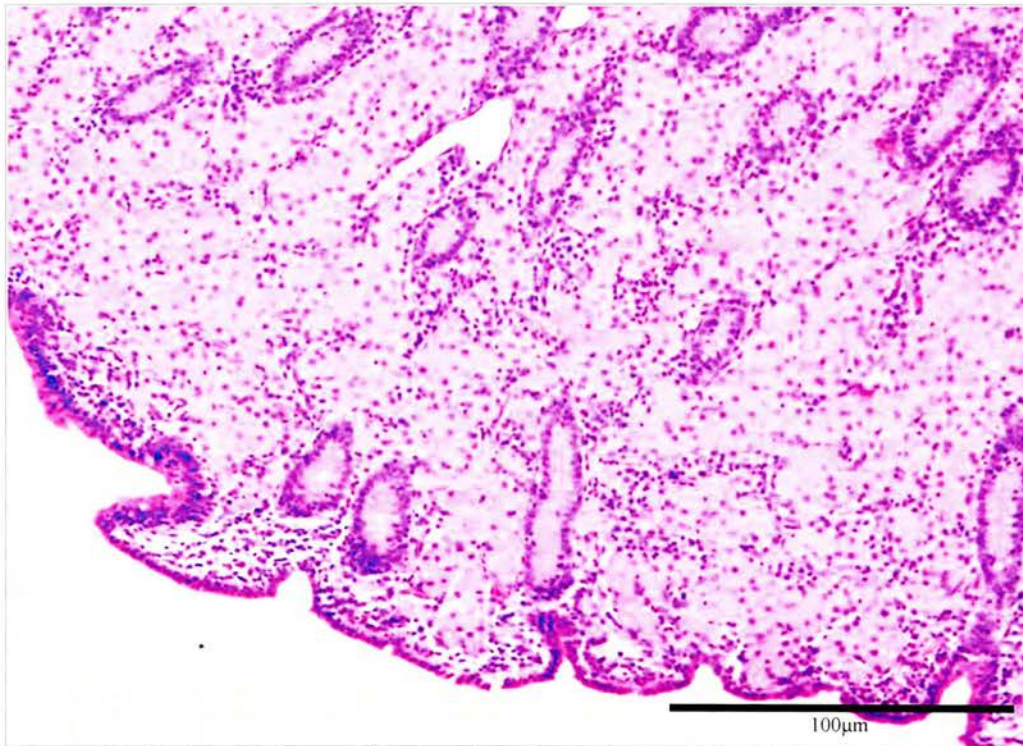


**Figure 3.9: Histopathology of the terminal ileum from multibacillary sheep**  
H&E stained low power (x250) showing infiltration of the lamina propria by sheets of epithelioid macrophages distending the propria and flattening the surface mucosa.

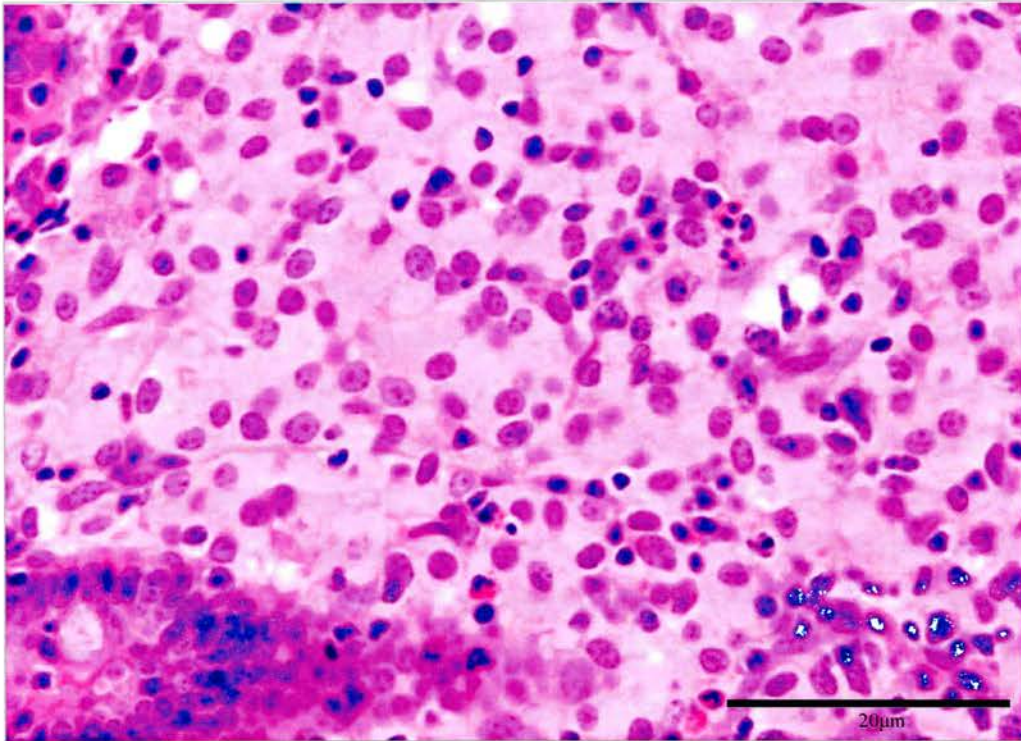


**Figure 3.10: Histopathology of the terminal ileum from multibacillary sheep**  
H&E stained high power (x400) demonstrating the uniform population of macrophages with abundant cytoplasm infiltrating around an intestinal crypt.

Table 3.1: PPD Elisa Results

Sample	Relative score
Positive Control	100
Negative control	0
4	111
6	33
7	3
8	25
10	147
32	56
11	89
12	114
13	138
14	152
16	109
18	165
30	120
20	2
21	3
22	3
23	2
24	8
25	10
26	2
34	43

Score of <60 is negative, >70 is positive

Table 3.2: Definition of pathological forms

Sample	MØ infiltrate in Ileum	Lymphocyte infiltrate in ileum	Antibody ELISA	IS900 real-time PCR on ileum	IS900 real-time PCR on MLN	Pathological form
3	-	+	ND*	+	ND	Paucibacillary
4	-	+	+	+	ND	Paucibacillary
5	-	+	ND	+	ND	Paucibacillary
6	-	+	-	+	ND	Paucibacillary
7	-	+	-	+	ND	Paucibacillary
8	-	+	-	+	ND	Paucibacillary
9	-	+	ND	+	ND	Paucibacillary
10	-	+	+	+	ND	Paucibacillary
32	-	+	-	+	ND	Paucibacillary
33	-	+	ND	+	ND	Paucibacillary
11	+	-	+	+	ND	Multibacillary
12	+	-	+	+	ND	Multibacillary
13	+	-	+	+	ND	Multibacillary
14	+	-	+	+	ND	Multibacillary
16	+	-	+	+	ND	Multibacillary
18	+	-	+	+	ND	Multibacillary
27	+	-	ND	+	ND	Multibacillary
28	+	-	ND	+	ND	Multibacillary
29	+	-	ND	+	ND	Multibacillary
30	+	-	+	+	ND	Multibacillary
19	-	-	ND	+	+	Asymptomatic
20	-	-	-	+	+	Asymptomatic
21	-	-	-	+	+	Asymptomatic
22	-	-	-	+	+	Asymptomatic
23	-	-	-	+	+	Asymptomatic
24	-	-	-	+	+	Asymptomatic
25	-	-	-	+	+	Asymptomatic
26	-	-	-	+	+	Asymptomatic
31	-	-	ND	+	+	Asymptomatic
34	-	-	-	+	+	Asymptomatic
35	ND	ND	ND	-	ND	Control
36	ND	ND	ND	-	ND	Control
37	ND	ND	ND	-	ND	Control
38	ND	ND	ND	-	ND	Control
39	ND	ND	ND	-	ND	Control
40	ND	ND	ND	-	ND	Control
41	ND	ND	ND	-	ND	Control
42	ND	ND	ND	-	ND	Control
43	ND	ND	ND	-	ND	Control

\*ND = not done

### 3.3 Discussion

The three major mycobacterial diseases of mammals - tuberculosis, leprosy and paratuberculosis affect different organ systems but share at least two important characteristics. Firstly, not all infected individuals become clinically affected and second, there are at least two pathological forms of each disease (89,173). In human leprosy, the tuberculoid form of the disease has lesions formed of infiltrating T cells and containing few bacteria; and the lepromatous form has lesions of infiltrating macrophages containing large numbers of bacteria (164). The pathological picture of ruminant paratuberculosis seems to mimic human leprosy (55) mainly in sheep where the pathology can be unambiguously differentiated into tuberculoid (paucibacillary), lepromatous (multibacillary) and asymptomatic (infected but no pathology) (53). There are also differences between ovine and bovine paratuberculosis, as in cattle the pathological form is thought to be related to the disease development (55,230), with early stage tuberculoid lesions developing into end-stage lepromatous disease. In addition, intermediate stages between these two extremes have also been reported (90,136).

This study has shown that the three pathological forms can be defined unambiguously by both histopathological and molecular means. Unlike cattle, where asymptomatic animals are regarded as 'preclinical' and show histological lesions (242), asymptomatic sheep show normal ileal histology and do not succumb to disease (52). The asymptomatic sheep in this study were shown to be infected by detection of IS900 by real-time RT-PCR of both ileum and mesenteric lymph node tissues, proving that these animals are infected with MAP. This result also allows asymptomatic animals to be easily differentiated from uninfected controls, which tested negative for IS900 in the ileum. MLN tissues from control animals were not available and thus were not tested for IS900.

Chapter 4: Differential cytokine gene expression

#### 4.1 Introduction

This study examined the expression of mRNA for thirteen candidate genes involved in the polarisation of the immune response. Of these, one (IL-3) was chosen from a preliminary microarray study carried out by other members of the research group (191). The remaining twelve genes – IL-1 $\alpha$ , IL-1 $\beta$ , IL-6, IL-8, IL-10, IL-12p40, IL-18, GM-CSF, IFN $\gamma$ , TGF $\beta$ , TNF $\alpha$  and TRAF-1 - were chosen from published sources. Several studies in cattle have shown up-regulation of IL-8, IL-10, IL-12, GM-CSF, IFN- $\gamma$ , TGF $\beta$ , TRAF-1, IL-1 $\alpha$ , IL-1 $\beta$ , IL-6 and TNF $\alpha$  and down-regulation of IL-18 in response to MAP infection (3,59,63,128,138,139,242,265,266). Although little research has been done into gene expression in sheep in response to MAP infection, studies using cytokine release assays and semi-quantitative RT-PCR have shown that multibacillary sheep have increased expression of TNF $\alpha$ , IL-1 $\beta$  and IL-6 and paucibacillary sheep have increased expression of TNF $\alpha$ , IFN- $\gamma$  and IL-2 during clinical infection (6,36).

The T cells response in ovine paratuberculosis is central to control of infection.  $\gamma\delta$  T cells are increased early at the site of infection (21,23,144), and CD4 $^{+}$  and CD8 $^{+}$  cells are increased later in infection (144,186). The T cell response later in infection is polarised, and leads to the observed differences in pathology. In paucibacillary lesions, IL-2 and IFN $\gamma$  are increased, leading to activation of macrophages and Th1 cells (36,144). Conversely, IFN $\gamma$  and TNF $\alpha$  are decreased in multibacillary lesions, leading to lower macrophage activation and an increase in Th2 responses (36,144). T regulatory cells (Tregs) have a CD4 $^{+}$ CD25 $^{+}$ FoxP3 $^{+}$  phenotype, and are capable of inducing anergy to self and foreign antigens and preventing migration of immune cells to the site of infection by the production of Th2 cytokines including IL-10 (273).

The aim of this study was therefore to quantify cytokine gene expression in the three pathologies of ovine paratuberculosis to gain insight into the type 1 / type 2 immune responses present.

#### **4.2 RNA extraction from ileum**

RNA was successfully extracted from thirty-nine samples in total – ten paucibacillary, ten multibacillary, ten asymptomatic and nine controls. The concentration of RNA and RNA integrity number (RIN) for each sample are given in Table 4.1. Samples without RIN numbers were analysed on an earlier version of the Agilent software, which did not assign a RIN number to the samples.

#### **4.3 Sequences of cloned PCR products**

Clones of PCR products were sequenced in one direction using T7 primer. The sequences of the clones and the percentage alignment with the expected sequence are given in Appendix 2.

#### **4.4 Gene expression analysis in ileal tissues**

##### **4.4.1 Generation of standard curves**

Standard curves were generated from linearised plasmid DNA for all candidate genes. Standard curves with an efficiency between 0.9 and 1.1, an M value (a measure of the gradient of the slope) of around -3.3 and R<sup>2</sup> values (a measure of how well the standards fit onto a curve) of as close to 1 as possible were acceptable. Figure 4.1b shows an acceptable standard curve, with values close to ideal. Sample cDNA is arrowed. Figure 4.1d shows an unacceptable standard curve. Standard curves with values like these were rejected, plasmid DNA samples replaced and the reactions repeated.

Table 4.1: RNA concentration and RIN

Sample	Type	RNA Concentration ( $\mu\text{g/ml}$ )	RIN
3	Pauci	888	8.9
4	Pauci	985.6	8.5
5	Pauci	998.4	9.1
6	Pauci	1032.8	9
7	Pauci	324	8
8	Pauci	458.4	9.7
9	Pauci	671.2	9.5
10	Pauci	730.4	6.8
32	Pauci	224	ND*
33	Pauci	496	ND
11	Multi	698.4	8.9
12	Multi	460	8.6
13	Multi	1072	7.3
14	Multi	1249	9.1
16	Multi	1035.2	8.6
17	Multi	1500.8	8.2
27	Multi	904	9.6
28	Multi	1216	8.6
29	Multi	456	ND
30	Multi	408	ND
19	Asymp	515.2	8
20	Asymp	265	9
21	Asymp	260.8	6
22	Asymp	730.4	8.2
23	Asymp	918.4	9
24	Asymp	928	8.4
25	Asymp	528	8.5
26	Asymp	872	8.9
31	Asymp	392	ND
34	Asymp	496	ND
35	Control	826	ND
36	Control	804	ND
37	Control	763.2	ND
38	Control	771.2	ND
39	Control	632	ND
40	Control	660.8	ND
41	Control	621.6	ND
42	Control	491.2	ND
43	Control	520.8	ND

\*ND = not done

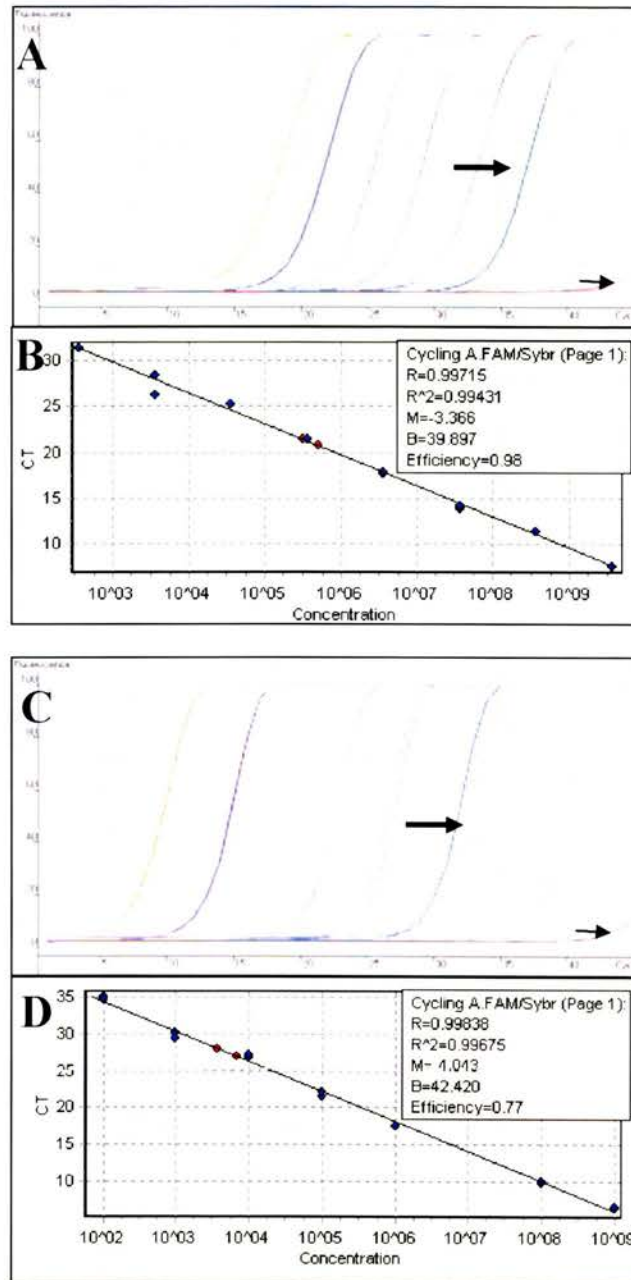


**Figure 4.1: Generation of linearised plasmid DNA standard curves for real-time PCR**

(a) Fluorescence versus cycle graph for a standard curve - spacing is even between plasmid dilutions. Large arrow indicates cDNA control, small arrow indicates no template control (NTC). (b) Standard curve taken from (a). All values are close to ideal, and points sit well on the line. (c) Fluorescence versus time graph for an unacceptable standard curve – uneven spacing between plasmid dilutions. Large arrow indicates cDNA control, small arrow indicates NTC. (d) Standard curves taken from (c). The efficiency is unacceptably low.

#### 4.4.2 Real-time RT-PCR analysis of mRNA expression

The expression levels of the thirteen candidate genes are shown in Table 4.2, which lists normalised mean copy numbers of each gene in the three disease types and controls. From these data it can be seen that the genes were expressed at very different levels, varying from less than 100 copies (e.g. IL-1 $\alpha$ , IL-3) to greater than 1x10<sup>6</sup> copies (e.g. IL-8). There was also a great deal of variation in the expression levels between the four types of samples, as reflected in the large standard deviations. The variation is due to the experimental animals being outbred, from different farms and of different ages.

The differences in gene expression can be seen more clearly in Figures 4.2 and 4.3. These graphs show statistically significant ( $p \leq 0.05$ ) fold-changes in the six comparisons. Fold-changes less than 2.2 but statistically significant are included in the comparisons (Section 2.8.5). Two genes - IL-1 $\alpha$  and GM-CSF - did not exceed 2.2 fold-change in any statistically significant comparison.

Figure 4.2 shows the comparison of the transcript levels between the infected groups and the uninfected control group. IL-1 $\alpha$ , IL-8, IL-12p40, GM-CSF, IFN $\gamma$ , TGF $\beta$ , TNF $\alpha$  and TRAF-1 were significantly up-regulated, and IL-18 was significantly down-regulated in paucibacillary samples. IL-8, IFN $\gamma$ , TGF $\beta$ , TNF $\alpha$  and TRAF-1 were significantly up-regulated in multibacillary samples. Interestingly, TNF $\alpha$  was significantly up-regulated and IL-18 significantly down-regulated in asymptomatic samples. IL-3 was detected at low levels in all infected animals but never in uninfected control samples; therefore it was not possible to produce fold-change figures for these comparisons. Nevertheless, IL-3 was statistically significantly up-regulated ( $p \leq 0.05$ ) in both multibacillary and asymptomatic samples (but not paucibacillary

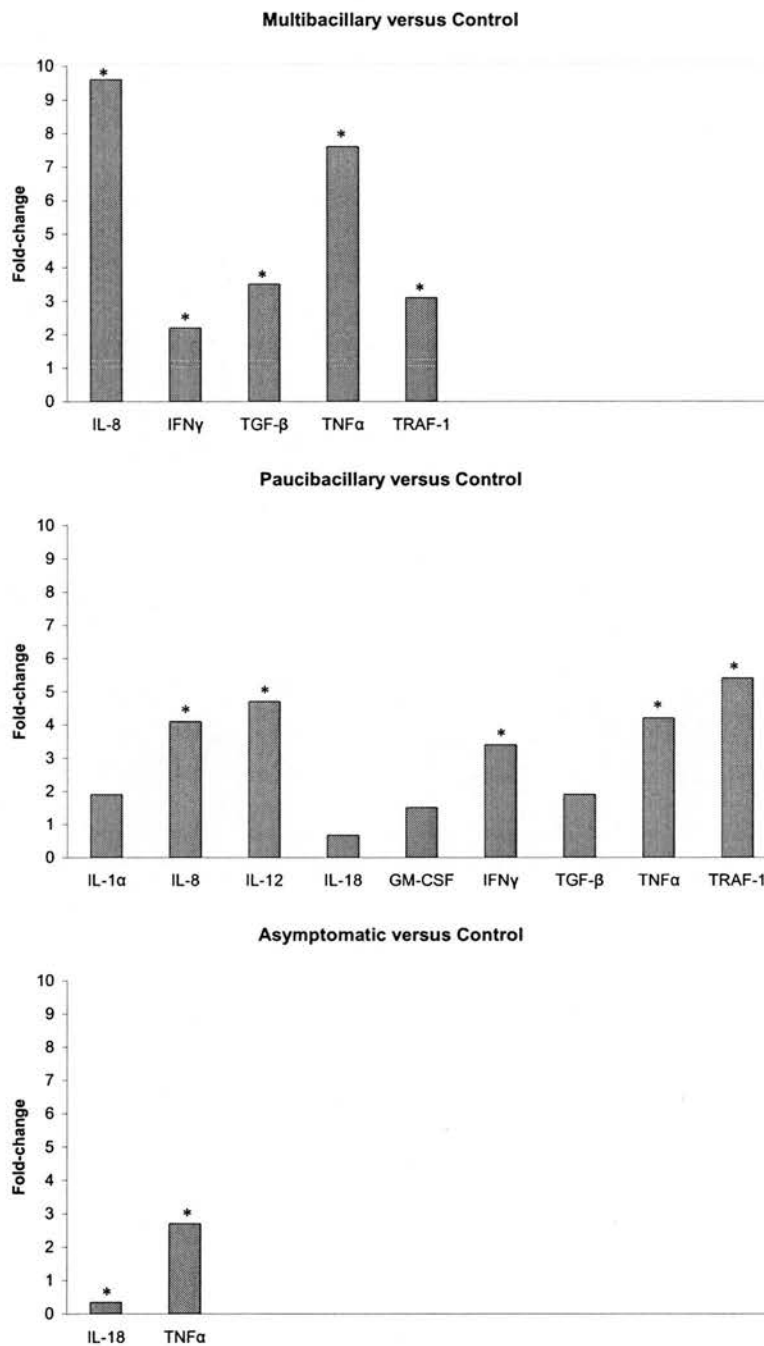
sheep) compared to controls using the non-parametric Mann-Whitney test.

Figure 4.3 shows the comparisons between the three infected groups of sheep. When the clinically diseased groups were compared to the asymptomatic group, IL-10, IL-18, TGF $\beta$ , TNF $\alpha$  and TRAF-1 were up-regulated in multibacillary animals and IL-1 $\beta$ , IL-6, IL-18, GM-CSF, IFN $\gamma$  and TRAF-1 were up-regulated in paucibacillary animals. IL-10 was down-regulated in paucibacillary samples compared to multibacillary samples.

Table 4.2: Copy numbers of all genes of interest in all groups normalised to reference gene expression.

	Multibacillary	Paucibacillary	Asymptomatic	Control
IL-1 $\alpha$	69 ± 56	<b>38</b> ± 14	51 ± 42	20 ± 8
IL-1 $\beta$	30,839 ± 41,353	16,470 ± 8559	4176 ± 2557	8613 ± 6090
IL-3	<b>29</b> ± 74	1 ± 3	87 ± 131	0 ± 0
IL-6	71,778 ± 124,310	11,023 ± 2980	4996 ± 1698	5473 ± 7583
IL-8	<b>1,448,098</b> ± 1,453,346	<b>609,805</b> ± 511,880	480,573 ± 601,312	150,388 ± 59,472
IL-10	305,964 ± 127,868	174,186 ± 82,536	126,941 ± 94,659	240,619 ± 185,599
IL-12p40	7178 ± 7381	<b>7589</b> ± 6467	4506 ± 5179	1615 ± 2436
IL-18	102,838 ± 45,161	<b>84,037</b> ± 34,888	<b>42,352</b> ± 10,066	126,047 ± 41,771
GM-CSF	2512 ± 1067	<b>2973</b> ± 963	1786 ± 684	1986 ± 552
IFN $\gamma$	<b>3354</b> ± 1063	<b>5209</b> ± 2554	2529 ± 1620	1537 ± 427
TGF $\beta$	<b>50,349</b> ± 30,161	<b>28,007</b> ± 13,809	21,871 ± 11,222	14,519 ± 6032
TNF $\alpha$	<b>21,113</b> ± 13,334	<b>11,681</b> ± 7914	<b>7492</b> ± 4925	2770 ± 2120
TRAF-1	<b>11,504</b> ± 6076	<b>20,087</b> ± 10,563	5018 ± 5134	3708 ± 1662

Bold denotes statistical significance ( $p \leq 0.05$ ) compared to uninfected control animals. Figures are shown  $\pm$  standard deviation.



**Figure 4.2: Statistically significant fold-changes in genes in infected animals compared to uninfected control groups** Results are given as fold-changes of mean copy-numbers relative to the mean copy-numbers of the uninfected control group and  $p \leq 0.05$ . IL-3 was not included, as the copy-number in the control samples was 0, thus fold change values could not be calculated. (\*) indicates fold-changes greater than 2.2.

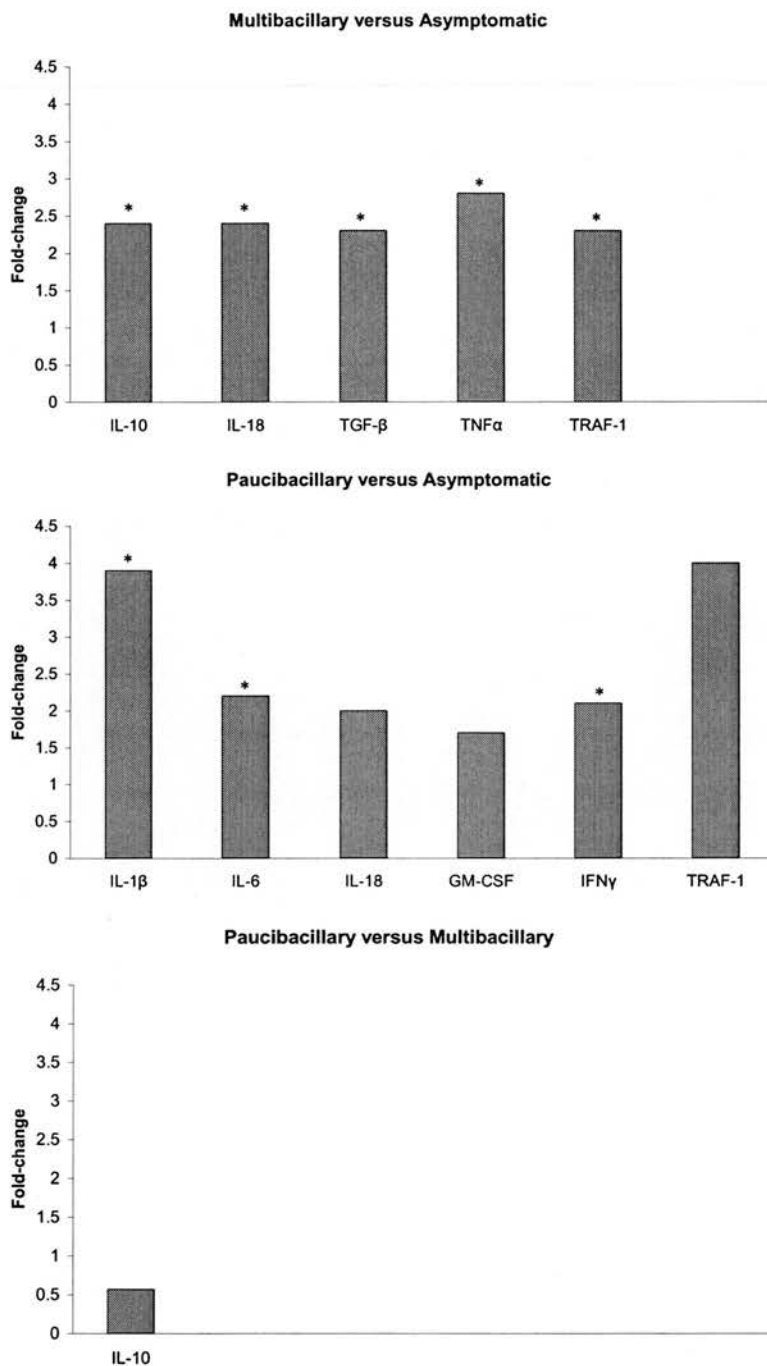


**Figure 4.3: Statistically significant fold-changes in genes in the three infected groups**  
Results are given as fold-changes of mean copy-numbers of infected groups relative to the mean copy-numbers of each other group and  $p \leq 0.05$ . (\*) indicates fold-changes greater than 2.2.

#### 4.5 Discussion

Despite the fact that there is a large variation in the levels of cytokine transcript expression, this study showed unambiguously that there is a relationship between the three pathological forms of sheep paratuberculosis and the immune response as represented by the cytokine transcript profiles within the target tissue. The large variation is probably due to the fact that these sheep are unrelated, of different breeds and are infected naturally rather than experimentally; in addition they carry a variable gastrointestinal worm burden (see section 2.1.1) that might influence ileal cytokine expression. We cannot measure levels of functional protein for all the cytokines within the ileum but assume that the relative quantities of cytokine protein and transcript are linked.

As has been shown with bovine paratuberculosis (63,138,242), the paucibacillary and multibacillary forms of the sheep disease are also associated with the polarization of the immune response. The comparison of each form of the disease with tissue from asymptomatic animals shows that IFN $\gamma$  is significantly increased in the paucibacillary lesions and IL-10 is raised in the multibacillary form, although only IL-10 is significantly different when the two clinical forms are directly compared. This confirms that in sheep paratuberculosis polarised Th1 and Th2 cells are associated with paucibacillary and multibacillary pathology respectively. However, the polarisation is incomplete. The major biological function of IL-18 seems to be linked to inducing type 1 responses and stimulating IFN $\gamma$  production (70). However, the pattern of IL-18 expression is up-regulated in both disease forms compared to asymptomatic samples. Similarly, both the paucibacillary and multibacillary groups displayed up-regulation of TGF $\beta$ , a regulatory cytokine with known anti-inflammatory and immunosuppressive functions in inflammatory bowel diseases (22). This up-regulation may explain why, unlike in other gastrointestinal inflammatory lesions (77),

the expression of large quantities of pro-inflammatory cytokines in paratuberculosis is not reflected in the large scale infiltration of neutrophils.

In addition, up-regulation of IL-8, TRAF-1, and TNF $\alpha$  was observed when both types of clinically diseased samples were compared to uninfected controls, reflecting the high levels of inflammation present in these samples. IL-1 $\alpha$  and IL-12 were also up-regulated in these samples, but the difference was not significant in multibacillary animals ( $p=0.081$  and  $0.06$ , respectively), again reflecting high levels of inflammation. The IL-12 result contradicts previous studies in bovine ileum tissues and stimulated PBMCs from infected cattle, that have shown down-regulation of IL-12 in infected cattle compared to controls (63,242). This may be due to differences in tissue source or in species specific host responses.

IL-18 and IL-6 were significantly up-regulated in paucibacillary samples compared to asymptomatic samples, and hugely up-regulated in multibacillary samples compared to asymptomatic samples, although this was not statistically significant ( $p=0.133$  and  $0.167$ , respectively). These genes have both previously been associated with multibacillary disease (6) and again probably indicate high levels of inflammation. The expression of IL-6 has long been known to be associated with parasitic worm infections (245). As the sheep in this study were kept outside and mixed with other sheep, many of them had parasitic infections, which may have contributed to the high levels of variation in expression levels.

GM-CSF, a cytokine produced by Th1 cells involved in production and activation of granulocytes and macrophages, was up-regulated in paucibacillary samples, leading to further polarisation of the response toward a Th1 profile.

Of particular interest was the comparison between the infected, asymptomatic and the uninfected, control sheep. Asymptomatic sheep show completely normal ileal histology and do not succumb to disease (52). This normality is largely confirmed by the fact that the majority of cytokines are expressed at 'normal' levels; however TNF $\alpha$  and IL-18 are exceptions - IL-18 was down-regulated and TNF $\alpha$  was up-regulated in asymptomatic sheep compared to controls. Up-regulation of proinflammatory cytokines such as TNF $\alpha$  would be expected to lead to an inflammatory response. However, these sheep have little or no inflammation in the gut, suggesting that this response is being well controlled. The down-regulation of IL-18 also suggests that a regulatory, anti-inflammatory response is dominating in these sheep.

IL-3 was detected at low levels in all infected samples but not in the uninfected controls. In tuberculosis in human cells, IL-3 is associated with the formation of granulomata containing multinucleated giant cells, and IL-3 treatment of infected cell cultures dramatically reduces the number of infectious bacteria present. IL-3 treatment also prevents cell-cell spread of the bacteria (38), and can enhance the survival of dendritic cells involved in Th2 cell differentiation (79,195,250). However, the extremely low level of detection of this cytokine leaves doubts as to its biological significance in the ileum of MAP infected sheep.

Although this study represents a robust and replicable quantification of cytokines involved in paratuberculosis pathologies, the method does have several drawbacks. Using pDNA for the standard curves, as is required for absolute quantification, may not be an accurate measure of the gene in a cDNA sample. The pDNA is not reverse transcribed, and thus cannot reflect or control for variation introduced during this step. Secondly, it cannot exactly reflect the behaviour of the cDNA samples during the assay, as it is a purer sample and does not contain DNA of any other

sequence which could interfere with the assay, unlike cDNA samples. Also, the presence and amount of cDNA quantified for a gene may not directly relate to the presence and quantity of that particular protein in a cell.

Chapter 5: Differential expression and SNP  
analysis of non-cytokine genes

### 5.1 Introduction

In addition to the cytokine genes described in Chapter 4, the expression of a further selection of relevant immune genes was quantified. Several genes – CD34, CXCR4, IGFBP-2 and IGFBP-6 - were again chosen from previous microarray data (191) on the basis of differential expression in multibacillary and paucibacillary animals. CXCR4 is known to be associated with type 2 immune responses, and CD34 is a marker for haematopoietic stem cells. Little is known about the role of IGFbps in pathogenesis, although they are known to control the actions of IGFs, leading to a reduction in proliferation. TIRAP and TRAM were chosen from published sources in order to further understand the role of TLR signalling in paratuberculosis (166). Only IGFBP-6 had been previously quantified in sheep paratuberculosis (62).

Of these additional genes, two were selected for SNP analysis based on their expression profiles – IGFBP-6 and CXCR4. Both of these genes were differentially expressed in paucibacillary animals compared to multibacillary animals, with CXCR4 being down-regulated and IGFBP-6 being up-regulated. SNPs are defined as single base pair positions in genomic DNA at which different sequence alleles exist in normal individuals in some populations, wherein the least frequent allele has an abundance of 1% or greater (33). SNPs account for much of the genetic variation between individuals in a population and if found within the coding region of a gene can lead to differences in the amino acid sequence coded for and thus can change the protein structure of the product of the gene. If found within the upstream promoter regions of a gene they can affect regulation of gene expression. They can also be used as markers for particular genetic traits (33). The aim of this study was to analyse the sequence of the coding regions of the IGFBP-6 and CXCR4 genes to look for disease specific SNPs, which could go some way towards explaining

the differences in gene expression between sheep with different forms of paratuberculosis.

The role of these two genes in clinical paratuberculosis is very unclear. CXCR4 is a receptor for CXCL12 and is expressed on the cell surface of all B cells, monocytes, natural killer cells and most T cells (31,121,160,190,194) and IGFBP-6 has been well known for some time as a regulator of IGF-II (13), a growth factor involved in cell proliferation.

## **5.2 Real-time RT-PCR analysis of gene expression**

RNA was extracted and PCR products cloned and sequenced and standard curves generated as described in Chapter 4. The expression levels of the six candidate genes are shown in Table 5.1, which lists mean copy numbers of each gene in the three disease types and controls normalised to SDHA expression. From these data it can be seen that the genes were expressed at very different levels, varying from less than 300 copies (e.g. IGFBP2, IGFBP6) to greater than 30000 copies (e.g. CXCR4). There was also a great deal of variation in the expression levels between the four types of samples.

The differences in gene expression can be seen more clearly in Figures 5.1 and 5.2. The high degree of variation in gene expression was due to the nature of the samples used – the sheep were out bred and from different farms, thus the external influences on these sheep varied greatly. These graphs show statistically significant ( $p \leq 0.05$ ) fold-changes in the six comparisons. Fold-changes less than 2.2 but statistically significant are included in the comparisons (Section 2.8.5). IGFBP-2 expression was not significantly different in any comparison, and in two genes – CD34 and TRAM – the fold-change did not exceed 2.2 for any comparison.

Table 5.1: Copy numbers of all genes of interest in all groups normalised to reference gene expression.

	<b>Multibacillary</b>	<b>Paucibacillary</b>	<b>Asymptomatic</b>	<b>Control</b>
CD34	<b>1901</b> ± 1017	2622 ± 1525	<b>1937</b> ± 1086	3568 ± 1097
CXCR4	26,980 ± 15,227	<b>12,702</b> ± 6646	<b>4401</b> ± 2153	31,495 ± 21,406
IGFBP-2	778 ± 578	485 ± 420	354 ± 237	271 ± 61
IGFBP-6	259 ± 106	<b>657</b> ± 303	354 ± 127	269 ± 117
TIRAP	<b>2863</b> ± 1244	<b>3905</b> ± 2115	8281 ± 2921	6263 ± 1716
TRAM	<b>329</b> ± 115	466 ± 159	<b>317</b> ± 108	584 ± 180

Bold denotes statistical significance compared to uninfected control animals. Figures are shown ± standard deviation

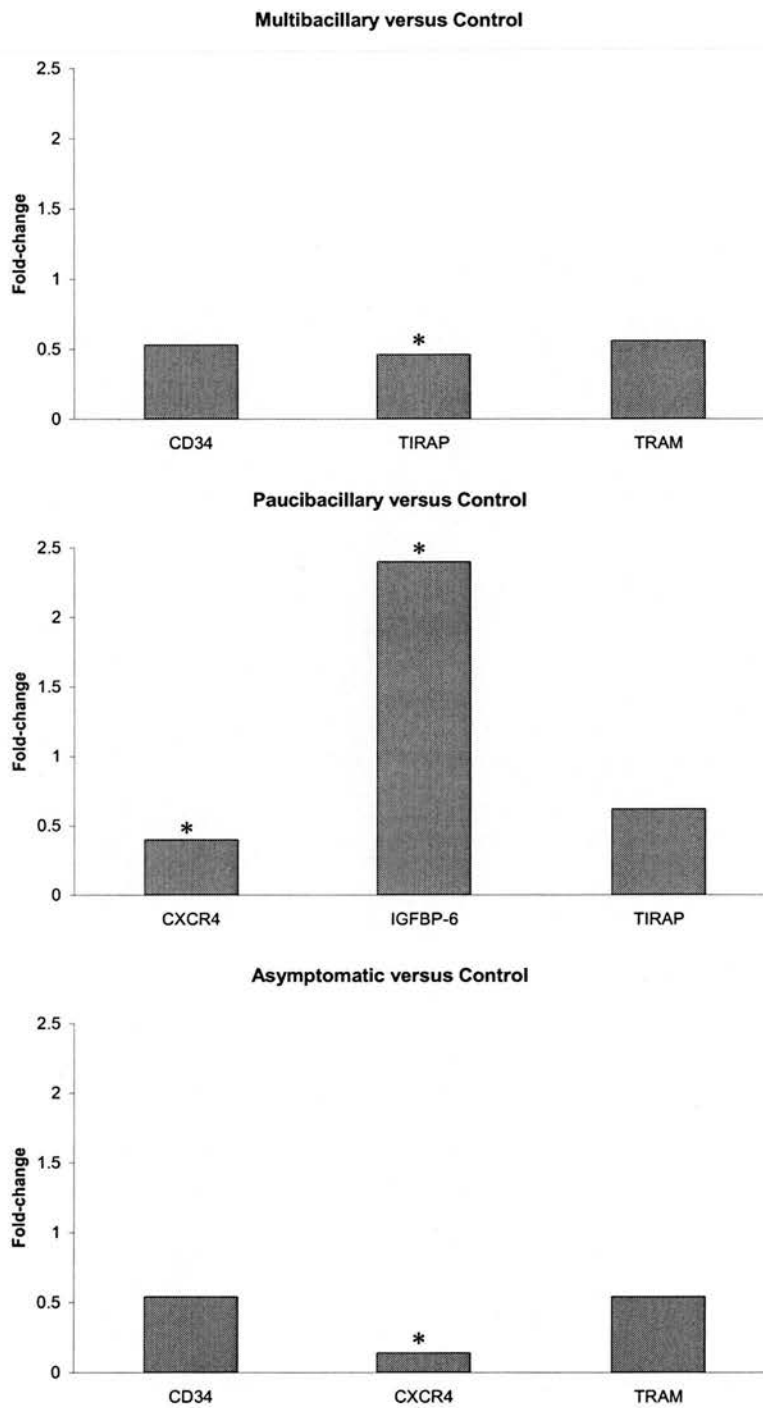


**Figure 5.1: Statistically significant fold-changes in genes in infected animals compared to uninfected control groups** Results are given as fold-changes of mean copy-numbers relative to the mean copy-numbers of the uninfected control group and  $p \leq 0.05$ . (\*) indicates fold-changes greater than 2.2.

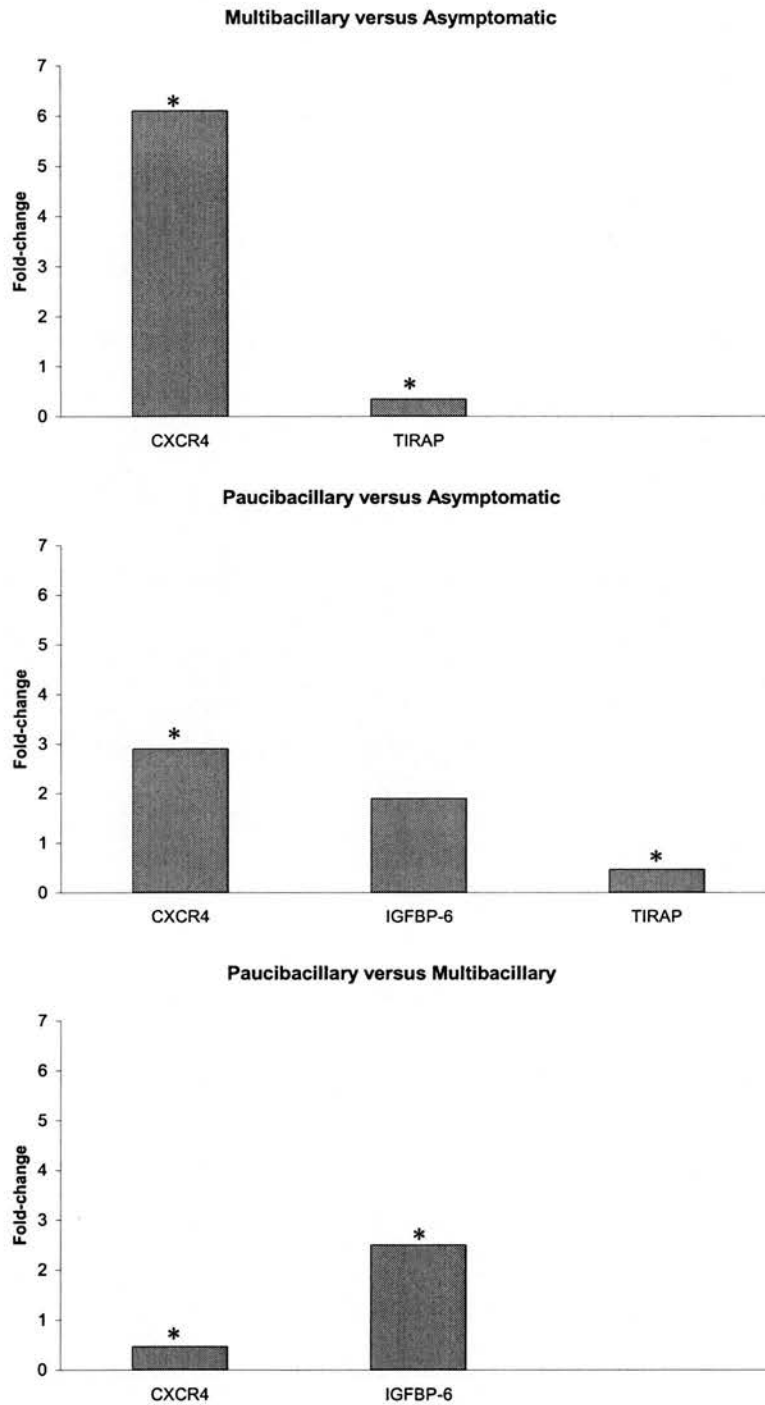


**Figure 5.2: Statistically significant fold-changes in genes in the three infected groups**  
Results are given as fold-changes of mean copy-numbers in infected groups relative to the mean copy-numbers in each of the other infected groups and  $p \leq 0.05$ . (\*) indicates fold-changes greater than 2.2.

Figure 5.1 shows the comparison of the transcript levels between the infected groups and the uninfected control group. CD34, TIRAP and TRAM were significantly down-regulated in multibacillary samples CXCR4 and TIRAP were significantly down-regulated, and IGFBP-6 up-regulated in paucibacillary samples. CXCR4, CD34 and TRAM were significantly down-regulated in asymptomatic samples.

Figure 5.2 shows the comparisons between the three infected groups of sheep. In both multibacillary and paucibacillary samples, CXCR4 was up-regulated and TIRAP down-regulated compared to asymptomatic samples. IGFBP-6 was also up-regulated in paucibacillary samples compared to asymptomatic samples. CXCR4 was down-regulated and IGFBP-6 up-regulated in paucibacillary samples compared to multibacillary samples.

CXCR4 and IGFBP-6 were selected for SNP analysis because they were differentially expressed in paucibacillary and multibacillary samples.

### **5.3 Extraction of genomic DNA from paratuberculosis tissues**

In order to perform the SNP analysis, genomic DNA was successfully extracted from thirty samples in total – ten paucibacillary, ten multibacillary and ten asymptomatic. The concentration of DNA extracted from each sample is given in Table 5.2.

### **5.4 CXCR4 sequence and PCR fragments**

Bovine genomic and full-length CXCR4 mRNA (Accession number: NM\_174301.3) sequences were obtained from Genbank and aligned to identify CXCR4 exons within the bovine genomic sequence. The CXCR4 gene is found on chromosome two and consists of two exons and one intron as depicted in Figure 5.3. Primers were designed to amplify all of

the coding regions and the intron/exon boundaries where possible. The positions of the CXCR4 primers are depicted in Figure 5.3.

### **5.5 IGFBP-6 sequence and PCR fragments**

Bovine genomic and full-length IGFBP-6 mRNA (Accession number: NM\_001040495.1) sequences were obtained from Genbank and aligned to identify IGFBP-6 exons within the bovine genomic sequence. The IGFBP-6 gene is found on chromosome five and consists of four exons and three introns as depicted in Figure 5.4. Primers were designed to amplify all of the coding regions and the intron/exon boundaries where possible. The positions of the IGFBP-6 primers are depicted in Figure 5.4.

### **5.6 Production of PCR products**

PCR products C1, C2, C3 and C4 and IG1, IG2, IG3 and IG4 were generated by PCR from all samples. PCR product C5 was generated from samples 3, 4, 6-22 and 24-32 by PCR. It was not possible to generate this product from samples 5 and 23 – possibly due to mutations in the genomic sequence of these samples preventing primer binding, or the presence of an inhibitor in the DNA sample. These samples were purified and quantified.

Table 5.2: DNA sample concentrations

Sample	Type	DNA Concentration ( $\mu\text{g}/\text{ml}$ )	Extraction kit
1*	Asymp	217.2	DNEasy
2*	Asymp	32.6	DNEasy
3	Pauci	33.5	DNEasy
4	Pauci	191.0	DNEasy
5	Pauci	67.0	DNEasy
6	Pauci	81.1	DNEasy
7	Pauci	50.6	DNEasy
8	Pauci	231.2	FastDNA
9	Pauci	211.3	FastDNA
10	Pauci	238.7	FastDNA
32	Pauci	53.1	DNEasy
34	Pauci	95.4	DNEasy
11	Multi	120.8	FastDNA
12	Multi	162.2	FastDNA
13	Multi	203.6	FastDNA
14	Multi	203.5	FastDNA
16	Multi	170.0	FastDNA
17	Multi	274.6	FastDNA
27	Multi	235.5	FastDNA
28	Multi	181.8	FastDNA
29	Multi	238.0	FastDNA
30	Multi	196.9	FastDNA
19	Asymp	35.6	DNEasy
20	Asymp	98.0	DNEasy
21	Asymp	47.1	DNEasy
22	Asymp	54.6	DNEasy
23	Asymp	62.3	DNEasy
24	Asymp	38.0	DNEasy
25	Asymp	59.0	DNEasy
26	Asymp	96.6	DNEasy
31	Asymp	84.9	DNEasy
33	Asymp	74.6	DNEasy

\*samples used for primer optimisation, but not in final analysis

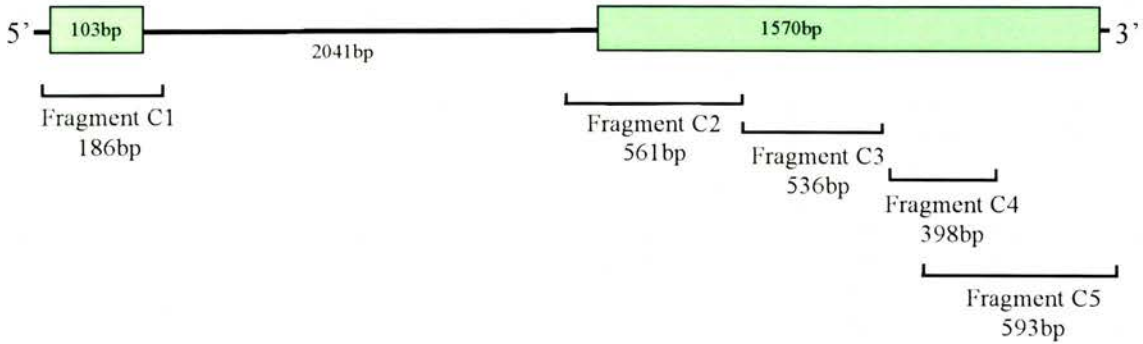


**Figure 5.3: Schematic diagram of the structure of the bovine CXCR4 gene.** Boxes represent exons and square brackets indicate the length of the fragments amplified by the sequencing primers.

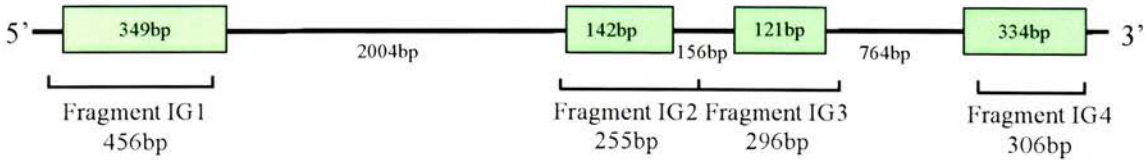


**Figure 5.4: Schematic diagram of the structure of the bovine IGFBP-6 gene.** Boxes represent exons and square brackets indicate the length of the fragments amplified by the sequencing primers.

### 5.7 Cloning and sequencing of PCR products

All PCR products were successfully cloned and the plasmid extracted and sequenced. At least three minipreps were prepared for each sample with each of the nine PCR products, and at least one correct sequence was obtained for each sample and PCR product. A correct sequence was classed as a plasmid containing the insert of interest and of sufficient quality to allow unambiguous reading of the sequence. The number of correct sequences obtained for each PCR product and sample are shown in table 5.3.

### 5.8 SNP analysis of CXCR4

Analysis of the consensus CXCR4 sequences revealed the presence of three SNPs – two in the second PCR fragment and one in the fifth. These were a C to T change at position 2169 (Figure 5.5a), a G to A change at position 2364 (Figure 5.5b) and a G to A change at position 3523 (Figure 5.5c). Sequences containing SNPs are shown aligned with the sequence of sample 6, which contained no SNPs.

When these SNPs were analysed by disease type, all the SNPs were found in all three disease types (Table 5.4), and there were no significant associations. The first SNP was equally common in asymptomatic and paucibacillary samples. The second SNP was most common in asymptomatic samples, and the third SNP was most common in multibacillary samples. The SNPs were also analysed by breed, to ensure that the SNPs were not breed specific. All of the SNPs were found in sheep of a mix of breeds.

Table 5.3: Number of correct sequences for each sample

PCR Product	Number of correct sequences	Samples
C1	3	3-32
C2	3	4-7, 9-11, 13-24, 26-34
	2	3, 8, 12, 25
C3	3	4, 7-9, 11-21, 23-26, 28, 30-34
	2	3, 5, 6, 10, 22, 29
	1	27
C4	3	3, 4, 6-11, 13-16, 19-23, 26-31, 33, 34
	2	5, 9, 12, 17, 24, 25, 32
C5	3	3-7, 9-22, 25, 26, 28-34
	2	8, 23, 24, 27
IG1	3	4-11, 13, 16-19, 21-27, 29-34
	2	14, 20, 28
	1	3, 12
IG2	3	4-9, 12-25, 27, 28, 31-34
	2	8, 10, 11, 26, 30
	1	29
IG3	3	3-8, 10-27, 29-34
	2	9, 28
IG4	3	3, 5, 6, 8-11, 13-31, 33, 34
	2	4, 7, 12, 32

**(A)**

```

2122 TCTATTCCCTTGCCTGTTTTTCAGATATTCACCTCCGATAATTACACCGAGGATGACTTG 2181
      |||
2122 TCTATTCCCTTGCCTGTTTTTCAGATATTCACCTCCGATAATTACACTGAGGATGACTTG 2181

```

**(B)**

```

2362 ACGTGCACCTGTCTGTGGCGGACCTCCTCTTTGTCCCTCACACTTCCCTTCTGGGCGGTT 2421
      |||
2362 AGACTGCACCTGTCTGTGGCGGACCTCCTCTTTGTCCCTCACACTTCCCTTCTGGGCGGTT 2421

```

**(C)**

```

3479 AAATGGTTCTCAGCTGTTTGTAATAAATGATCTCTCCATTCCAGTGAACATTTTCTTT 3538
      |||
3479 AAATGGTTCTCAGCTGTTTGTAATAAATGATCTCTCCATTCCAATGAACATTTTCTTT 3538

```

Figure 5.5: Position of SNPs in the CXCR4 gene (A) alignment of reference sequence 21 against sequence 31 containing SNP at position 2169. (B) alignment of reference sequence 21 against sequence 26 containing SNP at position 2364. (C) alignment of reference sequence 21 against sequence 30 containing SNP at position 3523.

Table 5.4: Samples and disease groups containing the three CXCR4 SNPs

SNP	Samples	Number of samples of each disease type		
		M	P	A
C>T 2169	3, 6, 10, 14, 22, 23, 24, 27, 31, 32	2	4	4
G>A 2364	4, 5, 19, 20, 26, 29, 30, 33	2	2	4
G>A 3523	9, 18, 20, 26, 28, 29, 30	4	2	1

### 5.9 SNP analysis of IGFBP-6

Analysis of the consensus IGFBP-6 sequences revealed the presence of three SNPs – one in each of the first, third and fourth PCR fragments. These were a C to A change at position 63 (Figure 5.6a), a G to A change at position 2776 (Figure 5.6b) and a G to A change at position 3822 (Figure 5.6c). Sequences containing SNPs are shown aligned with the sequence of sample 4, which contained no SNPs.

When these SNPs were analysed by disease type (Table 5.5), both of the first two SNPs (C>A at 63; G>A at 2776) were found in all three disease types, and were both equally distributed among the three types. The third SNP (G>A at 3822) was only found in clinically diseased animals, and most commonly in multibacillary samples. The SNPs were also analysed by breed, to ensure that the SNPs were not breed specific. All of the SNPs were found in sheep of a mix of breeds.

**(A)**

```

61  CACAGGCTGCTGCGCCACTGCTGCTAACTTTGCTGCTCGCTGCCCGCCAGGAGGCGCC 120
   |||
61  CAAAGGCTGCTGCGCCACTGCTGCTAACTTTGCTGCTCGCTGCCCGCCAGGAGGCGCC 120

```

**(B)**

```

2725 ACGTGCCTAATTGTGACCATAGGGGCTTCTATCGGAAGCGGCAGGTGAGGCCGTTTCCTCC 2784
     |||
2725 ACGTGCCTAATTGTGACCATAGGGGCTTCTATCGGAAGCGGCAGGTGAGGCCATTTCCTCC 2784

```

**(C)**

```

3800 CTCACCCCTGGGACCTCACATGTTGGAAAGATTGTTGGTGTGGCCTGGGGTATTAATAAA 3859
     |||
3800 CTCACCCCTGGGACCTCACATAATGGAAAGATTGTTGGTGTGGCCTGGGGTATTAATAAA 3859

```

Figure 5.6: Position of SNPs in the IGFBP-6 gene (A) alignment of reference sequence 23 against sequence 29 containing SNP at position 63 (B) alignment of reference sequence 23 against sequence 7 containing SNP at position 2776 (C) alignment of reference sequence 23 against sequence 6 containing SNP at position 3822.

Table 5.5: Samples and disease groups containing the three IGFBP-6 SNPs  
 Number of samples of each disease type

SNP	Samples	M	P	A
C>A 63	6, 24, 29	1	1	1
G>A 2776	5, 7, 8, 9, 13, 14, 19, 20, 24, 25, 29, 30, 31, 32	4	5	5
G>A 3822	6, 29, 30	2	1	0

### 5.10 Discussion

One of the most unexpected findings of this study was that several genes were significantly differently expressed in asymptomatic samples compared to uninfected controls - CD34, CXCR4 and TRAM were down-regulated. The decrease in CD34 expression probably reflects the lower number of haematopoietic cells present, and the down-regulation of CXCR4 may reflect good control of the immune response. As these sheep are known to be infected with MAP but show no clinical or histopathological signs of disease, these responses may represent the 'best-case scenario' after infection with MAP. This is further supported by the expression profiles in the other infected groups- CXCR4 is down-regulated in paucibacillary sheep, which control bacterial multiplication, and is up-regulated in multibacillary animals, which do not control bacterial proliferation. All of the groups have down-regulation of TIRAP, a TLR regulatory molecule, suggesting that MAP infection can lead to down-regulation of the TLR response. TRAM is involved production of secretory proteins. The down-regulation of TRAM in asymptomatic samples may reflect a reduction in cell activation and thus protein production.

One of the main aims of this study was to find genes differentially expressed in paucibacillary and multibacillary in order to try to understand what governs which type of end-stage disease develops. Two genes were significantly differentially expression - CXCR4 and IGFBP-6. Both of these genes were chosen from previous microarray data (191).

The CXCR4 gene has been recently cloned (145) and found to encode a G-protein-coupled receptor with seven transmembrane domains (121). It is a member of the  $\alpha$  chemokine family and the main receptor for CXCL12, also known as stromal cell derived factor-1 (SDF-1) (112). The CXCR4 signalling pathway is illustrated in Figure 5.7. When CXCL12 binds to

CXCR4, G-protein signalling pathways are activated. This can lead to regulation of gene expression through the production of NF $\kappa$ B, STAT3 and ELK1. BCAR1 is produced, which leads to enhanced cell migration. This is further enhanced by the activation of ITGA4, ITGAL and ITGAM, cell surface molecules involved in cell adhesion.

CXCL12 and CXCR4 play a central role in the chemotaxis of haematopoietic stem cells (HSC). CXCL12 is expressed on stromal cells in bone marrow and promotes trafficking of HSC to the bone marrow (39). CXCR4<sup>+</sup> bone marrow cells can develop into both B and T cells, and CXCR4 deficiency can result in reduced expansion of thymocyte populations during embryogenesis, suggesting that CXCR4 is involved in B and T cell development (106,129). CXCR4 may also play a role in the homing of B and T-cells to the lymph nodes and inflamed tissues (39,160). CXCR4 is expressed on the cell surface of all B cells, monocytes, natural killer cells and most T cells (31,121,160,190,194), and all subsets migrate towards CXCL12 (40). In T cells, CXCR4 expression is higher in naïve and T regulatory cells than in Th1 and Th2 cells (204). Most studies report no differences in expression of CXCR4 between Th1 and Th2 cells (31,64,194), although this is contradicted by a challenge study in mice using either *Mycobacterium bovis* purified protein derivative or *Schistosoma mansoni* egg-antigen coated beads. This showed that a CXCR4 antagonist had little effect on Th1 type granulomata induced by *M.bovis*, but the Th2 type lesions induced by *S.mansoni* were significantly reduced, suggesting that CXCL12 is more highly expressed in the Th2 model (112). It has been reported that CXCR4 can associate with T cell receptors (135) and may play a role in the survival of mature T cells and the generation of memory T cells (129). Recent studies have also suggested that CXCR4 could inhibit expression of MHC class II (215).

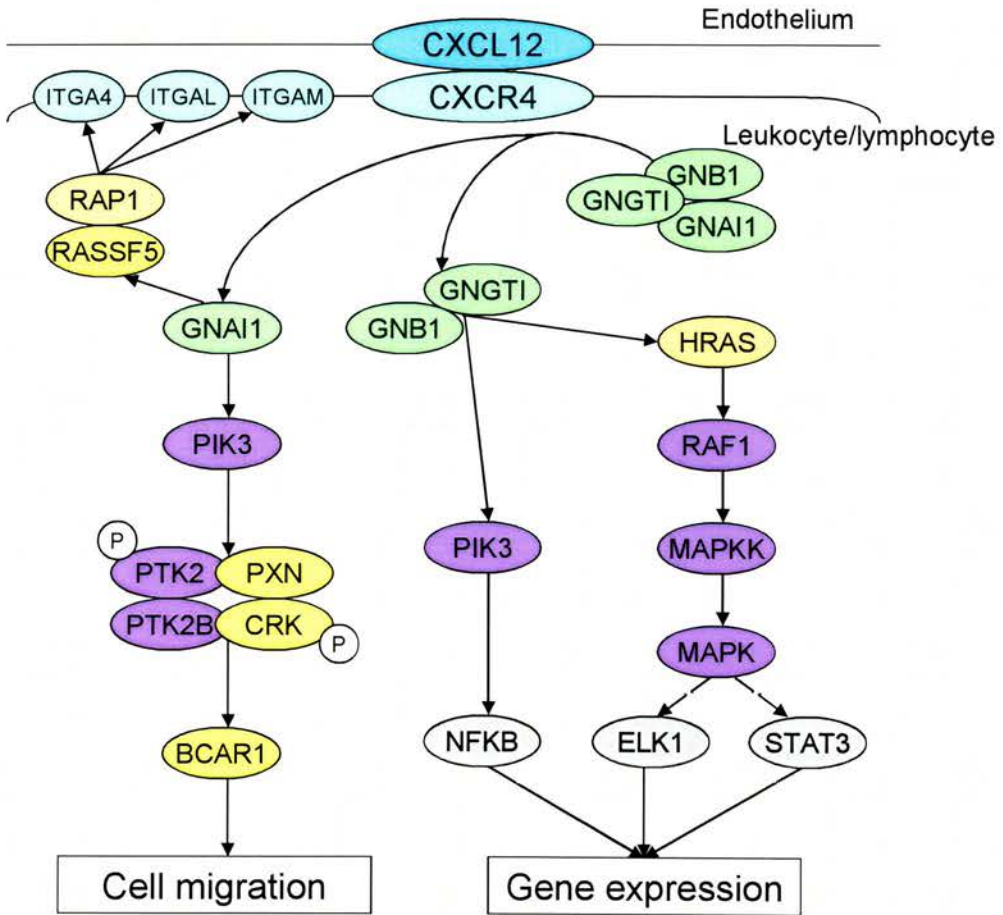


Figure 5.7: CXCR4 signalling pathways

The expression of CXCR4 has been shown to be up-regulated in patients with Crohn's disease (7) and in patients and cells infected with *Mycobacterium tuberculosis* (107,123,140).

CXCR4 expression is regulated by several inflammatory cytokines. CXCR4 expression is up-regulated by IFN $\gamma$  in whole blood (123,176) but down-regulated by IFN $\gamma$  in human monocytes (179). CXCR4 expression is also up-regulated by TNF $\alpha$ , IL-2, IL-4, IL-7, IL-10, IL-12 and IL-15 (7,121,129,176).

CXCR4 was found to be down-regulated in both paucibacillary and asymptomatic samples compared to uninfected controls. This is inconsistent with previous studies on macrophages showing up-regulation of CXCR4 in mycobacterial infection (107,158). Down-regulation of CXCR4 in paucibacillary and asymptomatic samples may be a mechanism to prevent CXCR4 mediated down-regulation of MHC class II.

There are currently six known insulin-like growth factor binding proteins (IGFBP-1-6), all of which bind insulin-like growth factors (IGF) I and II. IGFBP-6 is unique among these as it binds with high affinity to IGF-II, while binding with very low affinity to IGF-I (13,100,125). This difference in binding affinity is due to the unique structure of the C terminal of IGFBP-6, which is responsible for binding IGF-II (100). IGFBP-6 is also unique in its N terminal disulphide links, further differentiating it from other IGFBPs (14).

Through its high affinity binding to IGF-II, IGFBP-6 inhibits many of the functions of IGF-II, including proliferation and differentiation (92,241). Transgenic mice engineered to over express IGFBP-6 have reduced body weights and litter size, suggesting that IGF-II has central roles in growth and reproduction (30). IGFBP-6 also promotes apoptosis in some cell

types, including rhabdomyosarcoma cells and neurones (13,30), and may have a role to play in the development of the central nervous system. It is also important in the control of proliferation in several cancers, and can be up-regulated in some renal cell carcinomas (13,47).

As yet, little is known about the role of IGFBP-6 in infectious disease, although it has previously been shown to be up-regulated in cattle PBMCs stimulated with MAP (62). It is known to be up-regulated in humans in critical illness, and may play a role in transporting IGF-II from the blood into tissues (20). Expression of IGFBP-6 has previously been reported to be inhibited by the presence of TGF $\beta$  (150), although these results in paucibacillary animals contradict this, with up-regulation of both TGF $\beta$  and IGFBP-6. Previous studies have also shown that IGFBP-6 expression is required for pro-B cell development (241). This present study has shown significant up-regulation of IGFBP-6 in paucibacillary samples compared to all others. In paucibacillary infection, it is possible that IGFBP-6 expression could play a role in controlling proliferation in the infected tissues by preventing the actions of IGF-II and inducing apoptosis. Conversely, IGFBP-6 plays a role in transporting IGF-II to the infected tissues, thus increasing proliferation and differentiation of cells in the infected areas.

Due to their differential expression in multibacillary and paucibacillary sheep, CXCR4 and IGFBP-6 were selected for SNP analysis of their coding regions. This analysis aimed to discover whether similar SNPs exist within the coding regions of the CXCR4 and IGFBP-6 genes in sheep, and whether these SNPs were associated with the pathology.

This real-time PCR study found that CXCR4 was down-regulated in paucibacillary and asymptomatic samples compared to controls. Expression in multibacillary samples was similar to controls. It was

expected, therefore, that any SNPs discovered would be associated with the multibacillary form of the disease. Three SNPs were discovered in the CXCR4 gene. Functional analysis of these SNPs revealed that the SNPs at positions 2169 and 2364 are contained within the coding region of the gene, but are silent and thus unlikely to affect gene function. The SNP at position 3523 is in the 3' untranslated region of the gene, and thus cannot affect the gene function, but could affect gene regulation or mRNA translation.

As all of the CXCR4 SNPs are found in all of the types of disease, and none in all of one particular type, it is unlikely that these SNPs are responsible for the differential expression of CXCR4 seen in the three disease types. The samples size in this experiment is too small for any definite conclusions to be reached. However, it was considered unlikely that any of these changes could explain the difference in gene expression observed in the previous study.

This real-time PCR study found that IGFBP-6 was up-regulated only in paucibacillary samples. It was therefore expected that any SNPs found would associate with the paucibacillary form of the disease. Three SNPs were discovered in the IGFBP-6 gene. Functional analysis of these SNPs revealed that the SNP at position 63 is contained within the coding region of the gene which leads to a change in the fourth amino acid in the IGFBP-6 protein from a histidine to glutamine. Histidine is a polar, weakly basic amino acid and glutamine is a polar neutral amino acid of a similar size to histidine. The change may not be significant since the two amino acids have similar characteristics. This SNP was also found in samples of all disease types, so could not be linked to a particular pathology.

The SNP at position 2776 is contained within the intron between exons three and four. Although it could interfere with splicing and other modification of the mRNA, it was found in equal numbers in each of the three groups, suggesting that it does not affect gene function.

The SNP at position 3822 is in the 3' untranslated region of the gene, and thus cannot affect the protein structure, but could affect gene regulation or mRNA translation. It is possible that this SNP could be clinically relevant as it is not observed in asymptomatic animals but investigation of more animals would be needed to consolidate this finding. The SNP was also only found in 3 out of 20 clinically diseased samples – two multibacillary and one paucibacillary. Therefore many more sequences from clinically diseased sheep would have to be analysed before definite conclusions could be drawn.

In the future, it would be beneficial to expand these SNP analyses to include upstream non-coding regions. This is where promoter and regulatory regions are likely to be found, and any SNPs in these areas could have a profound effect on gene expression.

## Chapter 6: Microarray analysis of gene expression

### 6.1 Introduction

Competitive hybridisation of cDNA microarrays is a powerful method for comparing host gene expression in different pathologies. Microarray analysis allows hundreds of genes to be assayed in parallel and significant interactions between these genes to be elucidated. Lower consumption of reagents and samples results in a high number of genes being analysed from smaller samples. Competitive hybridisations are an ideal way of comparing gene expression between two different samples as they reduce between chip variations and differences in reaction conditions (198).

The results of such a host response study can be applied in several ways. They can be used to detect novel pathways involved in pathogenesis or to compare pathways involved in contrasting pathologies. Comparisons between resistant and susceptible hosts can allow identification of genes and pathways involved in protection and recovery, thus providing new targets for treatment and vaccination (108).

Although microarray analysis is powerful, it also has its limitations. There can be a high 'false-discovery' rate, leading to high numbers of genes seeming to be differentially expressed when they are not. This is controlled for during the normalisation process, when an adjusted  $p$  – value is produced. It is also essential to validate the array by using real-time PCR to analyse the expression of genes found to be differentially expressed in the microarray analysis. Microarray analysis must be done to Minimum Information About a Microarray Experiment (MIAME) standards, which allow easy interpretation and repetition of the experimental results (32).

This analysis utilised the ruminant immunoinflammatory gene universal array (RIGUA). The array has 4000 spots consisting of replicates of 600

genes, each represented as 75bp oligomers, picked to represent genes involved in all aspects of the ruminant immunoinflammatory response. The array is thus small and focussed, and can only provide information about immunoinflammatory responses. The four types of samples were analysed pairwise, and the array validated by the real-time RT-PCR analysis of seven genes, picked on the basis of their differential expression in multibacillary and paucibacillary ileum samples.

## **6.2 Microarray quality control**

### **6.2.1 Heat Plot**

A heat plot was produced for each channel on each array to check for trends in intensity across the chip. Ideally, the high and low intensity spots are uniformly distributed across the array, indicating that the hybridisation was successful. Figure 6.1 shows an example of an array with a uniform intensity. All of the arrays used in the analysis had R values of less than 0.4.

### **6.2.2 MA plot**

An MA (log ratios versus mean log intensities) plot was produced for each array both before and after normalisation. Points on an MA plot from a successful array should be in a cluster around 0 on the Y axis, as most genes would be expected to have no differential expression. Usually, spots of lower intensities are more spread out around 0, due to the background subtraction method used by Bluefuse. After normalisation, the points should be more linear and cluster more tightly together. MA plots can thus be used to identify any unusual trends in the microarray data. Figure 6.2 shows typical MA plots before and after normalisation. MA plots for all of the arrays were produced and examined to ensure that the arrays were hybridising as expected.

### 6.2.3 Inter-array variation

Figure 6.3 shows boxplots of normalised ratios for all spots on one set of six experiments, excluding blanks and buffer spots - these are the spots that are used in all the subsequent analyses. For all sets of experiments, the majority of the spots showed a similar distribution of values on all the six chips so a further normalisation between arrays was not required.

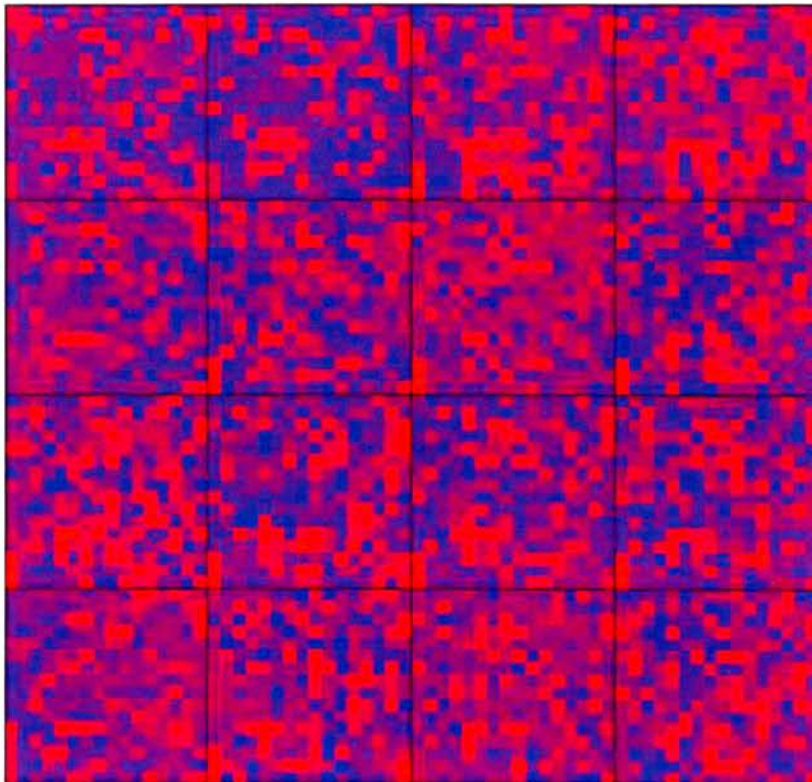


**Figure 6.1: Heat map of channel 2 on 3P vs. 2C chip.** Blue indicates low intensity and red high intensity. The landing lights (bottom left of each block on the image) are clearly visible as high intensity in most blocks. The high intensity spots are fairly uniformly distributed across the chip with no apparent trends in intensity

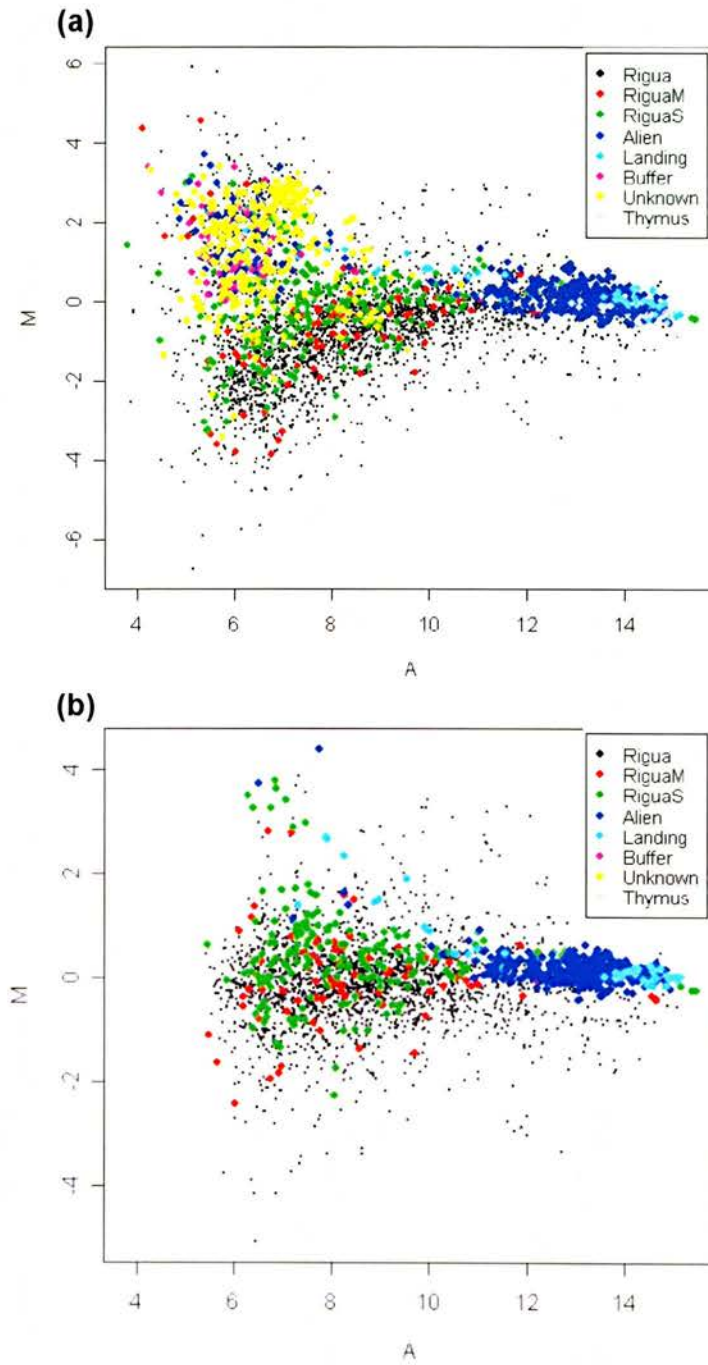


**Figure 6.2: MA plots of 3P vs. 2C chip.** (a) is a typical raw data MA plot. The points form a curved line, with a 'fish-tail' effect towards the lower intensity end of the plot. (b) is a plot of the same data after normalisation. The points now line up horizontally around 0 and the 'fish-tail' effect is no longer appreciable.

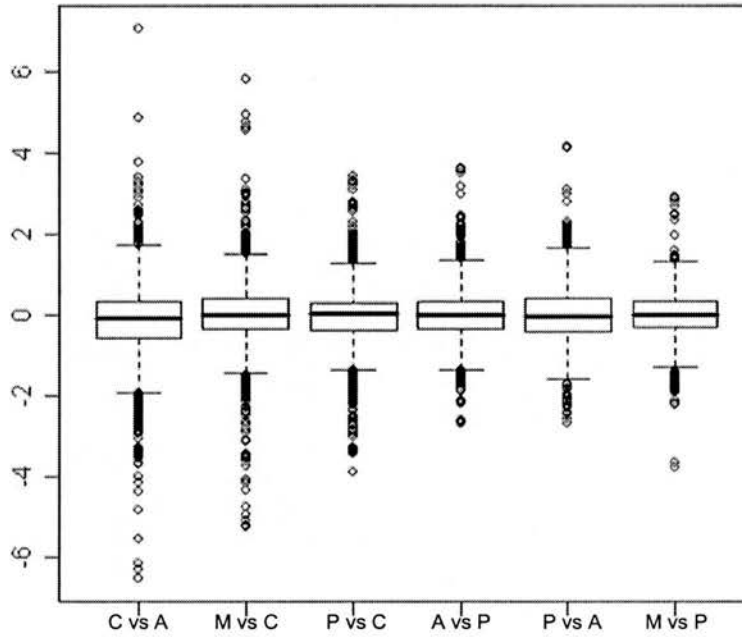


**Figure 6.3: Boxplot of one set of microarrays.** Boxes represent the interquartile range of ratios after normalisation, with the line representing the median, and the spots representing outliers. The six arrays have similar interquartile ranges and distribution of values, indicating that further normalisation would be unnecessary.

### 6.3 Gene expression analysis

The design of the array analysis divided the 24 samples of interest into groups of four, each containing one sample of each type. The four samples in each group were compared pair wise with each other sample, utilising six arrays. This was repeated for each group, using a total of 36 arrays. The samples and comparisons used are given in table 6.1.

Of the 600 genes analysed on the array, 63 fulfilled the criteria of fold-change greater than 1.5 and  $p < 0.05$  in at least one comparison. Additional microarray data is provided in Appendix 3 (CD). These genes and fold-changes are listed in Table 6.2. The fold-changes given are a mean of all probes for each gene. Four genes were found to be differentially expressed in infected samples compared to uninfected controls, and a further eight in clinically affected samples compared to uninfected controls. Eight genes - ANPEP, CD3E, CD3G, CD247, TRDC, IGFBP3, IGHA1 and CCL2 - were differentially expressed in clinically affected samples compared to asymptomatic samples.

Table 6.1: Samples and comparisons used for microarray analysis

Comparison	Sample	
	CH1	CH2
1	16M*	5P
2	24A	16M
3	38C	24A
4	5P	38C
5	24A	5P
6	38C	16M
7	27M	3P
8	19A	3P
9	3P	36C
10	19A	27M
11	36C	19A
12	36C	27M
13	28M	4P
14	37C	23A
15	23A	4P
16	4P	37C
17	28M	23A
18	37C	28M
19	11M	6P
20	22A	11M
21	39C	22A
22	22A	6P
23	39C	11M
24	6P	39C
25	14M	9P
26	25A	9P
27	40C	25A
28	9P	40C
29	40C	14M
30	25A	14M
31	26A	8P
32	43C	17M
33	43C	26A
34	8P	43C
35	26A	17M
36	17M	8P

\*M=multibacillary, P=paucibacillary, A=asymptomatic, C=control. Numbers represent RNA sample numbers (Table 4.1)

Table 6.2: Mean fold-changes of significantly differentially expressed genes. Bold denotes genes selected for validation by real-time RT-PCR. Changes less than 1.5 were included to show trends in the data.

Gene	Comparison					
	A vs. C	M vs. C	P vs. C	M vs. A	P vs. A	M vs. P
ANPEP		0.46	1.6	0.4	0.43	
C3		1.42		1.75	1.53	
C7		1.83		1.5		
C9	1.69		2.1			0.62
CCL2		1.73	1.51	1.64	1.65*	
CCL5		0.7	0.65		0.66	
CCR7	0.68	0.58	0.71			
CD247	0.75	0.52	0.64	0.69		
CD3D	0.67	0.48	0.58			
CD3E	0.73	0.55	0.63	0.63		
CD3G	0.68	0.41	0.54	0.6		
CD55	0.63	0.69				
<b>CD63</b>		1.77		1.87		1.62
CD74	0.56	0.68			1.49	
CD79A	0.47	0.41	0.52			
CFB			1.71		1.52	
CFH	1.38		1.83		1.43	
CLIC5		0.62				0.65
CP	0.59*	0.65	0.77			
CR2	0.34	0.34	0.43			
<b>CXCL10</b>			2.31		2.25	0.58*
CXCR3				1.54		
CXCR4	0.55		0.61	1.82		1.9
DEFB1	1.66	1.41	1.89			
FCER1G		1.87	2.28*	1.49	2.28*	
GAPDH	0.63					
<b>ICAM1</b>		1.55		1.9	1.45	1.31
<b>IGF2R</b>		1.65		1.74		1.51
IGFBP3		0.6	0.58	0.64	0.62	
IGHA1		1.85	1.96	1.85	1.96	
IGHE	1.59			0.59*	0.69	
IGHM	0.69		1.59	1.83	2.31	
IGJ		1.47	2.38		1.89	0.62
IL16	0.67	0.59	0.65			
IL18RAP			1.66		1.68	
ITGA4	0.54	0.52			1.52	0.63
ITGAL	0.56	1.91		3.58	1.9	1.95
ITGAM						1.51
<b>ITGB2</b>		1.89		2.03		1.95
MHC class II DQ B1/2	0.64				1.36	
MHC class II DQB1	0.66	0.57*				
MHC class II DR A		0.65				
MHC class II DR B1	0.63	0.64				
MHC class II DYA	0.65				1.67	

\*Changes not statistically significant, but >1.5 fold

Table 6.1 continued

Gene	Comparison					
	A vs. C	M vs. C	P vs. C	M vs. A	P vs. A	M vs. P
MHC class II DYB	1.63	1.5	1.48			
<b>MMP7</b>		1.93				1.84
<b>MMP9</b>		1.47		1.98		1.76
<b>OXT</b>		2.66		2.4		2.61
PI3			1.63			
PIGR			1.79		1.56	
PTPRC	0.55	0.62				
SELL		1.98		1.85	1.58*	1.83*
SIRPA	0.68			1.65	1.41	
<b>SLC11A1</b>				1.57		1.63*
STAT1				1.32	1.47	
STS	1.76					
<b>TLR2</b>		1.95		1.52		1.52
<b>TNFRSF1B</b>		1.6		1.62		1.5
TRDC		0.56	0.63			
TFRC		2.65*		2.79	1.78	1.81*
<b>TYROBP</b>		1.9		1.95		1.68
VIM		1.56		1.48		

\*Changes not statistically significant, but >1.5 fold

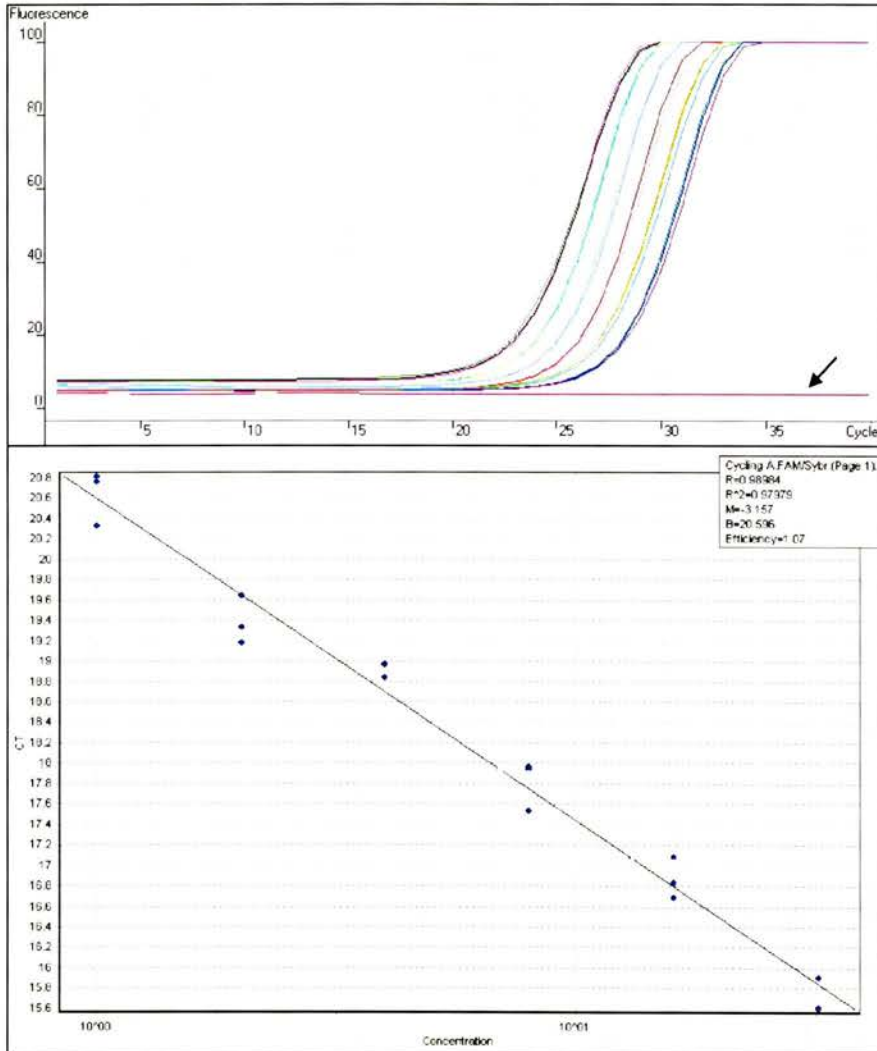
#### 6.4 Real-time RT-PCR validation of Microarray results

Of the 63 genes found to be differentially expressed in the microarray experiment, twelve were chosen for real-time RT-PCR validation – MMP9, ITGB2, ICAM1, CD63, CXCL10, TYROBP, IGF2R, MMP7, SLC11A1, OXT, TLR2 and TNFRSF1B. All of these genes were differentially expressed in paucibacillary and multibacillary samples. Primers were successfully designed and optimised for nine of the genes – primers were designed for SLC11A1 and TNFRSF1B but consistently produced multiple products, and primers for CXCL10 could not be optimised for use in real-time RT-PCR. A standard curve was produced for each gene using serial dilutions of a cDNA pool of all samples. An example of a typical standard curve is shown in Figure 6.4.

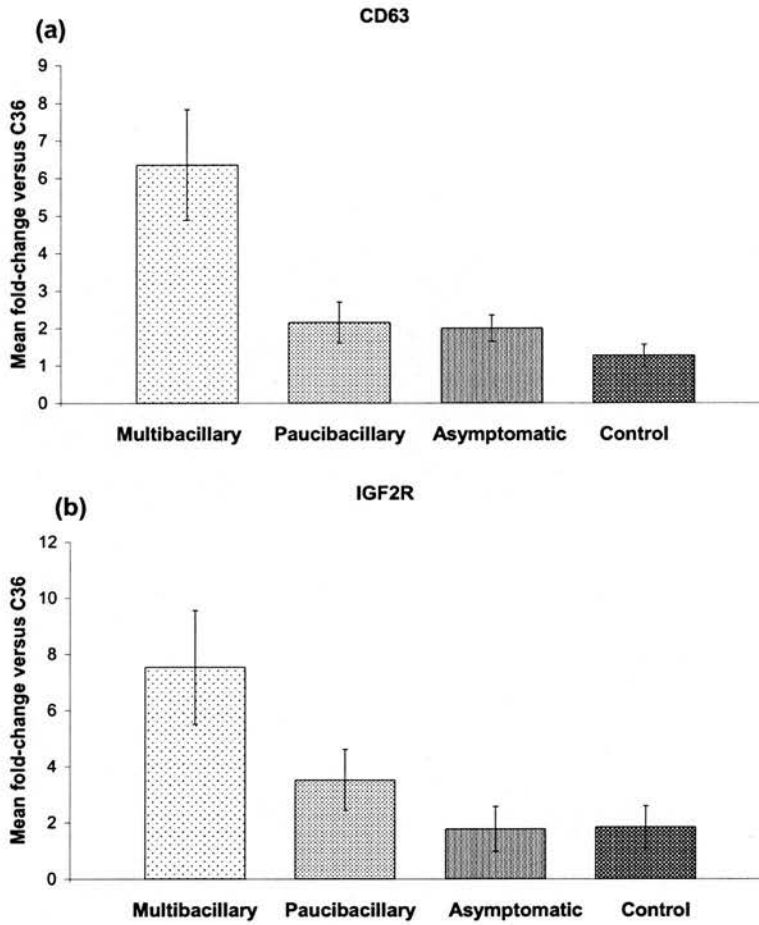
The remaining nine genes were analysed using real-time RT-PCR analysis, and expressed as fold-changes relative to an arbitrary calibrator sample. For all cases except OXT this was control sample 36. For OXT, the calibrator sample was paucibacillary sample 3, as OXT was not expressed in control or asymptomatic samples. The expression of MMP7 and CD54 was too low to be accurately quantified (fewer than 100 copies/reaction). The results of the real-time RT-PCR analysis confirmed the results from the microarray experiment, with minor differences in the magnitude of the fold-change, probably due to differences in sensitivity of the two methods. In addition, several borderline significant changes in the microarray results were significant in the real-time RT-PCR results.. Table 6.3 shows the results expressed as relative fold-changes in the six comparisons, and Figures 6.5a-g shows the fold-changes in each gene relative to a calibrator sample.

Table 6.3: Relative fold-changes of genes analysed in real-time RT-PCR. Bold denotes statistical significance.

	Comparison					
	M vs. C	P vs. C	A vs. C	M vs. A	P vs. A	M vs. P
CD63						
Fold-change	<b>5.0</b>	<b>1.7</b>	<b>1.6</b>	<b>3.2</b>	1.1	<b>3.0</b>
P-value	0.00	0.01	0.01	0.00	0.66	0.00
IGF2R						
Fold-change	<b>4.1</b>	<b>1.9</b>	0.97	<b>4.2</b>	<b>2.0</b>	<b>2.1</b>
P-value	0.00	0.03	0.91	0.00	0.02	0.00
ITGB2						
Fold-change	<b>4.5</b>	<b>2.2</b>	1.0	<b>4.3</b>	<b>2.1</b>	<b>2.1</b>
P-value	0.00	0.01	0.89	0.00	0.02	0.00
MMP9						
Fold-change	<b>9.7</b>	1.0	0.65	<b>14.9</b>	<b>1.6</b>	<b>9.3</b>
P-value	0.00	0.89	0.25	0.00	0.02	0.00
OXT						
Fold-change	-	-	-	-	-	<b>48.5</b>
P-value	-	-	-	-	-	0.02
TLR2						
Fold-change	<b>7.3</b>	1.7	1.1	<b>6.8</b>	1.6	<b>4.3</b>
P-value	0.00	0.22	0.87	0.00	0.40	0.00
TYROBP						
Fold-change	<b>7.4</b>	<b>2.5</b>	0.78	<b>9.4</b>	<b>3.1</b>	<b>3.0</b>
P-value	0.00	0.00	0.30	0.00	0.01	0.00



**Figure 6.4: Generation of cDNA standard curves for real-time PCR** (a) Fluorescence versus cycle number (time) graph for an acceptable standard curve - cDNA dilutions are spaced two cycles apart and efficiency is between 0.9 and 1.1. Arrow indicates NTC. (b) Standard curve taken from (a). All values are close to ideal, and points sit well on the line.



**Figure 6.5: Mean fold-change of genes compared to calibrator sample.** Error bars indicate the 95% confidence interval. (a) Shows the relative expression of CD63 (b) shows the relative expression of IGF2R.

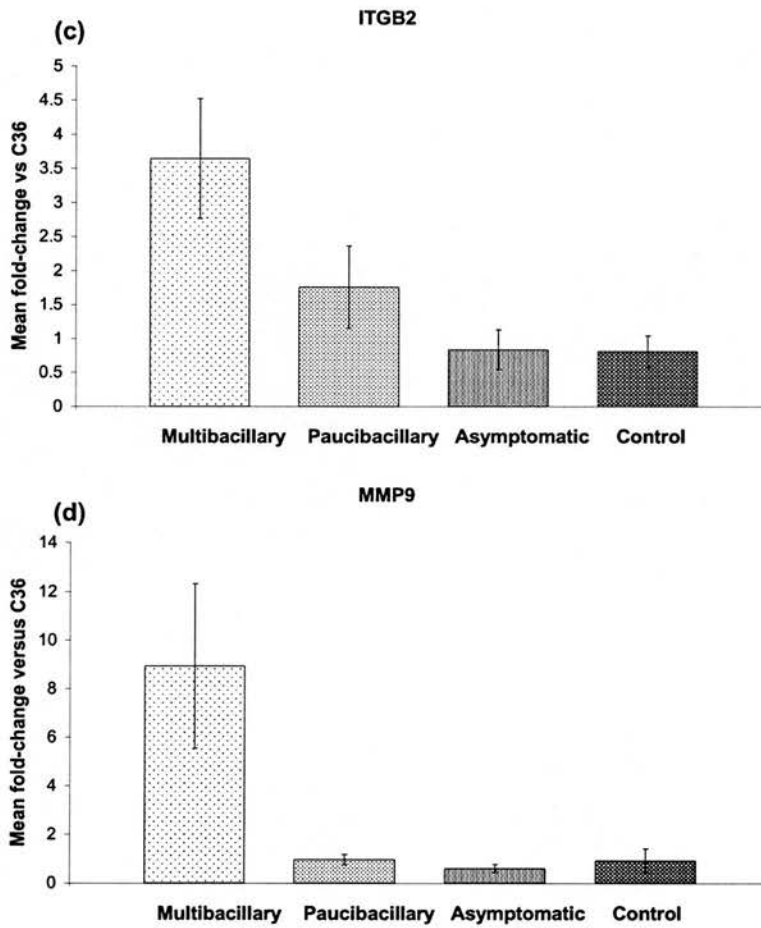


**Figure 6.5 cont.** (c) Shows the relative expression of ITGB2 (d) shows the relative expression of MMP9.

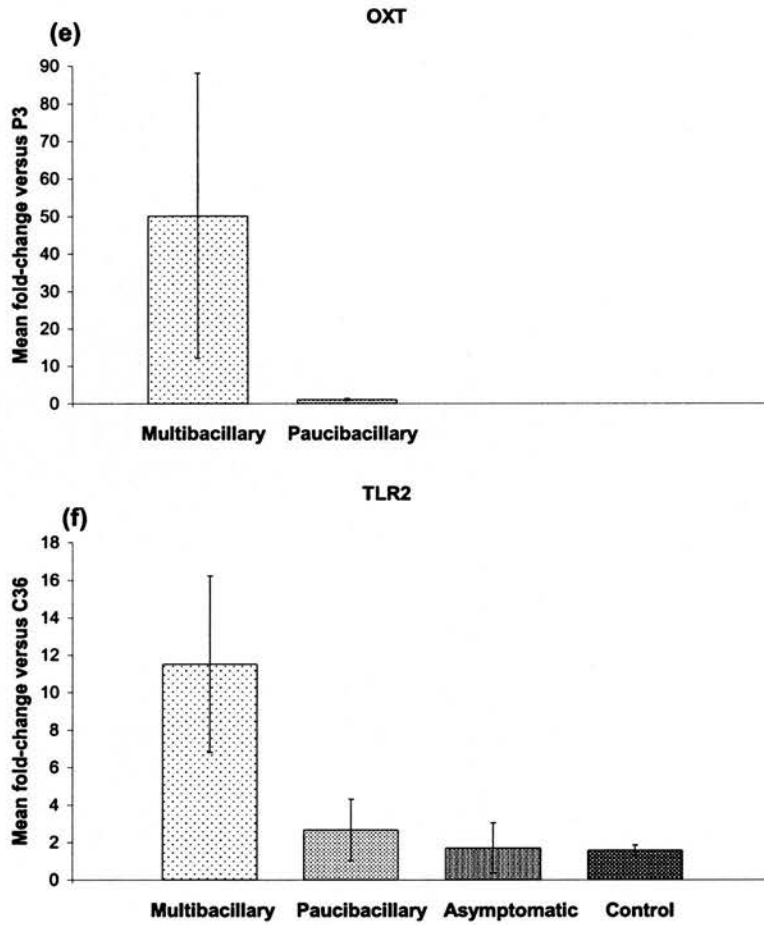
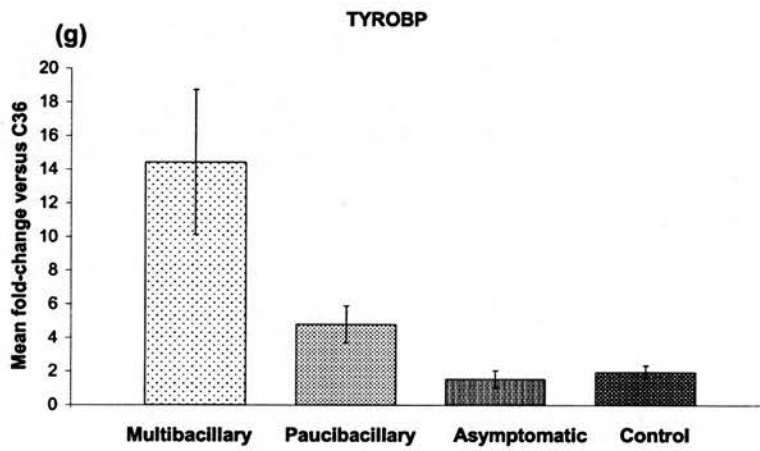


**Figure 6.5 cont.** (e) Shows the relative expression of OXT. OXT expression in asymptomatic and control samples was too low to be accurately quantified. (f) shows the relative expression of TLR2.



Figure

cont. (g) Shows the relative expression of TYROBP

6.5

The expression of all genes was significantly up-regulated in multibacillary samples compared to each of the other groups. This agrees well with the results of the microarray. CD63, IGF2R, ITGB2 and TYROBP were found to be up-regulated in paucibacillary samples compared to controls. All of these genes showed a slight up-regulation in the microarray results, but this was below the selection criteria for significant genes. CD63 was also found to be up-regulated in asymptomatic samples compared to controls, contradicting the array results which suggested that there was no change in the expression of CD63. CD63 was the only gene to be up-regulated in all infected samples. IGF2R, ITGB2, MMP9 and TYROBP were up-regulated in paucibacillary samples compared to asymptomatic samples. Again, these genes were slightly up-regulated in the microarray, but below the selection criteria.

### **6.5 Discussion**

This study has analysed the expression of a selection of genes in the three forms of paratuberculosis in sheep. Generally, the microarray results showed that there is a massive change in expression of immunoinflammatory genes in both paucibacillary and multibacillary infection, with 24 and 34 genes found to be significantly differentially expressed respectively. This was to be expected when the histopathology results are taken into account, showing massive inflammation and infiltration of immune cells to the site of infection. Perhaps less expected were the 21 genes differentially expressed in asymptomatic samples compared to controls, as the histopathology results for these samples show no signs of infection or inflammation.

Seven genes were chosen, on the basis of differential expression in multibacillary and paucibacillary samples, and their possible relation to paratuberculosis pathology, to be validated using real-time RT-PCR. The results of the real-time RT-PCR assays accurately reflected the results of

the microarray analysis. This firstly validates the microarray results and demonstrates consistency. Secondly, it gives a greater understanding of the differential expression of this selected group of genes.

The seven genes studied – CD63, IGF2R, ITGB2, MMP9, OXT, TLR2 and TYROBP – were all significantly up-regulated in multibacillary samples compared to all others, which was consistent with the microarray results. The real-time results differed from the microarray results in paucibacillary samples. Compared to control samples, CD63, IGF2R, ITGB2 and TYROBP were up-regulated in paucibacillary samples, results not reflected in the filtered microarray data. However, when the unfiltered normalised data were examined, it was found that these changes were evident in the microarray data, but they were below the cut-off criteria. Although the microarray results were well validated by the real-time RT-PCR analysis, none of the genes successfully quantified was significantly down-regulated in any comparison. Therefore, the validation does not fully reflect the range of fold-changes observed in the array data, and in future could be improved by either including more genes or picking genes at random for validation.

The array results did not, however, fully reflect the results of the previous real-time studies. Only CXCR4 was found to be significantly differently expressed in the array data. There are several reasons for the apparent discrepancy. The oligo for TRAF1 was designed using human sequence and thus may not have bound ovine TRAF1 with high affinity. The microarray is less sensitive than real-time PCR, as demonstrated by the differences in fold-change between the microarray and real-time validation results. Finally, the chosen method of analysis and normalisation for these arrays detected only those genes stably expressed across six comparisons. As many of the genes previously quantified were highly variable, these would not be detected by the microarray analysis.

Many of the genes found to be differentially expressed in the microarray and real-time RT-PCR analyses can be grouped together into different immune pathways, allowing a comparison of the pathways involved in the three different pathologies. This allows a more 'systems biology' approach to be taken in the analysis of these results, giving a more in depth picture of the pathologies.

Both paucibacillary and multibacillary samples displayed significant up-regulation of FCERG1, which may indicate up-regulation of the FCERG1 signalling pathway. This pathway is activated by IGHE, which is slightly up-regulated in these samples, but not significantly so. Activation of the FCER1G signalling pathway can lead to activation of the phosphatidyl inositol and MAPK signalling pathways, which in turn lead to production of cytokines including TNF $\alpha$ , which is up-regulated in both types of sample, and CSF2, which is up-regulated in paucibacillary samples. Although asymptomatic samples show a significant up-regulation of IGHE, the corresponding up-regulation of FCER1G was not observed.

Compared to asymptomatic samples, both multibacillary and paucibacillary show significant up-regulation of STAT1, as well as cytokines that activate the JAK-STAT signalling pathway including IL6 and IFNG. Activation of the JAK-STAT pathway leads to activation of genes involved in the activation of lymphocyte subsets. STAT1 is slightly, but not significantly, up-regulated in these samples compared to controls. It is therefore likely that activation of the JAK-STAT pathway is a significant step in the development of clinical paratuberculosis.

TLR2 was greatly up-regulated in multibacillary samples compared to all other groups, suggesting that the TLR2 signalling pathway is important in multibacillary pathogenesis. TLR2 is central to the immune response to mycobacteria – knockout mice are significantly more susceptible to

mycobacterial infections (243). In leprosy in humans, TLR2 signalling can alter the cytokine responses. Studies in monocytes with a TLR2 mutation have shown that normal TLR2 signalling leads to a type 1 response, whereas signalling through the mutated TLR2 leads to increased IL10 production and a type 2 immune response (124). A recent study in bovine monocytes infected with MAP has shown that TLR2 signalling is involved in phagosome trafficking and anti-microbial responses through the MAPK pathway (270). TLR2 acts a dimer with either TLR1 or TLR6. The expression of both of these genes was not significantly different in the microarray, contradicting the suggestion that TLR2 signalling is activated. However, the probes for both TLR1 and TLR6 were designed using human sequences, which may have affected the binding of the ovine cDNA to the probe, and thus the data may be unreliable. The TLR2 probe was designed using bovine sequence.

If a ligand is bound to TLR2, this can activate a series of TLR regulatory molecules. Both paucibacillary and multibacillary samples have displayed down-regulation of TIRAP, which acts as a co-regulator with MyD88. These data suggests that a MyD88-independent pathway is utilised in clinical paratuberculosis to regulate the activity of TLRs. The TLR signalling pathway leads to production of proinflammatory and chemotactic cytokines, both of which are up-regulated in clinical paratuberculosis.

All samples infected with MAP displayed down-regulation of several genes encoding elements of the T-cell receptor complex - CD3E, CD3D, CD247, and CD3G -and other genes involved in the TCR signalling pathway, including CR2 and PTPRC. The TCR signalling pathway has many functions, and can lead to activation and differentiation of T cells, T cell cytotoxicity and T helper cell functions, and the production of a host of cytokines, including IFNG and IL10. These TCR molecules are also

markers of various T cell subsets. As this response is seen in all infected samples, it is possible that this down-regulation is caused by infection by the mycobacteria, and may represent a method of host response modification by the mycobacteria.

The expression of several genes involved in leukocyte transendothelial migration, including ITGAL, ITGB2, ICAM1, CXCR4 and MMPs were up-regulated in multibacillary samples. The expression of these genes was either unchanged or down-regulated in asymptomatic and paucibacillary samples. This suggests that even at a late stage in the disease there are still a large number of leukocytes entering the site of infection in multibacillary animals. This agrees with the histopathological observations that the ileal tissue contains large numbers of macrophages. Up-regulation of both CXCR4 and MMP9 has previously been reported in bovine macrophages in response to MAP stimulation (117,158).

The results of the microarray suggest strongly that NK cell cytotoxicity is involved in paratuberculosis pathogenesis. Several genes involved in cytokine production and release by NK cells are up-regulated in multibacillary and paucibacillary samples, including ITGAL, FCER1G and TYROBP, as well as the cytokines themselves. However, there is no evidence from the array that this leads on to the synthesis of products such as FASL and perforin via the JAK-STAT pathway, which can lead to the initiation of apoptosis in an affected cell.

All infected samples displayed up-regulation of some elements of the complement cascade. These genes include C3 and C7 in multibacillary samples, CFB, CFH and C9 in paucibacillary and CFH and C9 in asymptomatic samples. The up-regulation of CFB suggests that, in paucibacillary and asymptomatic samples, the alternative complement pathway is activated. This would lead to production of the membrane attack complex and cell lysis, which would in turn lead to further

inflammation at the site of infection. However, the upregulation of CFH in these samples also suggests that the complement cascade is being controlled.

In both asymptomatic and multibacillary samples there is a general down-regulation of MHC class II and associated genes, including CD74, which is not observed in paucibacillary samples. This down-regulation would lead to lower levels of CD4 cell activation. As these cells are responsible for the activation of both cell-mediated and humoral acquired immune responses, this lack of activation would lead to a reduction in activation of the whole acquired immune response. The results agree with previous studies which have identified a reduction of MHC class II expression in paratuberculosis, which is thought to be due to mycobacteria-mediated modulation of the immune response (5,215,253,267).

Several of the genes found to be differentially expressed in the microarray and real-time RT-PCR results could not be easily classified into biologically functional pathways. Of these genes, five were differentially expressed in all infected samples – CD63 and DEFB1 were up-regulated, and CD79a, CP and IL16 were down-regulated. CD63 is a tetraspanin thought to complex with integrins and keep them clustered on the cell surface and DEFB1 is an anti-microbial peptide involved in the resistance of epithelial surfaces to colonisation. The up-regulation of these genes may simply reflect the immune activation already evident in this tissue. The down-regulation of CD79a, part of the B-cell receptor complex, may reflect a reduction in the number of B-cells present in the tissues. The down-regulation of CP, a copper carrying enzyme indicative of the acute phase response, and IL16, a chemoattractant and modulator of T-cell activation, further reflects a 'damping down' of the immune response, possibly related to the late stage of infection of these samples.

In addition, four genes were differentially expressed only in clinically affected sheep – IGF2R, IGHA1 and IGJ were up-regulated and IGFBP3 was down-regulated. IGHA1 and IGJ combine to form dimeric IgA, a secreted antibody produced by B cells. These results are supported by the antibody ELISA results, but is confused by the down-regulation of CD79a, which suggested either a reduction in activation of B cells, or a reduction in the number of B cells present, both of which should lead to a reduction in the amount of IgA produced. IGF2R was also up-regulated. IGF2R is a receptor for IGF2 and M6P. It plays a role in the activation of TGF $\beta$ , a gene shown to be up-regulated in these samples in the previous real-time RT-PCR study. IGFBP3 has similar functions to IGFBP6, discussed in detail in Chapter five, and its role in the immune system is unknown. Paucibacillary and asymptomatic samples both displayed differentially expressed IGHM, which was up-regulated in paucibacillary samples and down-regulated in asymptomatic samples. IGHE was also up-regulated in both paucibacillary and asymptomatic samples, although this was not significant in the paucibacillary samples. As previously discussed, IGHA1 was also up-regulated in paucibacillary samples, as was PIGR, a component of the immunoglobulin secretory pathway. These results taken together suggest that either the types of antibody expressed in the three pathologies may have an effect on disease progression, or simply that they are reflective of the type of disease that has developed. These results also contradict the antibody ELISA results described in Chapter 3, which state that most of the paucibacillary animals did not produce MAP specific antibodies.

Finally, there was a group of genes differentially expressed in only one of the three pathologies studied. In the asymptomatic samples, GAPDH and SIRPA were down-regulated and STS was up-regulated. These genes are not thought to be involved in the immune response, and are concerned

with normal cellular functions, growth and differentiation. The role of any of these genes in establishing asymptomatic paratuberculosis is unclear. In paucibacillary samples, IL18RAP and PI3 were up-regulated. IL18RAP is a subunit of the IL18 receptor and is required for the activation of the NF $\kappa$ B and MAPK8 pathways in response to IL18. As previously shown, IL18 is down-regulated in these samples. The up-regulation of the IL18 receptor may be an attempt to increase the sensitivity of the cell to low levels of IL18 at this late stage of the disease. PI3 is a serine antiprotease with anti-inflammatory effects in neutrophils. The expression of this gene has been linked to inflamed ulcerative colitis and may act to reduce tissue damage in the intestine (200). OXT, TFRC, VIM, SLC11A1 and SELL were up-regulated in multibacillary samples. OXT is a hormone involved in pregnancy and maternal behaviour, normally expressed in the pituitary gland. Which cells could be expressing OXT in the ileum and what role it is playing in multibacillary pathology are unknown. TFRC is involved in iron transport from the intestine to the rest of the body and has been previously shown to be up-regulated early in MAP infection in cattle (277), and VIM is a cytoskeletal element. Again, the role of these genes in multibacillary pathology is unclear. SLC11A1 functions as a divalent metal transporter and has been linked to susceptibility to Crohn's disease (44,205). SELL is a lymphocyte adhesion molecule. Previous studies of *M.bovis* infected deer have found up-regulation of SELL in infected lymph nodes. As effector CD4+ cells express low levels of SELL, it was suggested that up-regulation of SELL could lead to lower levels of macrophage activation (85).

Overall, this microarray study has identified several genes and pathways which warrant future investigation.

## Chapter 7: Discussion and conclusions

### 7.1 Discussion

Paratuberculosis is a chronic inflammatory disease of the gut of ruminants, caused by infection with MAP and characterised by granulomatous enterocolitis, lymphangitis and lymphadenitis (52). It has a global distribution, with the herd level prevalence in cattle ranging from 0% to 71% (155). It is a major problem for livestock producers. Cows with clinical paratuberculosis produce 19.5% less milk and those with sub-clinical paratuberculosis produce 16% less milk (24).

Paratuberculosis in livestock may also have an impact on human health, with a recent study concluding that current evidence strongly supports a causal relationship between MAP and CD (251).

Detecting infection with MAP before the onset of clinical symptoms, and the associated bacterial shedding, is problematic, and the most cost-effective way of preventing Johne's is by vaccination. The current Gudair™ vaccine is a whole cell preparation of heat-killed MAP which can offer some protection against shedding and mortality (114). However, of the few vaccinated sheep that do go on to develop paratuberculosis, all have the multibacillary form of the disease (185,274).

Once within the macrophage, MAP can prevent the maturation of the macrophage phagosome and may survive in these for several weeks (12,230,252). To do this, the mycobacteria prevent bacterial killing through several mechanisms (230). Antibodies are produced by all animals with multibacillary disease, but only some animals with paucibacillary disease (35,136). In sheep the T cell response is polarised and leads to the observed differences in pathology (36,144,224).

Few studies have been carried out on the expression profiles of sheep infected with MAP, perhaps assuming that the profiles would be similar to those seen in cattle. Overall, little is known about gene expression in

ovine paratuberculosis, and there have been no extensive microarray studies done in this area.

This study aimed to address several of the current concerns about paratuberculosis in sheep. Quantification of the gene expression profiles of sheep with the different pathologies provides a greater understanding of the differences in immune response in these sheep. This in turn may aid the understanding of T cell polarisation and how best to produce a successful response to paratuberculosis vaccine in sheep, and may give insights into other inflammatory bowel diseases, including Crohn's disease in humans.

In order to perform differential gene expression studies accurately, it was first essential to define unambiguously the three pathological forms of paratuberculosis in both histopathological and molecular terms. It was confirmed that the forms of the disease are similar to human leprosy where the pathology can be differentiated into tuberculoid (paucibacillary), lepromatous (multibacillary) and asymptomatic (infected but no pathology) (53). As with ovine paratuberculosis, the tuberculoid form of the disease has lesions formed of infiltrating T cells and contain few bacteria; and the lepromatous form has lesions of infiltrating macrophages containing large numbers of bacteria (164).

The differences between multibacillary and paucibacillary pathologies were easily defined in terms of pathology, but were more ambiguous in individual molecular tests. However, this work has provided the first unambiguous definition of asymptomatic sheep, as having normal ileal histology but being infected with MAP as shown by detection of IS900 by real-time RT-PCR of both ileum and mesenteric lymph node tissues.

These results form the foundation of a robust and useful definition of the three forms of paratuberculosis in sheep and as such will be useful for any future work on paratuberculosis in sheep. In future studies, it would be useful to analysis the cell populations present in these tissues by FACS or immunohistochemistry of the tissue sections. Although the histopathology results clearly show that, for example, there are more macrophages in multibacillary tissue than in paucibacillary tissue, it would nonetheless be helpful to know the relative population sizes of rarer cells, such as eosinophils and NK cells, and apply this knowledge to the gene expression data. A recent study in infected cattle revealed that the regulatory T cell population is expanded in the ileum and could be responsible for suppression of the immune response (268), therefore investigating the relative populations of T cells in these sheep could be valuable. A second avenue for future work in this area would be to look at ELISA score cut-offs in relation to paucibacillary animals. It was observed that paucibacillary animals had higher ELISA scores than asymptomatic animals, even when all were classed as negative as defined by the manufacturer. It would be of value to investigate whether this is the case in younger animals, and could form the basis of an ELISA test able to predict what type of disease is likely to develop.

The second stage of this study looked at the differential expression of a panel of cytokine and non-cytokine genes in ovine paratuberculosis. Despite a large variation in the levels of cytokine transcript expression, the study showed unambiguously that there is a relationship between the three pathological forms of sheep paratuberculosis and cytokine transcript profiles. Secondly, the study confirmed, as has been shown with bovine paratuberculosis (63,138,242), that the paucibacillary and multibacillary forms of the sheep disease are associated with the polarization of the immune response and that polarised Th1 and Th2 cells are associated with paucibacillary and multibacillary pathologies

respectively, when compared to asymptomatic animals. Lastly, these results highlighted that, although the pathologies are associated with immune polarisation, this is not a clear cut difference, with upregulation of the anti-inflammatory cytokine TGF $\beta$  and IFN $\gamma$  in both disease types when compared to control animals.

The gene expression analysis of non-cytokine genes revealed several genes differentially expressed in asymptomatic samples compared to controls, which, when combined with the cytokine gene data, may point towards what constitutes a successful response to MAP infection. This analysis also identified two non-cytokine genes that are differentially expressed in paucibacillary and multibacillary samples and thus may have an impact on what type of disease develops. These genes – CXCR4 and IGFBP6 – were analysed by SNP analysis. However, there was no association between 5 of the 6 SNPs and pathological type. Only the coding region of each gene was analysed in this study, so it may be of value to expand this analysis to include the upstream promoter regions of each gene, as SNPs in this area may be more likely to affect gene expression. A sixth SNP, found in the IGFBP-6 gene, was only found in clinical samples. However, the SNP was only found in 3 out of 20 clinical samples. It may therefore be of value in the future to analyse a large number of sheep to see if any association exists.

Although these studies represent a robust and reproducible quantification of cytokines involved in paratuberculosis pathologies, the method does have several drawbacks. In future it may be more valid to use a cDNA curve, instead of pDNA standards. Also, although absolute quantitation is useful, the copy numbers produced are still relative to the amount of starting material and to the reference gene, and it may thus improve such studies to use a more robust method incorporating relative quantitation.

Preliminary, non-statistical analysis of the relative worm burden in these sheep would suggest that a higher FEC is associated with the development of multibacillary disease and a lower worm burden is associated with development of paucibacillary disease. As animals with both types of disease have inflammation of the intestine, it is unlikely that this is the cause of the higher FEC in multibacillary animals. Having confirmed that the different pathologies are associated with immune response polarisation, future studies could address whether these higher worm burdens are skewing these responses towards a Th2 response, and thus multibacillary paratuberculosis, and whether better control of worm burden in sheep could reduce incidence of multibacillary disease.

The final part of this study involved carrying out the first extensive microarray study on paratuberculosis in sheep. The study identified 63 genes differentially expressed in the different types of disease, with 24, 34 and 21 genes found to be significantly differentially expressed in paucibacillary, multibacillary and asymptomatic samples respectively when compared to controls. 16 genes were identified as differentially expressed in paucibacillary and multibacillary samples. These results were well validated and then used to carry out pathway analysis. This analysis identified several pathways of interest. MAP regulation of the immune response was confirmed, with down-regulation of both MHC molecules and TLR signalling pathways. In addition, several novel pathways were identified for future analysis.

This study was performed using a small focussed array. Compared to a larger array, it was easier to analyse, and more detailed quality control was carried out, reducing the possibility of false positive results. It was also oligo-based, allowing rapid identification of the genes. However, although the results from the array study were robust and interesting, the study had certain limitations. The array concentrates on genes likely

to be involved in immunoinflammatory responses. This introduces problems when the array is used to quantify gene expression in immunoinflammatory diseases, because any change in gene expression will seem relevant to the observed pathology. This false discovery rate is accounted for when the data are normalised, but can be higher than for a less focussed array. The small number of genes analysed on the array also introduces difficulties when carrying the pathway analysis, as commonly only two or three genes from any pathway are represented. Finally, the low sensitivity of the array may lead to a loss of valuable data, as demonstrated by the lack of reproducibility of the real-time results in the array analysis.

Further microarray work on these samples using a large, less focussed array could provide more insights into the immune responses in the different pathologies. A larger array would allow a more extensive systems biology approach to be taken, by including more genes and providing the link between genes involved in the immune response as well as other cellular processes.

## **7.2 Conclusions**

Sheep paratuberculosis is not a spectrum of disease but three distinct pathologies. We produced the first unambiguous definition of these pathologies in both pathological and molecular terms, and revealed that asymptomatic animals are infected and can be distinguished, in terms of cytokine gene expression pattern, from uninfected controls.

The expression level of several cytokine and cytokine related genes in the three forms of ovine paratuberculosis were quantified using real-time PCR analyses and confirmed that sheep pauci- and multibacillary disease are linked to type 1 and type 2 T cell responses respectively, although the pathologies are not as polarised as expected. The expression patterns of

other cytokines shows that both disease forms have an inflammatory aetiology. The central role for IL-1 $\alpha$  in bovine paratuberculosis is not seen in the sheep infection.

We characterised the expression of a panel of non-cytokine genes, revealing several genes differentially expressed in asymptomatic samples compared to controls, which, when combined with the cytokine gene data, point towards what constitutes a controlled response to MAP infection. This analysis identified two non-cytokine genes differentially expressed in paucibacillary and multibacillary samples. Analysis of the sequence of these genes, CXCR4 and IGFBP6, revealed that there is no link between the coding regions and which paratuberculosis pathology develops.

Microarray analysis of the expression of a number of immunoinflammatory genes revealed that, although 63 genes are differentially expressed in the different types of disease, there is no definitive molecular signature for paratuberculosis pathologies. Using these data for pathway analysis identified novel pathways for future studies, including TLR and TCR signalling, complement activation and NK cell cytotoxicity.

## Chapter 8: Bibliography

1. **Abbott, K. A. and R. J. Whittington.** 2003. Monte Carlo simulation of flock-level sensitivity of abattoir surveillance for ovine paratuberculosis. *Preventative Veterinary Medicine* **61**:309-332.
2. **Abubakar, I., D. J. Myhill, A. R. Hart, I. R. Lake, I. Harvey, J. M. Rhodes, R. Robinson, A. J. Lobo, C. S. J. Probert, and P. R. Hunter.** 2007. A Case-Control Study of Drinking Water and Dairy Products in Crohn's Disease--Further Investigation of the Possible Role of *Mycobacterium avium* paratuberculosis. *Am. J. Epidemiol.* **165**:776-783.
3. **Aho, A. D., A. M. McNulty, and P. M. Coussens.** 2003. Enhanced expression of interleukin-1 $\alpha$  and tumor necrosis factor receptor-associated protein 1 in ileal tissues of cattle infected with *Mycobacterium avium* subsp. paratuberculosis. *Infect. Immun.* **71**:6486.
4. **Allen, S., J. Sotos, M. J. Sylte, and C. J. Czuprynski.** 2001. Use of Hoechst 33342 Staining To Detect Apoptotic Changes in Bovine Mononuclear Phagocytes Infected with *Mycobacterium avium* subsp. paratuberculosis. *Clin. Vaccine Immunol.* **8**:460-464.
5. **Alzuhherri, H. M., D. Little, and C. J. Clarke.** 1997. Altered intestinal macrophage phenotype in ovine paratuberculosis. *Research in Veterinary Science* **63**:139-143.
6. **Alzuhherri, H. M., C. J. Woodall, and C. J. Clarke.** 1996. Increased intestinal TNF- $\alpha$ , IL-1b and IL-6 expression in ovine paratuberculosis. *Veterinary Immunology and Immunopathology* **49**:331-345.
7. **Annunziato, F., L. Cosmi, G. Galli, C. Beltrame, P. Romagnani, R. Manetti, S. Romagnani, and E. Maggi.** 1999. Assessment of chemokine receptor expression by human Th1 and Th2 cells in vitro and in vivo. *J Leukoc Biol* **65**:691-699.
8. **Antognoli, M. C., H. L. Hirst, F. B. Garry, and M. D. Salman.** 2007. Immune Response to and Faecal Shedding of *Mycobacterium avium* ssp. paratuberculosis in Young Dairy Calves, and the Association Between Test Results in the Calves and the Infection Status of their Dams. *Zoonoses and Public Health* **54**:152-159.
9. **Autschbach, F., S. Eisold, U. Hinz, S. Zinser, M. Linnebacher, T. Giese, T. Loffler, M. W. Buchler, and J. Schmidt.** 2005. High prevalence of *Mycobacterium avium* subspecies paratuberculosis

- IS900 DNA in gut tissues from individuals with Crohn's disease. *Gut* **54**:944-949.
10. **Ayele, W. Y., M. Bartos, P. Svastova, and I. Pavlik.** 2004. Distribution of *Mycobacterium avium* subsp. *paratuberculosis* in organs of naturally infected bull-calves and breeding bulls. *Veterinary Microbiology* **103**:209-217.
  11. **Ayele, W. Y., P. Svastova, P. Roubal, M. Bartos, and I. Pavlik.** 2005. *Mycobacterium avium* subspecies *paratuberculosis* cultured from locally and commercially pasteurized cow's milk in the Czech Republic. *Appl. Environ. Microbiol.* **71**:1210-1214.
  12. **Bach, H., J. Sun, Z. Hmama, and Y. Av-Gay.** 2006. *Mycobacterium avium* subsp. *paratuberculosis* PtpA Is an Endogenous Tyrosine Phosphatase Secreted during Infection. *Infect. Immun.* **74**:6540-6546.
  13. **Bach, L. A.** 2005. IGFBP-6 five years on; not so 'forgotten'? *Growth Hormone & IGF Research* **15**:185-192.
  14. **Bach, L. A., S. J. Headey, and R. S. Norton.** 2005. IGF-binding proteins - the pieces are falling into place. *Trends in Endocrinology and Metabolism* **16**:228-234.
  15. **Bannantine, J. P., V. Rosu, S. Zanetti, S. Rocca, N. Ahmed, and L. A. Sechi.** Antigenic profiles of recombinant proteins from *Mycobacterium avium* subsp *paratuberculosis* in sheep with Johne's disease. *Veterinary Immunology and Immunopathology* **In Press, Accepted Manuscript.**
  16. **Bannantine, J. P. and J. R. Stabel.** 2007. Killing of *Mycobacterium avium* subspecies *paratuberculosis* within macrophages. *BMC Microbiology* **2**:2.
  17. **Barnes, P. F., S. Lu, J. S. Abrams, E. Wang, M. Yamamura, and R. L. Modlin.** 1993. Cytokine production at the site of disease in human tuberculosis. *Infect. Immun.* **61**:3482-3489.
  18. **Basler, T., S. Jeckstadt, P. Valentin-Weigand, and R. Goethe.** 2006. *Mycobacterium paratuberculosis*, *Mycobacterium smegmatis*, and lipopolysaccharide induce different transcriptional and post-transcriptional regulation of the IRG1 gene in murine macrophages. *J Leukoc Biol* **79**:628-638.
  19. **Bassey, E. O. and M. T. Collins.** 1997. Study of T-lymphocyte subsets of healthy and *Mycobacterium avium* subsp. *paratuberculosis*-infected cattle. *Infect. Immun.* **65**:4869-4872.

20. **Baxter, R. C.** 2001. Changes in the IGF-IGFBP axis in critical illness. *Best Practice & Research Clinical Endocrinology & Metabolism* **15**:421-434.
21. **Beard, P. M., S. M. Rhind, M. C. Sinclair, L. A. Wildblood, K. Stevenson, I. J. McKendrick, J. M. Sharp, and D. G. Jones.** 2000. Modulation of  $\gamma\delta$  T cells and CD1 in *Mycobacterium avium* subsp. paratuberculosis infection. *Veterinary Immunology and Immunopathology* **77**:311-319.
22. **Becker, C., M. C. Fantini, and M. F. Neurath.** 2006. TGF- $\beta$  as a T cell regulator in colitis and colon cancer. *Cytokine & Growth Factor Reviews* **17**:97-106.
23. **Begara-McGorum, I., L. A. Wildblood, C. J. Clarke, K. M. Connor, K. Stevenson, C. J. McInnes, J. M. Sharp, and D. G. Jones.** 1998. Early immunopathological events in experimental ovine paratuberculosis. *Veterinary Immunology and Immunopathology* **63**:265-287.
24. **Benedictus, G., A. A. Dijkhuizen, and J. Stelwagen.** 1987. Economic losses due to paratuberculosis in dairy cattle. *Veterinary Record* **121**:142-146.
25. **Benjamini, Y. and Y. Hochberg.** 1995. Controlling the False Discovery Rate: A Practical and Powerful Approach to Multiple Testing. *Journal of the Royal Statistical Society. Series B (Methodological)* **57**:289-300.
26. **Berger, S., J. P. Bannantine, and T. Griffin.** 2007. Autoreactive antibodies are present in sheep with Johne's disease and cross-react with *Mycobacterium avium* subsp. paratuberculosis antigens. *Microbes and Infection* **9**:963-970.
27. **Berghaus, R. D., T. B. Farver, R. J. Anderson, C. C. Jaravata, and I. A. Gardner.** 2006. Environmental Sampling for Detection of *Mycobacterium avium* ssp. paratuberculosis on Large California Dairies. *J. Dairy Sci.* **89**:963-970.
28. **Bernstein, C. N., M. H. Wang, M. Sargent, S. R. Brant, and M. T. Collins.** 2007. Testing the Interaction between NOD-2 Status and Serological Response to *Mycobacterium paratuberculosis* in Cases of Inflammatory Bowel Disease. *J. Clin. Microbiol.* **45**:968-971.
29. **Bhide, M., E. Chakurkar, L. Tkacikova, S. Barbuddhe, M. Novak, and I. Mikula.** 2005. IS900-PCR-based detection and characterization of *Mycobacterium avium* subsp. paratuberculosis

- from buffy coat of cattle and sheep. *Veterinary Microbiology* **112**:33-41.
30. **Bienvenu, G., D. Seurin, P. Grellier, P. Froment, M. Baudrimont, P. Monget, Y. Le Bouc, and S. Babajko.** 2004. Insulin-Like Growth Factor Binding Protein-6 Transgenic Mice: Postnatal Growth, Brain Development, and Reproduction Abnormalities. *Endocrinology* **145**:2412-2420.
  31. **Bonecchi, R., G. Bianchi, P. P. Bordignon, D. D'Ambrosio, R. Lang, A. Borsatti, S. Sozzani, P. Allavena, P. A. Gray, A. Mantovani, and F. Sinigaglia.** 1998. Differential Expression of Chemokine Receptors and Chemotactic Responsiveness of Type 1 T Helper Cells (Th1s) and Th2s. *J. Exp. Med.* **187**:129-134.
  32. **Brazma, A., P. Hingamp, J. Quackenbush, G. Sherlock, P. Spellman, C. Stoeckert, J. Aach, W. Ansorge, C. A. Ball, H. C. Causton, T. Gaasterland, P. Glenisson, F. C. P. Holstege, I. F. Kim, V. Markowitz, J. C. Matese, H. Parkinson, A. Robinson, U. Sarkans, S. Schulze-Kremer, J. Stewart, R. Taylor, J. Vilo, and M. Vingron.** 2001. Minimum information about a microarray experiment (MIAME) - toward standards for microarray data. *Nat Genet* **29**:365-371.
  33. **Brookes, A. J.** 1999. The essence of SNPs. *Gene* **234**:177-186.
  34. **Bull, T. J., S. C. Gilbert, S. Sridhar, R. Linedale, N. Dierkes, K. Sidi-Boumedine, and J. Hermon-Taylor.** 2007. A Novel Multi-Antigen Virally Vectored Vaccine against *Mycobacterium avium* Subspecies *paratuberculosis*. *PLoS One* **2**:e1229.
  35. **Burrells, C., C. J. Clarke, A. Colston, J. A. Kay, J. Porter, D. Little, and J. M. Sharp.** 1998. A study of immunological responses of sheep clinically-affected with paratuberculosis (Johne's disease): The relationship of blood, mesenteric lymph node and intestinal lymphocyte responses to gross and microscopic pathology. *Veterinary Immunology and Immunopathology* **66**:343-358.
  36. **Burrells, C., C. J. Clarke, A. Colston, J. A. Kay, J. Porter, D. Little, and J. M. Sharp.** 1999. Interferon-gamma and interleukin-2 release by lymphocytes derived from the blood, mesenteric lymph nodes and intestines of normal sheep and those affected with paratuberculosis (Johne's disease). *Veterinary Immunology and Immunopathology* **68**:139-148.
  37. **Buza, J. J., Y. Mori, A. M. Bari, H. Hikono, Aodon-Geril, S. Hirayama, Y. Shu, and E. Momotani.** 2003. *Mycobacterium avium*

- subsp. *paratuberculosis* infection causes suppression of RANTES, monocyte chemoattractant protein 1, and tumor necrosis factor alpha expression in peripheral blood of experimentally infected cattle. *Infect. Immun.* **71**:7223-7227.
38. **Byrd, T. F.** 1998. Multinucleated Giant Cell Formation Induced by IFN- $\gamma$ /IL-3 Is Associated with Restriction of Virulent *Mycobacterium tuberculosis* Cell to Cell Invasion in Human Monocyte Monolayers. *Cellular Immunology* **188**:89-96.
39. **Campbell, D. J., C. H. Kim, and E. C. Butcher.** 2003. Chemokines in the systemic organization of immunity. *Immunological Reviews* **195**:58-71.
40. **Campbell, J. J., G. Haraldsen, J. Pan, J. Rottman, S. Qin, P. Ponath, D. P. Andrew, R. Warnke, N. Ruffing, N. Kassam, L. Wu, and E. C. Butcher.** 1999. The chemokine receptor CCR4 in vascular recognition by cutaneous but not intestinal memory T cells. *Nature* **400**:776-780.
41. **Carrigan, M. J. and J. T. Seaman.** 1990. The pathology of Johne's disease in sheep. *Australian Veterinary Journal* **67**:47-50.
42. **Castellanos, E., A. Aranaz, B. Romero, L. de Juan, J. Alvarez, J. Bezos, S. Rodriguez, K. Stevenson, A. Mateos, and L. Dominguez.** 2007. Polymorphisms in *gyrA* and *gyrB* genes among *Mycobacterium avium* subspecies *paratuberculosis* Types I, II and III. *J. Clin. Microbiol.* **45**:3439-3442.
43. **Cetinkaya, B., K. Egan, D. A. Harbour, and K. L. Morgan.** 1996. An abattoir-based study of the prevalence of subclinical Johne's disease in adult cattle in south west England. *Epidemiol Infect* **116**:373-379.
44. **Chacon, O., L. E. Bermudez, and R. G. Barletta.** 2004. Johne's disease, inflammatory bowel disease and *Mycobacterium paratuberculosis*. *Annual Reviews Microbiology* **58**:329-363.
45. **Chamberlin, W. M. and Naser S.A.** 2006. Integrating theories of the etiology of Crohn's Disease On the etiology of Crohn's Disease: Questioning the Hypotheses. *Medical Science Monitor* **12**:27-33.
46. **Chen, X., B. Zhou, M. Li, Q. Deng, X. Wu, X. Le, C. Wu, N. Larmonier, W. Zhang, H. Zhang, H. Wang, and E. Katsanis.** 2007. CD4+CD25+FoxP3+ regulatory T cells suppress *Mycobacterium tuberculosis* immunity in patients with active disease. *Clinical Immunology* **123**:50-59.

47. **Cheung, C., D. Vesey, A. Cotterill, M. Douglas, G. Gobe, D. Nicol, and D. Johnson.** 2005. Altered messenger RNA and protein expressions for insulin-like growth factor family members in clear cell and papillary renal cell carcinomas. *International Journal of Urology* **12**:17-28.
48. **Chiang, S. K., S. Sommer, A. D. Aho, M. Kiupel, C. Colvin, B. Tooker, and P. M. Coussens.** 2007. Relationship between *Mycobacterium avium* subspecies paratuberculosis, IL-1 $\alpha$ , and TRAF1 in primary bovine monocyte-derived macrophages. *Veterinary Immunology and Immunopathology* **116**:131-144.
49. **Cho, D., S. J. Shin, A. M. Talaat, and M. T. Collins.** 2007. Cloning, expression, purification and serodiagnostic evaluation of fourteen *Mycobacterium paratuberculosis* proteins. *Protein Expression and Purification* **53**:411-420.
50. **Clancy, R., Z. Ren, J. Turton, G. Pang, and A. Wettstein.** 2007. Molecular evidence for *Mycobacterium avium* subspecies paratuberculosis (MAP) in Crohn's disease correlates with enhanced TNF- $\alpha$  secretion. *Digestive and Liver Disease* **39**:445-451.
51. **Clark, J., J. L. Anderson, J. J. Koziczkowski, and J. L. E. Ellingson.** 2006. Detection of *Mycobacterium avium* subspecies paratuberculosis genetic components in retail cheese curds purchased in Wisconsin and Minnesota by PCR. *Molecular and Cellular Probes* **20**:197-202.
52. **Clarke, C. J.** 1997. The pathology and pathogenesis of paratuberculosis in ruminants and other species. *Journal of Comparative Pathology* **116**:217-261.
53. **Clarke, C. J. and D. Little.** 1996. The pathology of ovine paratuberculosis: gross and histological changes in the intestine and other tissues. *Journal of Comparative Pathology* **114**:419-437.
54. **Clemens, D. L.** 1996. Characterization of the *Mycobacterium tuberculosis* phagosome. *Trends in Microbiology* **4**:113-118.
55. **Cocito, C., P. Gilot, M. Coene, M. de Kesel, P. Poupart, and P. Vannuffel.** 1994. Paratuberculosis. *Clin. Microbiol. Rev.* **7**:328-345.
56. **Corpa, J. M., J. Garrido, J. F. García Marín, and V. Pérez.** 2000. Classification of lesions observed in natural cases of paratuberculosis in goats. *Journal of Comparative Pathology* **122**:255-265.

57. **Corpa, J. M., V. Pérez, and J. F. García Marín.** 2000. Differences in the immune responses in lambs and kids vaccinated against paratuberculosis, according to the age of vaccination. *Veterinary Microbiology* **77**:475-485.
58. **Cousins, D. V., R. Whittington, I. Marsh, A. Masters, R. J. Evans, and P. Kluver.** 1999. Mycobacteria distinct from *Mycobacterium avium* subsp. *paratuberculosis* isolated from the faeces of ruminants possess IS 900 -like sequences detectable by IS 900 polymerase chain reaction: implications for diagnosis. *Molecular and Cellular Probes* **13**:431-442.
59. **Coussens P.M., Pudrith C., Skovgaard K., Ren X., Suchyta S., Stabel J., and Heegaard P.** 2005. Johne's disease in cattle is associated with enhanced expression of genes encoding IL-5, GATA-3, tissue inhibitors of matrix metalloproteinases 1 and 2, and factors promoting apoptosis in peripheral blood mononuclear cells. *Veterinary Immunology and Immunopathology* **105**:221-234.
60. **Coussens, P. M., C. J. Colvin, G. J. M. Rosa, J. P. Laspiur, and M. D. Elftman.** 2003. Evidence for a novel gene expression programme in peripheral blood mononuclear cells from *Mycobacterium avium* subsp. *paratuberculosis*-infected cattle. *Infect. Immun.* **71**:6487-6498.
61. **Coussens, P. M., C. J. Colvin, K. Wiersma, A. Abouzied, and S. Sipkovsky.** 2002. Gene expression profiling of peripheral blood mononuclear cells from cattle infected with *Mycobacterium paratuberculosis*. *Infect. Immun.* **70**:5494-5502.
62. **Coussens, P. M., A. Jeffers, and C. J. Colvin.** 2004. Rapid and transient activation of gene expression in peripheral blood mononuclear cells from Johne's disease positive cows exposed to *Mycobacterium paratuberculosis* in vitro. *Microbial Pathogenesis* **36**:93-108.
63. **Coussens, P. M., N. Verman, M. A. Coussens, M. D. Elftman, and A. M. McNulty.** 2004. Cytokine gene expression in peripheral blood mononuclear cells and tissues of cattle infected with *Mycobacterium avium* subsp. *paratuberculosis* : Evidence for an inherent proinflammatory gene expression pattern. *Infect. Immun.* **72**:1409-1422.
64. **Cubillas-Tejeda, A. C., A. Ruiz-Arguelles, G. Bernal-Fernandez, L. Quiroz-Compean, A. Lopez-Davila, E. Reynaga-Hernandez, and R. Gonzalez-Amaro.** 2003. Cytokine Production and Expression of Leucocyte-Differentiation Antigens by Human Mononuclear Cells

- in Response to Mycobacterium tuberculosis Antigens. *Scandinavian Journal of Immunology* **57**:115-124.
65. **Daniels M.J., Lees J.D., Hutchings M.R., and Greig A.** 2003. The ranging behavior and habitat use of rabbits on farmland and their potential role in the epidemiology of paratuberculosis. *The Veterinary Journal* **165**:248-257.
66. **de Juan, L., A. Mateos, L. Domínguez, J. M. Sharp, and K. Stevenson.** 2005. Genetic diversity of Mycobacterium avium subspecies paratuberculosis isolates from goats detected by pulsed-field gel electrophoresis. *Veterinary Microbiology* **106**:249-247.
67. **Denis, M., D. L. Keen, N. A. Parlane, A. K. Storset, and B. M. Buddle.** 2007. Bovine natural killer cells restrict the replication of Mycobacterium bovis in bovine macrophages and enhance IL-12 release by infected macrophages. *Tuberculosis* **87**:53-62.
68. **Dhand, N. K., J. Eppleston, R. J. Whittington, and J. A. Toribio.** 2007. Risk factors for ovine Johne's disease in infected sheep flocks in Australia. *Preventive Veterinary Medicine* **82**:51-71.
69. **Dieguez, F. J., I. Arnaiz, M. L. Sanjuan, M. J. Vilar, M. Lopez, and E. Yus.** 2007. Prevalence of serum antibodies to Mycobacterium avium subsp. paratuberculosis in cattle in Galicia (northwest Spain). *Preventive Veterinary Medicine* **82**:321-326.
70. **Dinarello, C. A.** 1999. IL-18: A TH1-inducing, proinflammatory cytokine and new member of the IL-1 family. *J Allergy Clin Immunol* **103**:11-24.
71. **Dohmann, K., B. Strommenger, K. Stevenson, L. de Juan, J. Stratmann, V. Kapur, T. J. Bull, and G. F. Gerlach.** 2003. Characterization of Genetic Differences between Mycobacterium avium subsp. paratuberculosis Type I and Type II Isolates. *J. Clin. Microbiol.* **41**:5215-5223.
72. **Donaghy, J. A., M. T. Rowe, J. L. W. Rademaker, P. Hammer, L. Herman, V. De Jonghe, B. Blanchard, K. Duhem, and E. Vindel.** 2008. An inter-laboratory ring trial for the detection and isolation of Mycobacterium avium subsp. paratuberculosis from raw milk artificially contaminated with naturally infected faeces. *Food Microbiology* **25**:128-135.
73. **Donaghy, J. A., N. L. Totton, and M. T. Rowe.** 2004. Persistence of Mycobacterium paratuberculosis during Manufacture and Ripening of Cheddar Cheese. *Appl. Environ. Microbiol.* **70**:4899-4905.

74. **Economou, M., T. A. Trikalinos, K. T. Loizou, E. V. Tsianos, and J. P. A. Ioannidis.** 2004. Differential Effects of NOD2 Variants on Crohn's Disease Risk and Phenotype in Diverse Populations: A Metaanalysis. *The American Journal of Gastroenterology* **99**:2393-2404.
75. **Eda, S., J. P. Bannantine, W. R. Waters, Y. Mori, R. H. Whitlock, M. C. Scott, and C. A. Speer.** 2006. A Highly Sensitive and Subspecies-Specific Surface Antigen Enzyme- Linked Immunosorbent Assay for Diagnosis of Johne's Disease. *Clin. Vaccine Immunol.* **13**:837-844.
76. **Eishi, Y., M. Suga, I. Ishige, D. Kobayashi, T. Yamada, T. Takemura, T. Takizawa, M. Koike, S. Kudoh, U. Costabel, J. Guzman, G. Rizzato, M. Gambacorta, R. du Bois, A. G. Nicholson, O. P. Sharma, and M. Ando.** 2002. Quantitative Analysis of Mycobacterial and Propionibacterial DNA in Lymph Nodes of Japanese and European Patients with Sarcoidosis. *J. Clin. Microbiol.* **40**:198-204.
77. **Elliot, S. N. and J. L. Wallace.** 1998. Neutrophil-mediated gastrointestinal injury. *Canadian Journal of Gastroenterology* **12**:559-568.
78. **Emery D.L. and Whittington R.J.** 2004. An evaluation of mycophage therapy, chemotherapy and vaccination for control of *Mycobacterium avium* subsp. *paratuberculosis* infection. *Veterinary Microbiology* **104**:143-155.
79. **Encabo, A., P. Solves, E. Mateu, P. Sepulveda, F. Carbonell-Uberos, and M. D. Minana.** 2004. Selective Generation of Different Dendritic Cell Precursors from CD34+ Cells by Interleukin-6 and Interleukin-3. *Stem Cells* **22**:725-740.
80. **Englund, S., G. Bölske, and K. E. Johansson.** 2002. An IS900-like sequence found in a *Mycobacterium* sp. other than *Mycobacterium avium* subsp. *paratuberculosis*. *FEMS Microbiology Letters* **209**:267-271.
81. **Eppleston J. and Whittington R.J.** 2001. Isolation of *Mycobacterium avium* subsp. *paratuberculosis* from the semen of rams with clinical Johne's disease. *Australian Veterinary Journal* **79**:776-777.
82. **Eppleston, J. and P. A. Windsor.** 2007. Lesions attributed to vaccination of sheep with Gudairtm for the control of ovine

- paratuberculosis: post farm economic impacts at slaughter. *Australian Veterinary Journal* 85:129-133.
83. **Feller, M., K. Huwiler, R. Stephan, E. Altpeter, A. Shang, H. Furrer, G. E. Pfyffer, T. Jemmi, A. Baumgartner, and M. Egger.** 2007. *Mycobacterium avium* subspecies paratuberculosis and Crohn's disease: a systematic review and meta-analysis. *The Lancet Infectious Diseases* 7:607-613.
  84. **Feng, C. G., M. Kaviratne, A. G. Rothfuchs, A. Cheever, S. Hieny, H. A. Young, T. A. Wynn, and A. Sher.** 2006. NK Cell-Derived IFN- $\gamma$  Differentially Regulates Innate Resistance and Neutrophil Response in T Cell-Deficient Hosts Infected with *Mycobacterium tuberculosis*. *J Immunol* 177:7086-7093.
  85. **Fernandez de Mera, I. G., J. M. Perez de la Lastra, P. Ayoubi, V. Naranjo, K. M. Kocan, C. Gortazar, and J. de la Fuente.** 2008. Differential expression of inflammatory and immune response genes in mesenteric lymph nodes of Iberian red deer (*Cervus elaphus hispanicus*) naturally infected with *Mycobacterium bovis*. *Developmental & Comparative Immunology* 32:85-91.
  86. **Frothingham, R.** 1999. Evolutionary bottlenecks in the agents of tuberculosis, leprosy, and paratuberculosis. *Medical Hypotheses* 52:95-99.
  87. **Gollnick, N. S., R. M. Mitchell, M. Baumgart, H. K. Janagama, S. Sreevatsan, and Y. H. Schukken.** 2007. Survival of *Mycobacterium avium* subsp. paratuberculosis in bovine monocyte-derived macrophages is not affected by host infection status but depends on the infecting bacterial genotype. *Veterinary Immunology and Immunopathology* 120:93-105.
  88. **Gonda, M. G., Y. M. Chang, G. E. Shook, M. T. Collins, and B. W. Kirkpatrick.** 2006. Genetic Variation of *Mycobacterium avium* ssp. paratuberculosis Infection in US Holsteins. *J. Dairy Sci.* 89:1804-1812.
  89. **Gonda, M. G., Y. M. Chang, G. E. Shook, M. T. Collins, and B. W. Kirkpatrick.** 2007. Effect of *Mycobacterium paratuberculosis* infection on production, reproduction, and health traits in US Holsteins. *Preventive Veterinary Medicine* 80:103-119.
  90. **González, J., M. V. Geijo, C. García-Pariente, A. Verna, J. M. Corpa, L. E. Reyes, M. C. Ferreras, R. A. Juste, J. F. García Marín, and V. Pérez.** 2005. Histopathological classification of lesions

- associated with natural paratuberculosis infection in cattle. *Journal of Comparative Pathology* **133**:184-196.
91. **Goodfellow, M. and J. G. Magee.** 1997. Taxonomy of Mycobacteria, p. 1-71. *In* P. R. J. Gangadharam and P. A. Jenkins (ed.), *Mycobacteria I Basic Aspects*. Chapman & Hall, New York.
  92. **Gotz, W., S. Lossdorfer, U. Kruger, B. Braumann, and A. Jager.** 2003. Immunohistochemical localization of insulin-like growth factor-II and its binding protein-6 in human epithelial cells of Malassez. *European Journal of Oral Sciences* **111**:26-33.
  93. **Grange, J. M.** 1980. The genus *Mycobacterium*, p. 7-19. *In* *Mycobacterial Diseases*. Edward Arnold, London.
  94. **Grange, J. M.** 1980. The species of mycobacteria, p. 20-31. *In* *Mycobacterial Diseases*. Edward Arnold, London.
  95. **Grant, I. R.** 2005. Zoonotic potential of *Mycobacterium avium* ssp. paratuberculosis: the current position. *Journal of Applied Microbiology* **98**:1282-1293.
  96. **Greenstein, R. J., L. Su, A. Shahidi, and S. T. Brown.** 2007. On the Action of 5-Amino-Salicylic Acid and Sulfapyridine on *M. avium* including Subspecies *paratuberculosis*. *PLoS One* **2**:e516.
  97. **Greenstein, R. J.** 2003. Is Crohn's disease caused by a mycobacterium? Comparisons with leprosy, tuberculosis, and Johne's disease. *The Lancet Infectious Diseases* **3**:507-514.
  98. **Gumber, S., G. Eamens, and R. J. Whittington.** 2006. Evaluation of a Pourquier ELISA kit in relation to agar gel immunodiffusion (AGID) test for assessment of the humoral immune response in sheep and goats with and without *Mycobacterium paratuberculosis* infection. *Veterinary Microbiology* **115**:91-101.
  99. **Gumber, S. and R. J. Whittington.** 2007. Comparison of BACTEC 460 and MGIT 960 systems for the culture of *Mycobacterium avium* subsp. paratuberculosis S strain and observations on the effect of inclusion of ampicillin in culture media to reduce contamination. *Veterinary Microbiology* **119**:42-52.
  100. **Headey, S. J., K. S. Leeding, R. S. Norton, and L. A. Bach.** 2004. Contributions of the N- and C-terminal domains of IGF binding protein-6 to IGF binding. *J Mol Endocrinol* **33**:377-386.
  101. **Heidemann, J., W. Domschke, T. Kucharzik, and C. Maaser.** 2006. Intestinal Microvascular Endothelium and Innate Immunity in

- Inflammatory Bowel Disease: a Second Line of Defense? *Infect. Immun.* **74**:5425-5432.
102. **Hein, W. R., T. Barber, S. Cole, L. Morrison, and A. Pernthaner.** 2004. Long-term collection and characterization of afferent lymph from the ovine small intestine. *Journal of Immunological Methods* **293**:153-168.
103. **Hellemans, J., G. Mortier, A. De Paepe, F. Speleman, and J. Vandesompele.** 2007. qBase relative quantification framework and software for management and automated analysis of real-time quantitative PCR data. *Genome Biology* **8**:R19.
104. **Hendrick S.H., Kelton D.F., Leslie K.E., Lissemore K.D., Archambault M., and Duffield T.F.** 2005. Effect of paratuberculosis on culling, milk production, and milk quality in dairy herds. *Journal of the American Veterinary Medical Association* **227**:1302-1308.
105. **Hines, M. E. and E. L. Styer.** 2003. Preliminary characterization of chemically generated *Mycobacterium avium* subsp. *paratuberculosis* cell wall deficient forms (Spheroplasts). *Veterinary Microbiology* **95**:247-258.
106. **Horuk, R.** 2001. Chemokine receptors. *Cytokine & Growth Factor Reviews* **12**:313-335.
107. **Hoshino, Y., D. B. Tse, G. Rochford, S. Prabhakar, S. Hoshino, N. Chitkara, K. Kuwabara, E. Ching, B. Raju, J. A. Gold, W. Borkowsky, W. N. Rom, R. Pine, and M. Weiden.** 2004. Mycobacterium tuberculosis-Induced CXCR4 and Chemokine Expression Leads to Preferential X4 HIV-1 Replication in Human Macrophages. *J Immunol* **172**:6251-6258.
108. **Hossain, H., S. Tchatalbachev, and T. Chakraborty.** 2006. Host gene expression profiling in pathogen-host interactions. *Current opinion in Immunology* **18**:422-429.
109. **Hostetter, J., E. Steadham, J. S. Haynes, T. B. Bailey, and N. F. Cheville.** 2002. Cytokine effects on maturation of the phagosomes containing *Mycobacterium avium* subsp. *paratuberculosis* in J774 cells. *FEMS Immunology and Medical Microbiology* **34**:127-134.
110. **Hostetter, J., E. Steadham, J. S. Haynes, T. B. Bailey, and N. F. Cheville.** 2003. Phagosomal maturation and intracellular survival of *Mycobacterium avium* subspecies *paratuberculosis* in J774 cells. *Comparative Immunology, Microbiology and Infectious Diseases* **26**:269-283.

111. **Hougardy, J. M., V. Verscheure, C. Locht, and F. Mascart.** 2007. In vitro expansion of CD4+CD25highFOXP3+CD127low/- regulatory T cells from peripheral blood lymphocytes of healthy Mycobacterium tuberculosis-infected humans. *Microbes and Infection* **9**:1325-1332.
112. **Hu, J. S., C. M. Freeman, V. R. Stolberg, B. Chin Chiu, G. J. Bridger, S. P. Fricker, N. W. Lukacs, and S. W. Chensue.** 2006. AMD3465, a Novel CXCR4 Receptor Antagonist, Abrogates Schistosomal Antigen-Elicited (Type-2) Pulmonary Granuloma Formation. *American Journal of Pathology* **169**:424-432.
113. **Huda, A., G. Jungersen, and P. Lind.** 2004. Longitudinal study of interferon-gamma, serum antibody and milk antibody responses in cattle infected with Mycobacterium avium subsp. paratuberculosis. *Veterinary Microbiology* **104**:43-53.
114. **Huntley, J. F., J. Stabel, M. L. Paustian, T. A. Reinhardt, and J. P. Bannatine.** 2005. Expression library immunization confers protection against *Mycobacterium avium* subsp. *paratuberculosis* infection. *Infect. Immun.* **73**:6877-6884.
115. **Ikonomopoulos J., Pavlik I., Bartos M., Svastova P., Ayele W.Y., Roubal P., Lukas J.C., Cook N., and Gazouli M.** 2005. Detection of Mycobacterium avium subsp. paratuberculosis in Retail Cheeses from Greece and the Czech Republic. *Appl. Environ. Microbiol.* **71**:8934-8936.
116. **Ikonomopoulos, J., C. Balaskas, B. Kantzoura, E. Fragiadaki, I. Pavlik, M. Bartos, J. C. Lukas, and M. Gazouli.** 2007. Comparative evaluation of positive tests to Mycobacterium avium subsp. paratuberculosis in clinically healthy sheep and goats in South-West Greece using molecular techniques, serology, and culture. *The Veterinary Journal* **174**:337-343.
117. **Janagama, H. K., i. J. Kwang, V. Kapur, Coussens P.M., and Sreevatsan S.** 2006. Cytokine responses of bovine macrophages to diverse clinical *Mycobacterium avium* subspecies *paratuberculosis* strains . *BMC Microbiology* **6**:10.
118. **Janeway, C. A., P. Travers, M. Walport, and M. Shlomchik.** 2001. *Immunobiology*. Garland Publishing.
119. **Jayachandran, R., V. Sundaramurthy, B. Combaluzier, P. Mueller, H. Korf, K. Huygen, T. Miyazaki, I. Albrecht, J. Massner, and J. Pieters.** 2007. Survival of Mycobacteria in Macrophages Is

- Mediated by Coronin 1-Dependent Activation of Calcineurin. *Cell* **130**:37-50.
120. **Jones, P. H., T. B. Farver, B. Beaman, B. C. etinkaya, and K. L. Morgan.** 2006. Crohn's disease in people exposed to clinical cases of bovine paratuberculosis. *Epidemiol. Infect.* **134**:49-56.
  121. **Jourdan, P., C. Abbal, N. Nora, T. Hori, T. Uchiyama, J. P. Vendrell, J. Bousquet, N. Taylor, J. Pene, and H. Yssel.** 1998. Cutting Edge: IL-4 Induces Functional Cell-Surface Expression of CXCR4 on Human T Cells. *J Immunol* **160**:4153-4157.
  122. **Judge J., Greig A, Kyriazakis I., and Hutchings M.R.** 2005. Ingestion of faeces by grazing herbivores – risk of interspecies disease transmission. *Agriculture, Ecosystems and Environment* **107**:267-274.
  123. **Juffermans, N. P., W. A. Paxton, P. E. P. Dekkers, A. Verbon, E. de Jonge, P. Speelman, S. J. H. van Deventer, and T. van der Poll.** 2000. Up-regulation of HIV coreceptors CXCR4 and CCR5 on CD4+ T cells during human endotoxemia and after stimulation with (myco)bacterial antigens: the role of cytokines. *Blood* **96**:2649-2654.
  124. **Kang, T. J., C. E. Yeum, B. C. Kim, E. Y. You, and G. T. Chae.** 2004. Differential production of interleukin-10 and interleukin-12 in mononuclear cells from leprosy patients with a Toll-like receptor 2 mutation. *Immunology* **112**:674-680.
  125. **Kelley, K. M., Y. Oh, S. E. Gargosky, Z. Gucev, T. Matsumoto, V. Hwa, L. Ng, D. M. Simpson, and R. G. Rosenfeld.** 1996. Insulin-like growth factor-binding proteins (IGFBPs) and their regulatory dynamics. *The International Journal of Biochemistry & Cell Biology* **28**:619-637.
  126. **Kent, P. T. and G. P. Kubica.** 1985. *Public Health Mycobacteriology: A Guide for the Level III Laboratory.* Centers for Disease Control, Atlanta, GA.
  127. **Khalifeh, M. S. and J. Stabel.** 2004. Effects of gamma interferon, interleukin-10 and transforming growth factor on the survival of *Mycobacterium avium* subsp. paratuberculosis in monocyte-derived macrophages from naturally infected cattle. *Infect. Immun.* **72**:1974-1982.
  128. **Khalifeh, M. S. and J. Stabel.** 2004. Upregulation of transforming growth factor-beta and interleukin-10 in cows with clinical Johne's disease. *Veterinary Immunology and Immunopathology* **99**:39-46.

129. **Klein, R. S. and J. B. Rubin.** 2004. Immune and nervous system CXCL12 and CXCR4: parallel roles in patterning and plasticity. *Trends in Immunology* **25**:306-314.
130. **Koets, A., A. Hoek, M. Langelaar, M. B. Overdijk, W. Santema, P. Franken, W. van Eden, and V. Rutten.** 2006. Mycobacterial 70 kD heat-shock protein is an effective subunit vaccine against bovine paratuberculosis. *Vaccine* **24**:2550-2559.
131. **Koets, A., V. Rutten, A. Hoek, F. van Mil, K. Müller, D. Bakker, E. Gruys, and W. van Eden.** 2002. Progressive bovine paratuberculosis is associated with local loss of CD4+ T cells, increased frequency of  $\gamma\delta$  T cells, and related changes in T-cell function. *Infect. Immun.* **70**:3856-3864.
132. **Köhler, H., H. Gyra, K. Zimmer, K. G. Dräger, B. Burkert, B. Lemser, D. Hausleithner, K. Cußler, W. Klawonn, and R. G. Heß.** 2001. Immune reactions in cattle after immunization with a Mycobacterium paratuberculosis vaccine and implications for the diagnosis of M. paratuberculosis and M. bovis infections. *Journal of Veterinary Medicine* **48**:185-195.
133. **Koo, H. C., Y. H. Park, M. J. Hamilton, G. M. Barrington, C. J. Davies, J. B. Kim, J. L. Dahl, W. R. Waters, and W. C. Davis.** 2004. Analysis of the Immune Response to Mycobacterium avium subsp. paratuberculosis in Experimentally Infected Calves. *Infect. Immun.* **72**:6870-6883.
134. **Kostoulas, P., L. Leontides, C. Billinis, G. S. Amiridis, and M. Florou.** 2006. The association of sub-clinical paratuberculosis with the fertility of Greek dairy ewes and goats varies with parity. *Preventive Veterinary Medicine* **74**:226-238.
135. **Kumar, A., T. D. Humphreys, K. N. Kremer, P. S. Bramati, L. Bradfield, C. E. Edgar, and K. E. Hedin.** 2006. CXCR4 Physically Associates with the T Cell Receptor to Signal in T Cells. *Immunity* **25**:213-224.
136. **Kurade, N. P., B. N. Tripathis, K. Rajukumar, and N. S. Parihar.** 2004. Sequential development of histologic lesions and their relationship with bacterial isolation, faecal shedding and immune responses during progressive stages of experimental infection of lambs with Mycobacterium avium subsp. paratuberculosis. *Vet Pathol* **41**:378-387.
137. **Kursar, M., M. Koch, H. W. Mittrucker, G. Nouailles, K. Bonhagen, T. Kamradt, and S. H. E. Kaufmann.** 2007. Cutting Edge:

- Regulatory T Cells Prevent Efficient Clearance of *Mycobacterium tuberculosis*. *J Immunol* **178**:2661-2665.
138. **Langelaar, M., C. N. Weber, M. B. Overdijk, K. Müller, A. Koets, and V. Rutten.** 2005. Cytokine gene expression profiles of bovine dendritic cells after interaction with *Mycobacterium avium* ssp. *paratuberculosis* (M.a.p.), *Escherichia coli* (E. coli) or recombinant M.a.p. heat shock protein 70. *Veterinary Immunology and Immunopathology* **107**:153-161.
139. **Lee, H., J. Stabel, and M. E. Kehrli.** 2001. Cytokine gene expression in ileal tissues of cattle infected with *Mycobacterium paratuberculosis*. *Veterinary Immunology and Immunopathology* **82**:73-85.
140. **Lei, J., C. Wu, X. Wang, and H. Wang.** 2005. p38 MAPK-dependent and YY1-mediated chemokine receptors CCR5 and CXCR4 up-regulation in U937 cell line infected by *Mycobacterium tuberculosis* or *Actinobacillus actinomycetemcomitans*. *Biochemical and Biophysical Research Communications* **329**:610-615.
141. **Lei, L. and J. M. Hostetter.** 2007. Limited phenotypic and functional maturation of bovine monocyte-derived dendritic cells following *Mycobacterium avium* subspecies *paratuberculosis* infection in vitro. *Veterinary Immunology and Immunopathology* **120**:177-186.
142. **Leroy, B., V. Roupie, I. Noël-Georis, V. Rosseels, K. Walravens, M. Govaerts, K. Huygen, and R. Wattiez.** 2007. Antigen discovery: A postgenomic approach to *paratuberculosis* diagnosis. *Proteomics* **7**:1164-1176.
143. **Lillie, R. D.** 1976. *Histopathologic technic and practical histochemistry*. McGraw-Hill, New York.
144. **Little, D., H. M. Alzuherri, and C. J. Clarke.** 1996. Phenotypic characterisation of intestinal lymphocytes in ovine *paratuberculosis* by immunohistochemistry. *Veterinary Immunology and Immunopathology* **55**:175-187.
145. **Loetscher, M., T. Geiser, T. O'Reilly, R. Zwahlen, M. Baggiolini, and B. Moser.** 1994. Cloning of a human seven-transmembrane domain receptor, LESTR, that is highly expressed in leukocytes. *J. Biol. Chem.* **269**:232-237.
146. **Losinger, W. C.** 2005. Economic impact of reduced milk production associated with Johne's disease on dairy operations in the USA. *Journal of Dairy Research* **72**:1-8.

147. **Mackintosh C.G., Labes R.E., R. G. Clark, de Lisle G.W., and J. F. T. Griffin.** 2007. Experimental infections in young red deer (*Cervus elaphus*) with a bovine and an ovine strain of *Mycobacterium avium* subsp *paratuberculosis*. *New Zealand Veterinary Journal* **55**:23-29.
148. **Mackintosh C.G., Labes R.E., and Griffin J.F.** 2005. The effect of Johne's vaccination on tuberculin testing in farmed red deer (*Cervus elaphus*). *New Zealand Veterinary Journal* **53**:216-222.
149. **Marri, P. R., J. P. Bannantine, and G. B. Golding.** 2006. Comparative genomics of metabolic pathways in *Mycobacterium* species: gene duplication, gene decay and lateral gene transfer. *FEMS Microbiology Reviews* **30**:906-925.
150. **Martin, J. L., J. A. Coverley, and R. C. Baxter.** 1994. Regulation of immunoreactive insulin-like growth factor binding protein- 6 in normal and transformed human fibroblasts. *J. Biol. Chem.* **269**:11470-11477.
151. **McKenna, S. L. B., H. W. Barkema, G. P. Keefe, and D. C. Sockett.** 2006. Agreement between three ELISAs for *Mycobacterium avium* subsp. *paratuberculosis* in dairy cattle. *Veterinary Microbiology* **114**:285-291.
152. **McKenna, S. L. B., G. P. Keefe, H. W. Barkema, and D. C. Sockett.** 2005. Evaluation of three ELISAs for *Mycobacterium avium* subsp. *paratuberculosis* using tissue and fecal culture as comparison standards. *Veterinary Microbiology* **110**:105-111.
153. **Molina, J. M., A. Anguiano, and O. Ferrer.** 1995. Study on immune response of goats vaccinated with a live strain of *Mycobacterium paratuberculosis*. *Comparative Immunology, Microbiology and Infectious Diseases* **19**:9-15.
154. **Moravkova, M., P. Hlozek, V. Beran, I. Pavlik, S. Preziuso, V. Cuteri, and M. Bartos.** Strategy for the detection and differentiation of *Mycobacterium avium* species in isolates and heavily infected tissues. *Research in Veterinary Science* **In Press, Corrected Proof**.
155. **Mortensen, H., S. S. Nielsen, and P. Berg.** 2004. Genetic variation and heritability of the antibody response to *Mycobacterium avium* subspecies *paratuberculosis* in Danish Holstein cows. *J. Dairy Sci.* **87**:2108-2113.

156. **Mosmann, T. R. and R. L. Coffman.** 1989. TH1 and TH2 Cells: Different Patterns of Lymphokine Secretion Lead to Different Functional Properties. *Annual Review of Immunology* **7**:145-173.
157. **Motiwala A.S., Amonsin A., Strother M., Manning E.J.B., Kapur V., and Sreevatsan S.** 2004. Molecular epidemiology of *Mycobacterium avium* subsp. *paratuberculosis* isolates recovered from wild animal species. *J. Clin. Microbiol.* **42**:1703-1712.
158. **Motiwala, A. S., H. K. Janagama, M. L. Paustian, X. Zhu, J. P. Bannantine, V. Kapur, and S. Sreevatsan.** 2006. Comparative Transcriptional Analysis of Human Macrophages Exposed to Animal and Human Isolates of *Mycobacterium avium* Subspecies *paratuberculosis* with Diverse Genotypes. *Infect. Immun.* **74**:6046-6056.
159. **Motiwala, A. S., L. Li, V. Kapur, and S. Sreevatsan.** 2006. Current understanding of the genetic diversity of *Mycobacterium avium* subsp. *paratuberculosis*. *Microbes and Infection* **8**:1406-1418.
160. **Muehlinghaus, G., L. Cigliano, S. Huehn, A. Peddinghaus, H. Leyendeckers, A. E. Hauser, F. Hiepe, A. Radbruch, S. Arce, and R. A. Manz.** 2005. Regulation of CXCR3 and CXCR4 expression during terminal differentiation of memory B cells into plasma cells. *Blood* **105**:3965-3971.
161. **Mullerad, J., A. Hovav, R. Nahary, Y. Fishman, and H. Bercovier.** 2003. Immunogenicity of a 16.7 kDa *Mycobacterium paratuberculosis* antigen. *Microbial Pathogenesis* **34**:81-90.
162. **Munjal, S. K., B. N. Tripathi, O. P. Paliwal, J. Boehmer, and M. Homuth.** 2007. Application of Different Methods for the Diagnosis of Experimental Paratuberculosis in Goats. *Zoonoses and Public Health* **54**:140-146.
163. **Muskens J., Bakker D., de Boer J., and van Keulen L.** 2001. Paratuberculosis in sheep: its possible role in the epidemiology of paratuberculosis in cattle. *Veterinary Microbiology* **78**:101-109.
164. **Myrvang, B., T. Godal, Ridley.D.S., S. S. Fröland, and Y. K. Song.** 1973. Immune responsiveness to *Mycobacterium leprae* and other mycobacterial antigens throughout the clinical and histopathological spectrum of leprosy. *Clinical & Experimental Immunology* **14**:541-553.
165. **Nagata, R., Y. Muneta, K. Yoshihara, Y. Yokomizo, and Y. Mori.** 2005. Expression cloning of gamma interferon-inducing antigens of

- Mycobacterium avium* subsp. *Paratuberculosis*. *Infect. Immun.* **73**:3778-3782.
166. **Nalubamba, K., J. Smeed, A. Gossner, C. Watkins, R. Dalziel, and J. Hopkins.** 2008. Differential expression of pattern recognition receptors in the three pathological forms of sheep paratuberculosis. *Microbes and Infection* **10**:598-604.
167. **Naser, S. A., G. Ghobrial, C. Romero, and J. F. Valentine.** 2004. Culture of *Mycobacterium avium* subspecies *paratuberculosis* from the blood of patients with Crohn's disease. *Lancet* **364**:1039-1044.
168. **Nebbia, P., P. Robino, S. Zoppi, and D. De Meneghi.** 2005. Detection and excretion pattern of *Mycobacterium avium* subspecies *paratuberculosis* in milk of asymptomatic sheep and goats by nested-PCR. *Small Ruminant Research* **66**:116-120.
169. **Nedrow, A. J., J. Gavalchin, M. C. Smith, S. M. Stehman, J. K. Maul, S. P. McDonough, and M. L. Thonney.** 2007. Antibody and skin-test responses of sheep vaccinated against Johne's Disease. *Veterinary Immunology and Immunopathology* **116**:109-112.
170. **Neill, S. D., R. A. Skuce, and J. M. Pollock.** 2007. Tuberculosis – new light from an old window. *Journal of Applied Microbiology* **98**:1261-1269.
171. **Nielsen, S. S. and N. Toft.** 2006. Age-Specific Characteristics of ELISA and Fecal Culture for Purpose-Specific Testing for Paratuberculosis. *J. Dairy Sci.* **89**:569-579.
172. **Norby, B., G. T. Fosgate, E. J. B. Manning, M. T. Collins, and A. J. Roussel.** 2007. Environmental mycobacteria in soil and water on beef ranches: Association between presence of cultivable mycobacteria and soil and water physicochemical characteristics. *Veterinary Microbiology* **124**:153-159.
173. **North, R. J. and Y. J. Jung.** 2004. Immunity to Tuberculosis. *Annual Review of Immunology* **22**:599-623.
174. **O'Brien, R., C. G. Mackintosh, D. Bakker, M. Kopečna, I. Pavlik, and J. F. T. Griffin.** 2006. Immunological and Molecular Characterization of Susceptibility in Relationship to Bacterial Strain Differences in *Mycobacterium avium* subsp. *paratuberculosis* Infection in the Red Deer (*Cervus elaphus*). *Infect. Immun.* **74**:3530-3537.

175. **Ott, S. L., S. J. Wells, and B. A. Wagner.** 1999. Herd-level economic losses associated with Johne's disease on US dairy operations. *Preventative Veterinary Medicine* **40**:179-192.
176. **Patterson, B. K., M. Czerniewski, J. Andersson, Y. Sullivan, F. Su, D. Jiyamapa, Z. Burki, and A. Landay.** 1999. Regulation of CCR5 and CXCR4 Expression by Type 1 and Type 2 Cytokines: CCR5 Expression Is Downregulated by IL-10 in CD4-Positive Lymphocytes. *Clinical Immunology* **91**:254-262.
177. **Pavlik, I., L. Matlova, J. Bartl, P. Svastova, L. Dvorska, and R. Whitlock.** 2000. Parallel faecal and organ *Mycobacterium avium* subsp. *paratuberculosis* culture of different productivity types of cattle. *Veterinary Microbiology* **77**:309-324.
178. **Pavlik, I., A. Horvathova, L. Dvorska, J. Bartl, P. Svastova, R. du Maine, and I. Rychlik.** 1999. Standardisation of restriction fragment length polymorphism analysis for *Mycobacterium avium* subspecies *paratuberculosis*. *Journal of Microbiological Methods* **38**:155-167.
179. **Penton-Rol, G., N. Polentarutti, W. Luini, A. Borsatti, R. Mancinelli, A. Sica, S. Sozzani, and A. Mantovani.** 1998. Selective Inhibition of Expression of the Chemokine Receptor CCR2 in Human Monocytes by IFN- $\gamma$ . *J Immunol* **160**:3869-3873.
180. **Pickup, R. W., G. Rhodes, T. J. Bull, S. Arnott, K. Sidi-Boumedine, M. Hurley, and J. Hermon-Taylor.** 2006. *Mycobacterium avium* subsp. *paratuberculosis* in Lake Catchments, in River Water Abstracted for Domestic Use, and in Effluent from Domestic Sewage Treatment Works: Diverse Opportunities for Environmental Cycling and Human Exposure. *Appl. Environ. Microbiol.* **72**:4067-4077.
181. **Pieters, J.** 2001. Evasion of host cell defense mechanisms by pathogenic bacteria. *Current opinion in Immunology* **13**:37-44.
182. **Pinedo, P. J., C. D. Buergelt, R. Wu, G. A. Donovan, J. E. Williams, P. G. Melendez, L. Morel, and D. O. Rae.** 2007. Association between two polymorphisms in the bovine CARD15/NOD2 gene and *paratuberculosis* infection in Florida dairy and beef cattle, *In* 9th International Colloquium on *Paratuberculosis*.
183. **Rajya, B. S. and C. M. Singh.** 1961. Studies on the Pathology of Johne's Disease in Sheep III. Pathologic Changes in Sheep with Naturally Occuring Infections. *American Journal of Veterinary Research* **22**:189-203.

184. **Raupach, B. and S. H. E. Kaufmann.** 2001. Immune responses to intracellular bacteria. *Current opinion in Immunology* **13**:417-428.
185. **Reddacliff, L., J. Eppleston, P. Windsor, R. Whittington, and S. Jones.** 2006. Efficacy of a killed vaccine for the control of paratuberculosis in Australian sheep flocks. *Veterinary Microbiology* **115**:77-90.
186. **Reddacliff, L. A., S. J. McClure, and R. J. Whittington.** 2004. Immunoperoxidase studies of cell mediated immune effector cell populations in early *Mycobacterium avium* subsp. paratuberculosis infection in sheep. *Veterinary Immunology and Immunopathology* **97**:149-162.
187. **Reddacliff, L. A. and R. J. Whittington.** 2003. Experimental infection of weaner sheep with S strain *Mycobacterium avium* subspecies paratuberculosis. *Veterinary Microbiology* **96**:247-258.
188. **Reimers, M. and J. Weinstein.** 2005. Quality assessment of microarrays: Visualization of spatial artifacts and quantitation of regional biases. *BMC Bioinformatics* **6**:166.
189. **Ristow, P., C. D. Marassi, A. B. Rodrigues, W. M. Oelemann, F. Rocha, A. S. O. Santos, E. C. Q. Carvalho, C. B. Carvalho, R. Ferreira, L. S. Fonseca, and W. Lilenbaum.** 2007. Diagnosis of paratuberculosis in a dairy herd native to Brazil. *The Veterinary Journal* **174**:432-434.
190. **Robertson, M. J.** 2002. Role of chemokines in the biology of natural killer cells. *J Leukoc Biol* **71**:173-183.
191. **Roupaka, S.** 2004. Functional Genomics of Ovine Johne's Disease. MSc Thesis The University of Edinburgh.
192. **Rowe, M. T. and I. R. Grant.** 2006. *Mycobacterium avium* ssp. paratuberculosis and its potential survival tactics. *Letters in Applied Microbiology* **42**:305-311.
193. **Ruiz, O., C. Manzano, M. Iriondo, J. Garrido, R. Juste, and A. Estonba.** 2007. Genetic association study between bovine NRAMP1 and CARD15 genes and infection by *M.a.paratuberculosis*, *In* 9th International Colloquium on Paratuberculosis.
194. **Sallusto, F., A. Lanzavecchia, and C. R. Mackay.** 1998. Chemokines and chemokine receptors in T-cell priming and Th1/Th2-mediated responses. *Immunology Today* **19**:568-574.

195. **Sato, M., K. Iwakabe, S. Kimura, and T. Nishimura.** 1999. Functional skewing of bone marrow-derived dendritic cells by Th1- or Th2-inducing cytokines. *Immunology Letters* **67**:63-68.
196. **Saunders, B. M. and A. M. Cooper.** 2000. Restraining mycobacteria: Role of granulomas in mycobacterial infections. *Immunology and Cell Biology* **78**:334-341.
197. **Scanu, A. M., T. J. Bull, S. Cannas, J. D. Sanderson, L. A. Sechi, G. Dettori, S. Zanetti, and J. Hermon-Taylor.** 2007. Mycobacterium avium subspecies paratuberculosis infection in Irritable Bowel Syndrome and comparison with Crohn's and Johnne's diseases: common neural and immune pathogenicity. *J. Clin. Microbiol.* **45**:3883-3890.
198. **Schena, M., R. A. Heller, T. P. Theriault, K. Konrad, E. Lachenmeier, and R. W. Davis.** 1998. Microarrays: biotechnology's discovery platform for functional genomics. *Trends in Biotechnology* **16**:301-306.
199. **Schleig, P. M., C. D. Buergelt, J. K. Davis, E. Williams, G. R. G. Monif, and M. K. Davidson.** 2005. Attachment of Mycobacterium avium subspecies paratuberculosis to bovine intestinal organ cultures: Method development and strain differences. *Veterinary Microbiology* **108**:263-270.
200. **Schmid, M., K. Fellermann, P. Fritz, O. Wiedow, E. F. Stange, and J. Wehkamp.** 2007. Attenuated induction of epithelial and leukocyte serine antiproteases elafin and secretory leukocyte protease inhibitor in Crohn's disease. *J Leukoc Biol* **81**:907-915.
201. **Schorey, J. S., M. C. Carroll, and E. J. Brown.** 1997. A Macrophage Invasion Mechanism of Pathogenic Mycobacteria. *Science* **277**:1091-1093.
202. **Schroeder, A., O. Mueller, S. Stocker, R. Salowsky, M. Leiber, M. Gassmann, S. Lightfoot, W. Menzel, M. Granzow, and T. Ragg.** 2006. The RIN: an RNA integrity number for assigning integrity values to RNA measurements. *BMC Molecular Biology* **7**:3.
203. **Scott-Browne, J. P., S. Shafiani, G. Tucker-Heard, K. Ishida-Tsubota, J. D. Fontenot, A. Y. Rudensky, M. J. Bevan, and K. B. Urdahl.** 2007. Expansion and function of Foxp3-expressing T regulatory cells during tuberculosis. *J. Exp. Med.* **204**:2159-2169.
204. **Sebastiani, S., P. Allavena, C. Albanesi, F. Nasorri, G. Bianchi, C. Traidl, S. Sozzani, G. Girolomoni, and A. Cavani.** 2001. Chemokine

- Receptor Expression and Function in CD4+ T Lymphocytes with Regulatory Activity. *J Immunol* **166**:996-1002.
205. **Sechi, L. A., M. Gazouli, L. E. Sieswerda, P. Molicotti, N. Ahmed, J. Ikonopoulou, A. M. Scanu, D. Paccagnini, and S. Zanetti.** 2006. Relationship between Crohn's disease, infection with *Mycobacterium avium* subspecies *paratuberculosis* and SLC11A1 gene polymorphisms in Sardinian patients. *World Journal of Gastroenterology* **12**:7161-7164.
206. **Sechi, L. A., L. Mara, P. Cappai, R. Frothingam, S. Ortu, A. Leoni, N. Ahmed, and S. Zanetti.** 2006. Immunization with DNA vaccines encoding different mycobacterial antigens elicits a Th1 type immune response in lambs and protects against *Mycobacterium avium* subspecies *paratuberculosis* infection. *Vaccine* **24**:229-235.
207. **Sechi, L. A., A. M. Scanu, P. Molicotti, S. Cannas, M. Mura, G. Dettori, G. Fadda, and S. Zanetti.** 2005. Detection and isolation of *Mycobacterium avium* subspecies *paratuberculosis* from intestinal mucosal biopsies of patients with and without Crohn's disease in Sardinia. *American Journal of Gastroenterology* **100**:1529-1536.
208. **Sechi, L. A., A. Ruehl, N. Ahmed, D. Usai, D. Paccagnini, G. E. Felis, and S. Zanetti.** 2007. *Mycobacterium avium* subspecies *paratuberculosis* infects and multiplies in enteric glial cells. *World Journal of Gastroenterology* **13**:5731-5735.
209. **Secott, T. E., T. L. Lin, and C. C. Wu.** 2001. Fibronectin Attachment Protein Homologue Mediates Fibronectin Binding by *Mycobacterium avium* subsp. *paratuberculosis*. *Infect. Immun.* **69**:2075-2082.
210. **Secott, T. E., T. L. Lin, and C. C. Wu.** 2002. Fibronectin Attachment Protein Is Necessary for Efficient Attachment and Invasion of Epithelial Cells by *Mycobacterium avium* subsp. *paratuberculosis*. *Infect. Immun.* **70**:2670-2675.
211. **Secott, T. E., T. L. Lin, and C. C. Wu.** 2004. *Mycobacterium avium* subsp. *Paratuberculosis* fibronectin attachment protein facilitates M-cell targeting and invasion through a fibronectin bridge with host integrins. *Infect. Immun.* **72**:3724-3732.
212. **Selby, W., P. Pavli, B. Crotty, T. Florin, G. Radford-Smith, P. Gibson, B. Mitchell, W. Connell, R. Read, M. Merrett, H. Ee, and D. Hetzel.** 2007. Two-Year Combination Antibiotic Therapy With Clarithromycin, Rifabutin, and Clofazimine for Crohn's Disease. *Gastroenterology* **132**:2313-2319.

213. **Sevilla, I., J. Garrido, M. Geijo, and R. Juste.** 2007. Pulsed-field gel electrophoresis profile homogeneity of *Mycobacterium avium* subsp. *paratuberculosis* isolates from cattle and heterogeneity of those from sheep and goats. *BMC Microbiology* 7:18.
214. **Sharma, G., S. V. Singh, I. Sevilla, A. V. Singh, R. J. Whittington, R. A. Juste, S. Kumar, V. K. Gupta, P. K. Singh, J. S. Sohal, and V. S. Vihan.** Evaluation of indigenous milk ELISA with m-culture and m-PCR for the diagnosis of Bovine Johne's disease (BJD) in lactating Indian dairy cattle. *Research in Veterinary Science* **In Press, Corrected Proof.**
215. **Sheridan, C., M. Sadaria, P. Bhat-Nakshatri, J. Goulet, H. J. Edenberg, B. P. McCarthy, C. H. Chang, E. F. Srour, and H. Nakshatri.** 2006. Negative regulation of MHC class II gene expression by CXCR4. *Experimental Hematology* 34:1085-1092.
216. **Sigurðardóttir, Ó. G., A. M. Bakke-McKellep, B. Dønnea, and Ø. Evensen.** 2005. *Mycobacterium avium* subsp. *Paratuberculosis* enters the small intestinal mucosa of goat kids in areas with and without Peyer's patches as demonstrated with the everted sleeve method. *Comparative Immunology, Microbiology and Infectious Diseases* 28:223-230.
217. **Sigurðardóttir, Ó. G., C. M. Press, and Ø. Evensen.** 2001. Uptake of *Mycobacterium avium* subsp. *paratuberculosis* through the distal small intestinal mucosa in goats: an ultrastructural study. *Vet Pathol* 38:184-189.
218. **Sigurðardóttir, Ó. G., M. Valheim, and C. M. Press.** 2004. Establishment of *Mycobacterium avium* subsp. *paratuberculosis* infection in the intestine of ruminants. *Advanced Drug Delivery Reviews* 56:819-834.
219. **Simutis, F. J., D. E. Jones, and J. M. Hostetter.** 2007. Failure of antigen-stimulated  $\gamma\delta$  T cells and CD4+ T cells from sensitized cattle to upregulate nitric oxide and mycobactericidal activity of autologous *Mycobacterium avium* subsp. *paratuberculosis*-infected macrophages. *Veterinary Immunology and Immunopathology* 116:1-12.
220. **Singh, A. V., S. V. Singh, G. K. Makharia, P. K. Singh, and J. S. Sohal.** 2008. Presence and characterization of *Mycobacterium avium* subspecies *paratuberculosis* from clinical and suspected cases of Crohn's disease and in the healthy human population in India. *International Journal of Infectious Diseases* 12:190-197.

221. **Singh, S. V., P. K. Singh, A. V. Singh, J. S. Sohal, V. K. Gupta, and V. S. Vihan.** 2007. Comparative efficacy of an indigenous 'inactivated vaccine' using highly pathogenic field strain of *Mycobacterium avium* subspecies paratuberculosis 'Bison type' with a commercial vaccine for the control of Capri-paratuberculosis in India. *Vaccine* **41**:41-7102.
222. **Singh, U. P., S. Singh, R. Singh, R. K. Karls, F. D. Quinn, M. E. Potter, and J. W. Lillard, Jr.** 2007. Influence of *Mycobacterium avium* subsp. paratuberculosis on Colitis Development and Specific Immune Responses during Disease. *Infect. Immun.* **75**:3722-3728.
223. **Skovgaard, K., S. N. Grell, P. M. H. Heegaard, G. Jungersen, C. B. Pudrith, and P. M. Coussens.** 2006. Differential expression of genes encoding CD30L and P-selectin in cattle with Johnne's disease: Progress toward a diagnostic gene expression signature. *Veterinary Immunology and Immunopathology* **112**:210-224.
224. **Smeed, J. A., C. A. Watkins, S. M. Rhind, and J. Hopkins.** 2007. Differential cytokine gene expression profiles in the three pathological forms of sheep paratuberculosis. *BMC Veterinary Research* **3**:18.
225. **Sohal, J. S., S. V. Singh, S. Subodh, N. Sheoran, K. Narayanasamy, P. K. Singh, A. V. Singh, and A. Maitra.** *Mycobacterium avium* subspecies paratuberculosis diagnosis and geno-typing: Genomic insights. *Microbiological Research* **In Press, Corrected Proof.**
226. **Souza, C. D., O. A. Evanson, S. Sreevatsan, and D. J. Weiss.** 2007. Cell membrane receptors on bovine mononuclear phagocytes involved in phagocytosis of *Mycobacterium avium* subsp paratuberculosis. *American Journal of Veterinary Research* **68**:975-980.
227. **Souza, C. D., O. A. Evanson, and D. J. Weiss.** 2006. Mitogen activated protein kinase38 pathway is an important component of the anti-inflammatory response in *Mycobacterium avium* subsp. paratuberculosis-infected bovine monocytes. *Microbial Pathogenesis* **41**:59-66.
228. **Souza, C. D., O. A. Evanson, and D. J. Weiss.** 2007. Role of the mitogen-activated protein kinase pathway in the differential response of bovine monocytes to *Mycobacterium avium* subsp. paratuberculosis and *Mycobacterium avium* subsp. avium. *Microbes and Infection* **9**:1545-1552.

229. **Souza, C. D., O. A. Evanson, and D. J. Weiss.** 2008. Role of cell membrane receptors in the suppression of monocyte anti-microbial activity against *Mycobacterium avium* subsp. *paratuberculosis*. *Microbial Pathogenesis* **44**:215-223.
230. **Stabel, J.** 2000. Transitions in immune response to *Mycobacterium paratuberculosis*. *Veterinary Microbiology* **77**:465-473.
231. **Stamp, J. T. and J. A. Watt.** 1954. Johne's Disease in Sheep. *Journal of Comparative Pathology* **64**:26-39.
232. **Stevenson, K. and J. M. Sharp.** 1997. The contribution of molecular biology to *Mycobacterium avium* subspecies *paratuberculosis* research. *The Veterinary Journal* **153**:269-286.
233. **Stevenson, K., V. M. Hughes, L. de Juan, N. F. Inglis, F. Wright, and J. M. Sharp.** 2002. Molecular Characterization of Pigmented and Nonpigmented Isolates of *Mycobacterium avium* subsp. *paratuberculosis*. *J. Clin. Microbiol.* **40**:1798-1804.
234. **Stewart W.C., Pollock K.G.J., Browning L.M., Young D., Smith-Palmer A., and Reilly W.J.** 2005. Survey of zoonoses recorded in Scotland between 1993 and 2002. *Veterinary Record* **157**:697-702.
235. **Stewart, D. J., J. A. Vaughan, P. L. Stiles, P. J. Noske, M. L. V. Tizard, S. J. Prowse, W. P. Michalski, K. L. Butler, and S. L. Jones.** 2004. A long-term study in Merino sheep experimentally infected with *Mycobacterium avium* subspecies *paratuberculosis*: clinical disease, faecal culture and immunological studies. *Veterinary Microbiology* **104**:165-178.
236. **Stewart, D. J., J. A. Vaughan, P. L. Stiles, P. J. Noske, M. L. V. Tizard, S. J. Prowse, W. P. Michalski, K. L. Butler, and S. L. Jones.** 2005. A long-term study in Angora goats experimentally infected with *Mycobacterium avium* subsp. *paratuberculosis*: Clinical disease, faecal culture and immunological studies. *Veterinary Microbiology* **113**:13-24.
237. **Stewart, D. J., J. A. Vaughan, P. L. Stiles, P. J. Noske, M. L. V. Tizard, S. J. Prowse, W. P. Michalski, K. L. Butler, and S. L. Jones.** 2007. A long-term bacteriological and immunological study in Holstein-Friesian cattle experimentally infected with *Mycobacterium avium* subsp. *paratuberculosis* and necropsy culture results for Holstein-Friesian cattle, Merino sheep and Angora goats. *Veterinary Microbiology* **122**:83-96.
238. **Stott A.W., Jones G.M., Humphry R.W., and Gunn G.J.** 2005. Financial incentive to control paratuberculosis (Johne's disease) on

- dairy farms in the United Kingdom. *The Veterinary Record* **156**:825-831.
239. **Strickland S.J., Scott H.M., Libal M.C., Roussel A.J., and Jordan E.R.** 2005. Effects of seasonal climatic conditions on the diagnosis of *Mycobacterium avium* subspecies *paratuberculosis* in dairy cattle. *Journal of Dairy Science* **88**:2432-2440.
240. **Sweeny R.W., Uzonna J., Whitlock R.H., Habecker P.L., Chilton P., and Scott P.** 2005. Tissue predilection sites and effect of dose on *Mycobacterium avium* subs. *paratuberculosis* organism recovery in a short-term bovine experimental oral infection model. *Research in Veterinary Science* **80**:253-259.
241. **Taguchi, T., H. Takenouchi, J. Matsui, W. R. Tang, M. Itagaki, Y. Shiozawa, K. Suzuki, S. Sakaguchi, Y. U. Ktagiri, and T. Takahashi.** 2006. Involvement of insulin-like growth factor-I and insulin-like growth factor binding proteins in pro-B-cell development. *Experimental Hematology* **34**:508-518.
242. **Tanaka, S., M. Sato, T. Onitsuka, H. Kamata, and Y. Yokomizo.** 2005. Inflammatory cytokine gene expression in different types of granulomatous lesions during asymptomatic stages of bovine *paratuberculosis*. *Vet Pathol* **42**:579-588.
243. **Texereau, J., J. D. Chiche, W. Taylor, G. Choukroun, B. Comba, and J. P. Mira.** 2005. The Importance of Toll-Like Receptor 2 Polymorphisms in Severe Infections. *Clin Infect Dis* **41**:S408-S415.
244. **Thorel, M. F., M. Krichevsky, and V. V. Lévy-Frébault.** 1990. Numerical taxonomy of mycobactin-dependent mycobacteria, emended description of *Mycobacterium avium*, and description of *Mycobacterium avium* subsp. *avium* subsp. nov., *Mycobacterium avium* subsp. *paratuberculosis* subsp. nov., and *Mycobacterium avium* subsp. *silvaticum* subsp. nov. *International Journal of Systemic Bacteriology* **40**:254-260.
245. **Titus, R. G., B. Sherry, and A. Cerami.** 2007. The involvement of TNF, IL-1 and IL-6 in the immune response to protozoan parasites. *Immunology Today* **12**:13-16.
246. **Tiwari A., Van Leeuwen J.A., Dohoo I.R., Stryhn H., Keefe G.P., and Haddad J.P.** 2005. Effects of seropositivity for bovine leukemia virus, bovine viral diarrhoea virus, *Mycobacterium avium* subspecies *paratuberculosis*, and *Neospora caninum* on culling in dairy cattle in four Canadian provinces. *Veterinary Microbiology* **30**:147-158.

247. **Tooker, B. C. and P. M. Coussens.** 2004. Phagocytosis of *M. paratuberculosis* fails to activate expression of NADH dehydrogenase and nucleolin-related protein in bovine macrophages. *Immunology Letters* **93**:137-142.
248. **Tripathi, B. N., S. Periasamy, O. P. Paliwal, and N. Singh.** 2006. Comparison of IS900 tissue PCR, bacterial culture, johnin and serological tests for diagnosis of naturally occurring paratuberculosis in goats. *Veterinary Microbiology* **116**:129-137.
249. **Twort, F. W. and G. L. Y. Ingram.** 1912. A Method for Isolating and Cultivating the *Mycobacterium enteritidis chronicae pseudotuberculosis bovis*, Johne, and some Experiments on the Preparation of a Diagnostic Vaccine for Pseudo-tuberculous Enteritis of Bovines. *Proceedings of the Royal Society of London Series B* **84**:517-542.
250. **Uchida, Y., K. Kurasawa, H. Nakajima, N. Nakagawa, E. Tanabe, M. Sueishi, Y. Saito, and I. Iwamoto.** 2001. Increase of dendritic cells of type 2 (DC2) by altered response to IL-4 in atopic patients. *Journal of Allergy and Clinical Immunology* **108**:1005-1011.
251. **Uzoigwe, J. C., M. L. Khaitza, and P. S. Gibbs.** 2007. Epidemiological evidence for *Mycobacterium avium* subspecies *paratuberculosis* as a cause of Crohn's disease. *Epidemiol. Infect.* **135**:1057-1068.
252. **Valentin-Weigand, P. and R. Goethe.** 1999. Pathogenesis of *Mycobacterium avium* subspecies paratuberculosis infections in ruminants: still more questions than answers. *Microbes and Infection* **1**:1121-1127.
253. **Valheim, M., Ó. G. Sigurðardóttir, A. K. Storset, L. G. Aune, and C. M. Press.** 2004. Characterisation of macrophages and occurrence of T cells in intestinal lesions of subclinical paratuberculosis in goats. *Journal of Comparative Pathology* **131**:221-232.
254. **van Roermund, H. J. W., D. Bakker, P. T. J. Willemsen, and M. C. M. de Jong.** 2007. Horizontal transmission of *Mycobacterium avium* subsp. paratuberculosis in cattle in an experimental setting: Calves can transmit the infection to other calves. *Veterinary Microbiology* **122**:270-279.
255. **van Schaik, G., S. M. Stehman, R. H. Jacobson, Y. H. Schukken, S. J. Shin, and D. H. Lein.** 2005. Cow-level evaluation of a kinetics ELISA with multiple cutoff values to detect faecal shedding of

- Mycobacterium avium* subspecies paratuberculosis in New York State dairy cows. *Preventative Veterinary Medicine* **72**:221-236.
256. **van Weering, H., G. van Schaik, A. van der Meulen, M. Waal, P. Franken, and K. van Maanen.** 2007. Diagnostic performance of the Pourquier ELISA for detection of antibodies against *Mycobacterium avium* subspecies paratuberculosis in individual milk and bulk milk samples of dairy herds. *Veterinary Microbiology* **125**:49-58.
257. **Vandesompele, J., K. De Preter, F. Pattyn, B. Poppe, N. Van Roy, A. De Paepe, and F. Speleman.** 2002. Accurate normalization of real-time quantitative RT-PCR data by geometric averaging of multiple internal control genes. *Genome Biology* **3**:research0034.1-research0034.11.
258. **Vansnick, E., de Rijk P., Vercammen F., Rigouts L., Portaels F., and Geysen D.** 2007. A DNA sequence capture extraction method for detection of *Mycobacterium avium* subspecies paratuberculosis in feces and tissue samples. *Veterinary Microbiology* **122**:166-171.
259. **Vaughan, J. A., C. Lenghaus, D. J. Stewart, M. L. V. Tizard, and W. P. Michalsk.** 2005. Development of a Johne's disease infection model in laboratory rabbits following oral administration of *Mycobacterium avium* subspecies paratuberculosis. *Veterinary Microbiology* **105**:207-213.
260. **Verna, A. E., C. Garcia-Pariente, M. Munoz, O. Moreno, J. F. Garcia-Marin, M. I. Romano, F. Paolicchi, and V. Perez.** 2007. Variation in the Immuno-pathological Responses of Lambs after Experimental Infection with Different Strains of *Mycobacterium avium* subsp. paratuberculosis. *Zoonoses and Public Health* **54**:243-252.
261. **Wang, H., g. Aodon, Y. Shu, Y. Momotani, X. Wang, Y. Mori, and E. Momotani.** 2007. Corticotropin-releasing hormone and urocortin expression in peripheral blood cells from experimentally infected cattle with *Mycobacterium avium* subsp. paratuberculosis. *Microbes and Infection* **9**:1061-1069.
262. **Warth, A.** Is [alpha]-dystroglycan the missing link in the mechanism of enterocyte uptake and translocation of *Mycobacterium avium* paratuberculosis? *Medical Hypotheses* **In Press, Corrected Proof.**
263. **Waters, W. R., J. M. Miller, M. V. Palmer, J. Stabel, D. E. Jones, K. A. Koistinen, E. Steadham, M. J. Hamilton, W. C. Davis, and J. P.**

- Bannatine.** 2003. Early induction of humoral and cellular immune responses during experimental *Mycobacterium avium* subsp. *paratuberculosis* infection of calves. *Infect. Immun.* **71**:5130-5138.
264. **Weber, M. F., H. J. W. van Roermund, J. C. M. Vernooij, C. H. J. Kalis, and J. A. Stegeman.** 2006. Cattle transfers between herds under paratuberculosis surveillance in The Netherlands are not random. *Preventive Veterinary Medicine* **76**:222-236.
265. **Weiss, D. J., O. A. Evanson, and C. de Souza.** 2005. Expression of interleukin-10 and suppressor of cytokine signaling-3 associated with susceptibility of cattle to infection with *Mycobacterium avium* subsp. *paratuberculosis*. *American Journal of Veterinary Research* **66**:1114-1120.
266. **Weiss, D. J., O. A. Evanson, M. Deng, and M. S. Abrahamsen.** 2004. Gene expression and antimicrobial activity of bovine macrophages in response to *Mycobacterium avium* subsp. *Paratuberculosis*. *Vet Pathol* **41**:326-337.
267. **Weiss, D. J., O. A. Evanson, D. J. McClenahan, M. S. Abrahamsen, and B. K. Walcheck.** 2001. Regulation of expression of major histocompatibility antigens by bovine macrophages infected with *Mycobacterium avium* subsp. *paratuberculosis* or *Mycobacterium avium* subsp. *avium*. *Infect. Immun.* **69**:1002-1008.
268. **Weiss, D. J., O. A. Evanson, and C. D. Souza.** 2006. Mucosal Immune Response in Cattle with Subclinical Johne's Disease. *Vet Pathol* **43**:127-135.
269. **Weiss, D. J., O. A. Evanson, A. Moritz, M. Q. Deng, and M. S. Abrahamsen.** 2002. Differential Responses of Bovine Macrophages to *Mycobacterium avium* subsp. *paratuberculosis* and *Mycobacterium avium* subsp. *avium*. *Infect. Immun.* **70**:5556-5561.
270. **Weiss, D. J., C. D. Souza, O. A. Evanson, M. Sanders, and M. Rutherford.** 2007. Bovine monocyte TLR2 receptors differentially regulate the intracellular fate of *Mycobacterium avium* subsp. *paratuberculosis* and *Mycobacterium avium* subsp. *avium*. *J Leukoc Biol* **83**:48-55.
271. **Whan L., Ball J.B., Grant I.R., and Rowe M.T.** 2005. Occurrence of *Mycobacterium avium* subsp. *paratuberculosis* in Untreated Water in Northern Ireland. *Appl. Environ. Microbiol.* **71**:7107-7112.
272. **Whittington, R. J., I. Marsh, M. J. Turner, S. McAllister, E. Choy, G. J. Eamens, D. J. Marshall, and S. Ottaway.** 1998. Rapid Detection of *Mycobacterium paratuberculosis* in Clinical Samples

- from Ruminants and in Spiked Environmental Samples by Modified BACTEC 12B Radiometric Culture and Direct Confirmation by IS900 PCR. *J. Clin. Microbiol.* **36**:701-707.
273. **Wilczynski, J. R., M. Radwan, and J. Kalinka.** 2008. The characterisation and role of regulatory T cells in immune reactions. *Frontiers in Bioscience* **13**:2266-2274.
274. **Windsor, P.** 2006. Research into vaccination against ovine Johne's disease in Australia. *Small Ruminant Research* **62**:139-142.
275. **Withers, F. W.** 1959. Incidence of the disease. *The Veterinary Record* **71**:1150-1153.
276. **Woo, S. R., J. A. Heintz, R. Albrecht, R. G. Barletta, and C. J. Czuprynski.** 2007. Life and death in bovine monocytes: The fate of *Mycobacterium avium* subsp. *paratuberculosis*. *Microbial Pathogenesis* **43**:106-113.
277. **Wu, C. w., M. Livesey, S. K. Schmoller, E. J. B. Manning, H. Steinberg, W. C. Davis, M. J. Hamilton, and A. M. Talaat.** 2007. Invasion and Persistence of *Mycobacterium avium* subsp. *paratuberculosis* during Early Stages of Johne's Disease in Calves. *Infect. Immun.* **75**:2110-2119.
278. **Zur Lage, S., R. Goethe, A. Darji, P. Valentin-Weigand, and S. Weiss.** 2003. Activation of macrophages and interference with CD4+ T-cell stimulation by *Mycobacterium avium* subspecies *paratuberculosis* and *Mycobacterium avium* subspecies *avium*. *Immunology* **108**:62-69.

**Appendix 1: Names and addresses of suppliers**

<b>Supplier</b>	<b>Address</b>
Agilent Technologies UK Ltd	710 Wharfedale Road Winnersh Triangle Wokingham Berkshire RG41 5TP
Ambion, Inc	Lingley House 120 Birchwood Boulevard Warrington WA3 7QH UK
BD Biosciences	The Danby Building Edmund Halley Road Oxford Science Park Oxford OX4 4DQ UK
Biobest Laboratories Ltd	6 Charles Darwin House The Edinburgh Technopole Milton Bridge Nr Penicuik EH26 0PY
BlueGnome Ltd	Breaks House Mill Court Great Shelford Cambridge CB22 5LD United Kingdom
Cambridge Bioscience Ltd	24-25 Signet Court Newmarket Road Cambridge CB5 8LA United Kingdom

Corbett Life Science / Corbett Robotics	Unit 1, Terek House Sandpiper Court Phoenix Business Park Eaton Socon St Neots Cambridgeshire PE19 8EP United Kingdom
Corning Inc Life Sciences	Koolhovenlaan 12 1119 NE Schiphol-Rijk The Netherlands
GE Healthcare	The Grove Centre White Lion Road Amersham Bucks HP7 9LL
Implen UK Ltd	Cumberland House 24 - 28 Baxter Avenue Southend on Sea Essex SS2 6HZ
Institut Pourquier	326, rue de la Galéra Parc Euromédecine 34090 Montpellier France
Invitrogen Ltd	3 Fountain Drive Inchinnan Business Park Paisley UK PA4 9RF
Molecular Devices Ltd	660 - 665 Eskdale Road Winnersh Triangle Wokingham Berkshire RG41 5TS UK

Nanodrop Technologies, Inc	3411 Silverside Rd Bancroft Building Wilmington DE 19810 USA
New England Biolabs (UK) Ltd	75/77 Knowl Piece Wilbury Way Hitchin Hertfordshire SG4 0TY UK
Promega UK	Delta House Southampton Science Park Southampton SO16 7NS UK
Q-Biogene	Wellington House East Rd. Cambridge CB1 1BH
Qiagen	QIAGEN HOUSE Fleming Way Crawley West Sussex RH10 9NQ
Roche Applied Science	Charles Avenue Burgess Hill RH15 9RY UK
Sigma-Aldrich Company Ltd	Sigma-Aldrich Company Ltd. The Old Brickyard New Road Gillingham Dorset SP8 4XT
Stratagene Europe	Gebouw California Hogehilweg 15 1101 CB Amsterdam Zuidoost The Netherlands

Thermo-hybaid

ABgene House  
Blenheim Road  
Epsom  
KT19 9AP  
UK

VWR

Hunter Boulevard  
Magna Park  
Lutterworth  
Leicestershire  
LE17 4XN

## Appendix 2: Sequences of cloned plasmids

Gene	Sequence
CXCR4	TGGCTGAAAAGGTGGTCTATNTTGGTGTCTGGCTACCCGCTGTCCTG TTGACTATTCTGATCTCATCTTTGCCGACATCAAGGAAGCGGATGAG AGGTACATCTGTGATCGCTTCTATCCCAGCGACCTGTGGCTAGTGGT GTTTCAGTTTCAGCACATCGT
CD34	CCTTTTCCTGTTTCTTCCTTGATTTTTCTTTCTACTTTAGGAACAC CAAAGCAATCCCTCGAACTTGCCCTTTGTAATGACCGGTCAGAAAAT CATGCCATCTTAACCCATCTCCACCATTCCCCTCTCTGAGGCACTGAG CGTTTACTCACCAGCTCCCCTCTTGCTCTCTAAGGTCCCTGAGCNCCA CAGATAAACCACCCCC
CD54	GCTGATNGATAGTNACNCTTANTGNGGGCACTCTGGGCACCGCTGGT TATATTTACAACCTACCAGCGGAAGATCCAGAAATACGAGCTGCAGAA GGCCCAAAAAGAGGCTGCCTTGAAACTGAAATCCACGCC
CD63	GGGCTGTGTGGAGAAGATTGCCGCCTGGCTGAGGAAGAATGTGCTGG TGGTGGCTGCGGCAGCCCTGGGCATTGCCTTNGTGGAGATCCTGGGT ATTGTCTTAGCATGCTGCCTTGTGAAGAGCATCCGAAGTGNCTATGA GGTGATGTAGGGGTGTGTNTTCTTCGACGCATAC
CXCL10	ACCAAGCCAGTCACCAAATCANCNGCTACTACTCCTGCAGGGGGGAG GGTGGCTCATCACCCCTGAGCTGTTTCAGTAGTGACTCTGCCCTGGCAC TGTGACTGTAAGCTATAACCGGGGCGCTACGTTCTCAGTTAATGTGCTA AGTCCCAGCCTTGCTACTGACAGCTTCTTCCCCTTCCAATCAATCAC TAGTGAATTC
CD18	CTCACCGACAACCTCCAAACAGTTCGAGACAGAAGTCGGGAAGCAGCT GATCTCGGGAACTTGGACGCCCTGAAGGGTGGGCTGGACGCCATG ATGCAAGTGGCCGCGTGCCCGGAGGAAATTGGCTGGCGCAATGTCAC CAGGCTGCTGGTGTTCGCCACAGACGATGGGTTCACCT
DAP12	GACCTGATGCTGACCCTCCTCATCGCTCTGGCTGTGTACTCCCTGGGT CGGCTGGTCCCTCGGGGGCGAGGGGCTGCGGAGGTGACCCGGAAC AGCACATCACGGAGACAG
GM-CSF*	GCCTGCTTCACTTCTGGACTGGTTCACAGCAGTCAAAGGGAATGATA AAAAGGAAATCCTTCAGGTTCTCTTTGAAACTTTTGAAGGTGATAATC TGGGTTTACAGGAAGTTTCTGGGTGGGGGGCAGTGTTCCTTGTA GTGGCTGGCCATCATGGTCAAGGAGCCCGTGAGACTGGTGAGGCTGC CCCGCAGGCCCTGCTTGTACAGCTCCAGGCGAGTCTGCAGGCATGTC GGCTCCTGGGAGTCAAACATTTTCAGAGACGACTTCTACTGTTTCATCC ATCACAGCAGCAGTGTGCTGCTGTCGTTTCAGAAGGCTCAGGGCCTC CTTGATGGCATCCACATGCTGCCAGGGCCGGGTGACAGGGCTGGGT GGCGAGTGGGTGCGGAGAAGCTGCAGACCACAGTGCCAGGAGAAG C

IFN $\gamma$ *	TCACCTTGATGAGTTCATTGATGGCTTTGCGCTGGATCTGCAGATCAT CCACCGGAATTTGAATCAGCCTTTTGAAGTCCTCCAGTTTCTCAGAGC TGCCGTTCAAGAACTTCTGAAACATGTCTTGCTTGATGATATCCATGC TCCTTTGAATGACCTGGTTATCTTTGAGGTTTTCAAAGAGTTTGAAGT AGAAGGAGACAATTTGGCTCTGAATAATCTTTTGTCACTCTCCTCTT TCCAATTCTTCAAAAATTTCTGAGAAAAGAGGCCACCCTTAGCTACAT CTGGGTTACTTGCATTAATAACTCCTTTAAGTTTTCTATTTCTTTAAA AAATGGGCCCTGGCCATAAGAACCAGAAAAACCCAAAAGCACACAGA GCAGTAAAGCTAAGAAGGAGCTTGTGTATTTT
IGF2R	GACGACCTGAAGACCCCTGAAGCCGGGCAGGCTGGTGGGCCTGGAGA AGAGCCTGCAGCTGTCCACCGAGGGCTTTATAACCCTGAACTACACG GGGCTTCCCTCCACCCCAATGGGAGGGNTGATGCTTTCATCATNCN NNTCNNNNNC
IGFBP-2	CCTCTATTCCCTACCCCTNTNAAACTGTGACAAGCATGGCCTGTACAA CCTCAAACAGTGNAAGATGTCTCTGAACGGGCAGCGTGGGGAGTGCT GGTGTGTGAAC
IGFBP-6	AAGGAGAGTAAGCCCCAAGCAGGGACTGCTCGCTCGCAGGACGTGAA CCGCAGAGACCAACAGAGGAACTCGGGGACCTTACCACTCCTTCCC G
IL-1 $\alpha$	TTGGTGCACATGGCAAGTGGNCCTNNCTCGATCACTGACTTTCAGAT ATTGGAAAAATAGCCTTGACTGTGC
IL-1 $\beta$ *	CTGTGTTCTTCCCTTCCCTTCTGCCAGTCCTCGGGGTTATTCAGCCCA CGTGGACTCCCTGCGTATGGCTTTCTTTAGGGAGAGAGGGTTTCCATT CTGAAGTCAGTTATATCCTGGCCACCTCTAAAACGTCCCAGGAAGAC GGGCTTTTCTCGATTTGAGAAGTGCTGATGTACCAGTTAGGGTACAG GACAGACTCAAATTCAACTGTGTTCTTGATTTCTGTCTTGTAAGAC GAATCGCTTTTCCATATTCCTCTTGGGGTAGACTTTGGGGTCTACTTC CTCCAGCTGCAGGGTCGGTGTATCACCTTTTTTTCACACAAGACAGGTA TAGATTCTTGTCCCTGATACCCAAGGCCACAGGAATCTTGTGTCTCT TTCTCTCCTTGTACGAAGCTCATGCAGAACCACCTTCTCGGCTCAT TTCTGTGAGAGGAGGTGGAGAGCCTTTCAGCACACATGGGCTATCCA GCACCAGGGATTTTTG
IL-3	GAAGTCTGAAGCCCAGTTCCTCTCTGAAGCCTCAGATCATCAGTGAC AACAGACTGTCCTAAATTTCTTTCGATGTTTCTCACATGGTCCAGGCCT GGAAGAATTAATTTTCTCCTGTGGAGCCAGATGAATCGTTAATTTATTT AACTCCTGATATGTGTGGCCCCATTTGTCTTTTGGGATTATGTT
IL-6*	CCACAATCATGCGAGCCGCAGCTACTTCATCCGAATAGCTCTCAGGCT GAACTGCAGGAAATTTCTCAAGGCTTCTCAGGATGATGATAACCTTTGC GTTCTTTACCCACTCGTTTGGAGACTGCATCTTCTCCAGCATGTCAGT GTGTGTGGCTGGAGTGGTTATTAGACCTGCGATCTTTTCTCAGGAT CTGGATCAGTGTCTGATACTGCTCTGCAACTCCATGACAGTTTCTTG ATTTCCCTCAAACCTCGTTCTGGAGGAAGTCCAGGTATATCTGATACTC CAGAAGACCAGCAGTGGTTTTGATCAAGCAAATCGCCTGATTGAACC CAGATTGGAAGC

IL-8*	GAAGTCCTCTGGGACAGCAGAGCTCACAAAGCATCTAGAACGAGAGCC AGAAGAAACCTGACAAAAAGCCTCTTGCTCAAGNATGACTTCCAAGC TGGCTGTTGCTCTCTTGGCCGCTTTCCTGCTCTCTGCAGCTCTGTGTG AAGCTGCAGTTCTGTCAAGAATGAGTACAGAACTTCGATGCCAATGC ATAAAAACACATTCCACACCTTTCACCCCAAATTTATCAAAGAACTG AGAGTTATTGAGAGTGGGCCACACTGCGAAAATTCAGAAAATCATTGTT AAGCTTACCAACGGAAAAGAGGTGTGCTTAGACCCCAAGGAAAAGTG GGTGCAGAAGGTTGTGCAGGCATTTTTGAAGAGAGCTGAGAAGCAAG ATCCATGAAAAAGAAAAACAACCAAAAATCCTTTTTTTCNTTGGCTT CCAA
IL-10*	CTGTTGACCCAGTCTCTGCTGGATGACTTTAAGGGTTACCTGGGTTGC CAAGCCTTGTGCGAAATGATCCAGTTTTACCTGGAGGAGGTGATGCC ACAGGCTGAGAACCATGGGCCTGACATCAAGGAGCACGTGAACTCGC TGGGGGAGAAGCTGAAGACCCTCCGGCTGCGGCTGCGGCGCTGTCAT CGCTTCTGCCCTGCGAAAACAAGAGCAAGGCGG
IL-12p40*	CTGCTGCTTTTGACACTGCAATTTCCAGATTAGTACTGATTGCTGTCAG CCACGAGCAGGTGAAGTGTCCAGAATAATCCTTTGCCTCACATTTTAA AAAACCTTAGCTTTGGGTTCTTTCTGATCCTTTAAAATATCAGTGGA CCAAATCCATCTTCCTTTTGTGTCAGCAGGAGGAGTGAACGACTCAG AACCCTCGCTCCTTTGTGACAGGTGTACTGCCAGCATCCAAACTC TTTGACTTGGATGGTCAAGGTTTTGCCAGAGCCAGGACCTCACTGCT CTGGTCTGAGGTCCAGGTGATGCCGCTTCTTTCAGGAGTGTACACG TGAGGACCACTGTTTCTCCAGGAGCATTAGGATACCAATCCAATTCTA CAACATAAACATTTTTCTCCAGTTCCCATATGGCCACGATGGGAGATG CCAGCAAAACCAGGGAAAACCAG
IL-18*	TCAGATCACGTTTCCTCTCCTAGGAAGCTATTGAGCACAGGCATAAAG ATGGCTGCAGAACCAGTAGAAGACAATTGCATCAGCTTTGTGGAAAT GAAATTTATTAACAATACACTTTATTTTTGTAGCTGAAAATGGCGACCT GGAATCAGATCACTTTGGCAAGCTTGAACCTAAGCTCTCAATCATAAG AAATTTGAACGACCAAGTTCTCTTCATTAGCCAGGGAAATCAACCTGT CTTTGAGGATATGCCTGATTCTGACTGTTCCAGATAATGCACCCAGAC CATATTTATCATATATATGTATAAGGACAGCCTCACTAGAGGTCTGGC TGTAACCATC
MMP7	CAGCAAAACACACCTTCATTTCATTGGGTTCTATGTAACTGTTCCCAAC CAGAATTAAGAACACTGTTCCCTGCCTTCCATTTAACACTTGCTGCCT CCAACNTGTATTGNGGTNGGNNTNAGTCTNTNC
MMP9	AGCACGCACGACATCTTTCAGTACCAAGAGAAAGCTTACTTCTGCCAG GATCACTTCTTCTGGCGTGTGAGTTCCCGGAATGAGGTGAATNCNGN TGGANNTANGTGGNNT
Oxytocin	GTCTCCGTGATGACATTTCCATTGCCCCCTGGGCGGNAAGCGTGCGG TGCTGGACCTCGACGTGCGCACGTGTCTCCCTGCGGCCCCGGGGGC NTTTGCCGCTGCTTCGGGCCCAGCATCTGCTGCGGGGACGAGCTGGG CTGCTTCGTGGGCACGGCCGAGGCGCTGCGCTGCCGAGAGGAGAACT ACCTGCCGTCGCC

TGFβ*	GCCCTGGACACCAACTACTGCTTCAGCTCCACAGAAAAGAACTGCTG TGTTTCGTCAGCTCTACATTGACTTCCGGAAGGACCTGGGCTGGAAGT GGATTCACGAACCCAAGGGGTACCACGCCAATTTCTGCCTGGGGCCC TGCCCTTACATCTGGAGCCTGGACACGCAGTACAGCAAGGTCCTGGC CCTGTACAACCAGCACAACCCGGGCGCATCGGCGGCGCCGTGCTGCG TGCCTCAGGCGCTGGAACCCCTGCCATCGTGTACTACGTGGGCCGC AAGCCCAAGGTGGAGCAGTTATCCAACATGATCGTGCCTCCTGCAA GTGCAGCTG
TIRAP	CTTTATCCTGACGCCTGCTGAGGGCTTCCCCGGACACCGTGGAAAAC CACGCAGCTGAGGCAAGTGGTCCAGGATTCCAGCTCCTTACTCAGGT GAGCCACCTCTTCAAGAGGAATGCACCTCAACACCAGTGCCCGATTA CAGGGGATGAAGACACAGACACGACA
TLR2	GCACTTCAACCCTCCCTTTTAGCTGTGTCTTCATAAGCGAGACTTCGT CCCTGGCAAATGGATCATCGACAACATCATCGACTCCATGAAAAGA GCCGAAAACCATCTTTGTGCTTTCGGAGA
TNFα*	TCCTTGGTGATGGTTGGTGGCCCGTTGTCCAGGCCTCACTTCCCTACA TCCCTAATTTCTAAGTGCAGCTGTTGTTTAAAGTTGGACGCTTGGAGC CCAGCCCTGAGCCCCTAATTCCTTTCTAAACCAGAAGGGGATGAGG AGGGTCTGAAGGAGTAAATAATAAGGTAACCTGAGGTGGGAGAGGATG CATGTCCTGCGCCCTCACAGGGCGATGATCCCAAAGT
TRAF-1	AGCAGAGGGTGTGGAGTTGCCCCATACCCTGGCCCAGAAGGACCAG GCCTTGGGCAAGCTGGAGCAGAGCCTGCACCTCATGGAGGAGGCCTC CTACGATGGCACCTTCCTGTGGAAGATCACCAACGTTACCCGGCGGT GCCATGAGTCAGCCTGCGGCAGGACTGTCAGCCTC
TRAM	CACATTTCCCGCCTATTTTACCCNNTAATGAAAAGTATCAGAAAAGGA TTTTCTCTGTGGGCANNCTGTGTTTGTGTTTGGGAAGACTTCTGACTTTA ATTCTCTCGGTACTCACTGTTGGCTTTGGCCTAGCAAGAGCAGAGAAC CAGA

---

Clones marked with (\*) were kindly provided by T McNeilly.

## Differential cytokine gene expression profiles in the three pathological forms of sheep paratuberculosis

Jennifer A Smeed<sup>1</sup>, Craig A Watkins<sup>2</sup>, Susan M Rhind<sup>3</sup> and John Hopkins\*<sup>1</sup>

Address: <sup>1</sup>Centre for Infectious Diseases, Royal (Dick) School of Veterinary Studies, Summerhall, Edinburgh, EH9 1QH, UK, <sup>2</sup>Moredun Research Institute, International Research Centre, Pentlands Science Park, Penicuik, Midlothian EH26 0PZ, UK and <sup>3</sup>Division of Veterinary Clinical Studies, Royal (Dick) School of Veterinary Studies, University of Edinburgh, Easter Bush Veterinary Centre, Midlothian EH25 9RC, UK

Email: Jennifer A Smeed - [j.a.smeed@sms.ed.ac.uk](mailto:j.a.smeed@sms.ed.ac.uk); Craig A Watkins - [craig.watkins@moredun.ac.uk](mailto:craig.watkins@moredun.ac.uk); Susan M Rhind - [susan.rhind@ed.ac.uk](mailto:susan.rhind@ed.ac.uk); John Hopkins\* - [john.hopkins@ed.ac.uk](mailto:john.hopkins@ed.ac.uk)

\* Corresponding author

Published: 14 August 2007

Received: 16 May 2007

BMC Veterinary Research 2007, 3:18 doi:10.1186/1746-6148-3-18

Accepted: 14 August 2007

This article is available from: <http://www.biomedcentral.com/1746-6148/3/18>

© 2007 Smeed et al; licensee BioMed Central Ltd.

This is an Open Access article distributed under the terms of the Creative Commons Attribution License (<http://creativecommons.org/licenses/by/2.0>), which permits unrestricted use, distribution, and reproduction in any medium, provided the original work is properly cited.

### Abstract

**Background:** Johne's disease is a chronic inflammatory disease of the gut caused by infection with *Mycobacterium avium* subspecies *paratuberculosis* (MAP). Symptoms include wasting, diarrhoea, loss of condition and eventual death. Three forms of Johne's disease have been described in sheep – paucibacillary, multibacillary and asymptomatic. The paucibacillary form is characterized by an inflammatory, Th1-type immune response. The multibacillary form of the disease, which disseminates the infection, is characterized by macrophage infiltration mediated by a Th2-type immune response, and asymptomatic animals have no clinical symptoms or pathology but are infected with MAP. What determines these three forms of the disease is unknown. To further understand these differences, we used real-time RT-PCR to compare the expression of thirteen cytokine and cytokine-related genes in ileal tissue from sheep with the three forms of the disease.

**Results:** Three pathological forms of sheep paratuberculosis were defined on the basis of histopathology, cytochemistry (Ziehl-Neelsen) and IS900 PCR. Paucibacillary lesions have largely T cell and eosinophil infiltration and are ZN negative; multibacillary lesions have macrophage infiltration and large numbers of acid-fast bacteria. The pauci- and multibacillary forms are linked to the differential expression of IFN $\gamma$  and IL-10 respectively. In addition the increased levels of the proinflammatory cytokines (IL-1 $\beta$  and TNF $\alpha$ ), IL-8, IL-18 and TRAF-1 in both diseased forms is indicative of persistent inflammatory lesions. No changes were seen in IL-1 $\alpha$  in any sheep ileum tissues. Asymptomatic animals are IS900+ with normal histology but have significantly decreased levels of IL-18 and increased levels TNF $\alpha$ .

**Conclusion:** We have quantified the expression levels of thirteen cytokine and cytokine related genes in three forms of ovine paratuberculosis using real-time PCR analyses and confirm that sheep pauci- and multibacillary disease are linked to type 1 and type 2 T cell responses respectively. The expression patterns of other cytokines shows that both disease forms have an inflammatory aetiology but that the central role for IL-1 $\alpha$  in bovine paratuberculosis is not seen in the sheep infection. Asymptomatic animals are infected and show no pathology but can be distinguished, in terms of cytokine expression pattern, from uninfected controls.

## Background

Paratuberculosis (Johne's disease) is a chronic intestinal disease of ruminants caused by the bacterium *Mycobacterium avium* subspecies *paratuberculosis*. The disease is responsible for extensive economic losses worldwide related to fatality and loss of productivity [1,2]. The route of disease transmission is mainly faecal-oral; and neonates, when not infected congenitally are infected by ingestion of bacteria from infected teats or the pasture transmitted via the dissemination of diarrhoea from infected animals [3]. Consequently the majority of animals within an infected herd or flock become infected [3]. However, in sheep infection can give rise to three different forms of disease with only about 30% of animals in an infected flock becoming clinically affected. The majority of animals are asymptomatic; they are infected but show no pathology and do not develop clinical disease [4]. The remaining clinically-affected sheep show two distinct forms of the disease. Approximately 30% of disease cases are affected by the paucibacillary form of Johne's disease; they have very few bacteria and show a T cell infiltration into the gut. About 70% of cases have the multibacillary form, which is characterized by a high level of bacterial infection and a macrophage and B cell infiltration into the gut lamina propria. Both the pauci- and multibacillary forms are equally fatal but there is no evidence that the asymptomatic animals ever succumb to disease [4,5].

Johne's disease pathogenesis in cattle may differ from that in sheep as it is presumed that there is disease progression from the asymptomatic to paucibacillary and then to the fatal multibacillary form [6]. However, even in cattle 4–11% of animals in affected herds are infected but only 2–4% develop the disease [7,8]. Like the two other major mycobacterial diseases, tuberculosis and leprosy, the epidemiology of paratuberculosis suggests a genetic susceptibility [9]. The paucibacillary cases (tubercloid pathology) tend to have a strong cell-mediated immunity (CMI), high levels of IFN $\gamma$  and IL-2 and low levels of antibody [10–12]; the multibacillary cases (lepromatous pathology) have high antibody and pro-inflammatory cytokine levels and weak CMI [10,12]. Little is known about the asymptomatic form although they are positive for bacterial growth, IS900 and specific antibody [13,14].

As with tuberculosis and leprosy it seems clear that the polarization of the immune response is critical to the clinical outcome of the paratuberculosis infection [15–17]. The intestinal tissue damage that results from a Th1 response (paucibacillary disease) is fundamentally different to that caused by a Th2 response, which leads to multibacillary disease and dissemination of infection. The polarization of the immune response is controlled by the differential expression of T cell polarizing cytokines [18] and it seems that there is differential expression of some

of these cytokines in Johne's disease [19]. Several studies describe the changes in expression of cytokines in peripheral blood cells in cattle [20,21] and ileal tissue of both sheep [11,12] and cattle [19,21–24]. Burrells et al. (1999) [11] examined IL-2 and IFN $\gamma$  in both pauci- and multibacillary forms but not the asymptomatic animals while Tanaka et al. [19] quantified cytokines in granulomatous lesions during the preclinical stages of disease; all other studies on the target organ concentrated on analysis of the multibacillary form, including all studies on the ileal tissue in cattle.

This study tested the hypothesis that expression levels of a panel of thirteen cytokine and cytokine associated genes would be different at the site of infection in the three forms of sheep paratuberculosis, and that these differences could relate to the observed pathologies. Furthermore, this study also analyses the asymptomatic form of sheep Johne's disease in relation to uninfected control animals.

## Results

### Definition of pathological forms

All animals from the Johne's disease infected flocks were identified as IS900 positive by PCR analysis and therefore judged to be infected with MAP. Three groups of IS900+ animals could be discriminated on the basis of gross pathology, ZN staining and histopathology. The asymptomatic group had no clinical signs or lesions consistent with Johne's disease, at post mortem. Examination of histological sections of the terminal ileum showed normal histology and no evidence of the presence of acid-fast bacteria (ZN-) (Figure 1A–1C). All other sheep showed clinical signs and post mortem lesions consistent with Johne's disease and could be further differentiated into two groups (paucibacillary and multibacillary) on the basis of ZN staining of histological sections of terminal ileum. The paucibacillary sheep had no detectable ZN+ bacteria (Figure 2A) and showed a mixed inflammatory infiltrate into the lamina propria (Figure 2B) comprising lymphocytes, eosinophils and multinucleate giant cells (arrowed) with fewer macrophages (Figure 2C). The multibacillary sheep had high numbers of ZN+ acid-fast bacteria (Figure 3A), mostly within the cytoplasm of the large numbers of epithelioid macrophages, which distend the lamina propria (Figure 3B and 3C) and result in flattening of the surface mucosa (Figure 3B). A fourth group of unrelated, control sheep were IS900 negative and were judged to be uninfected with MAP.

### Gene expression analysis in ileal tissues

The expression levels of cytokine transcripts in sheep ileum from the three groups of paratuberculosis-infected sheep and in uninfected controls is shown in Table 1 which shows transcript copy number in relation to the

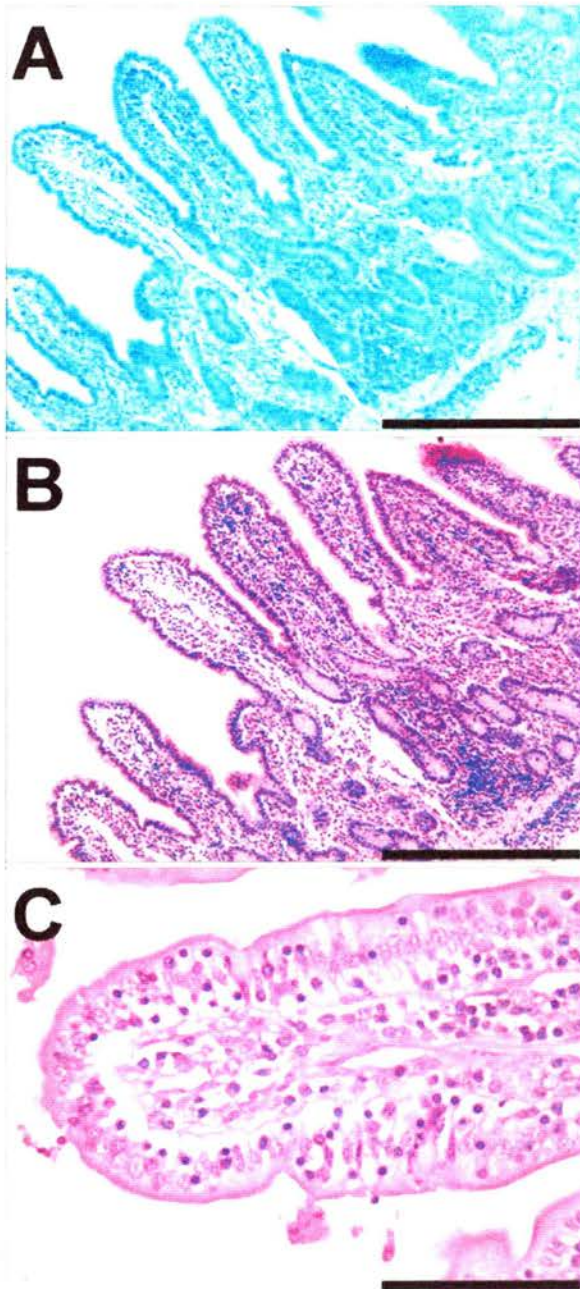


**Figure 1**  
**Histopathology of the terminal ileum from asymptomatic sheep.** (a) Ziehl-Neelsen stain for acid-fast bacteria ( $\times 250$ ) showing the absence of mycobacteria. (b) H&E stained low power ( $\times 250$ ) and (c) high power ( $\times 400$ ) show normal histology.

two housekeeping genes, GAPDH and SDHA. These data show that different cytokines are present at very different levels in ileal tissue, varying from less than 100 copies

(e.g. IL-3) to greater than 100,000 copies (e.g. IL-8 and IL-10). They also show that levels of individual cytokine transcripts show a high variability between animals, even within the same pathological group.

Furthermore, it shows that individual cytokines are differentially expressed in the distinct disease states.

This is more clearly shown in Figures 4 and 5 where the results are expressed as statistically significant ( $p = 0.05$ ) fold change where data are compared in six pairs – paucibacillary vs asymptomatic, multibacillary vs asymptomatic, paucibacillary vs multibacillary (Figure 4), paucibacillary vs control, multibacillary vs control and asymptomatic vs control (Figure 5). The expression levels of two genes, IL-1 $\alpha$  and GM-CSF was relatively consistent in all the animals regardless of disease status.

Figure 4 shows the comparison of cytokine transcripts between the three infected groups of sheep. When the two diseased forms were compared with the asymptomatic samples TRAF-1, IL-1 $\beta$ , IL-6, IL-18 and IFN $\gamma$  were significantly up-regulated in paucibacillary ileum, (Figure 4a) and TRAF-1, IL-10, IL-18, TNF $\alpha$  and TGF $\beta$  were up-regulated in multibacillary samples (Figure 4b). Comparison of the pauci- and multibacillary forms showed that only IL-10 was significantly different, with the expression levels in the paucibacillary ileum being approximately half that in multibacillary tissue. In contrast the level of IFN $\gamma$  and TRAF-1 were much higher in paucibacillary tissue, however neither was quite significant ( $p = 0.057$  and  $0.062$  respectively). If one outlier point in the TRAF-1 data was removed from the ten samples the significance level was increased to  $p = 0.02$  (Figure 4c).

Figure 5 shows the comparison of cytokine transcripts between the three infected groups and the uninfected control animals. TRAF-1, IL-8, IL-12p40, IFN $\gamma$ , TNF $\alpha$  and TGF $\beta$  were significantly increased in paucibacillary samples (Figure 5a). The multibacillary sheep showed significantly increased levels of TRAF-1, IL-8, IFN $\gamma$ , TNF $\alpha$  and TGF $\beta$  (Figure 5b). The multibacillary ileum also showed increased levels of IL-12p40 but this was not quite statistically significant ( $p = 0.06$ ). Interestingly there were significant differences between the asymptomatic and uninfected control samples, which showed that IL-18 was down-regulated and TNF $\alpha$  was up-regulated in the asymptomatic sheep. IL-3 was detected at low levels in all infected animals but never in uninfected control samples; therefore it was not possible to produce fold-change figures for these comparisons. Nevertheless, IL-3 was statistically significantly up-regulated ( $p = 0.05$ ) in both multibacillary and asymptomatic samples (but not paucibacillary sheep) compared to controls, using the non-parametric Mann-Whitney test.

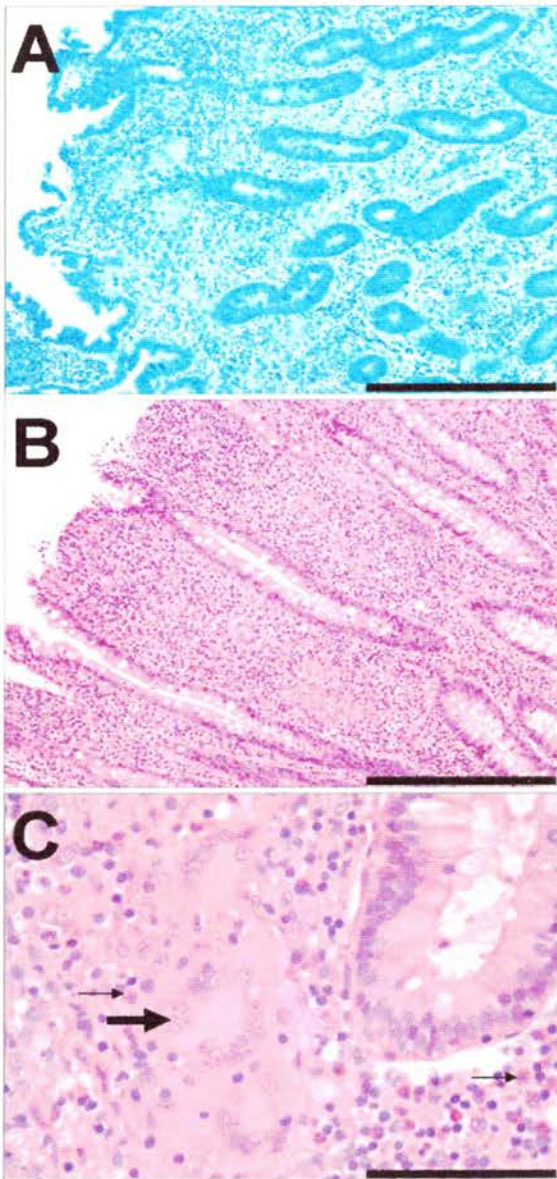


**Figure 2**  
**Histopathology of the terminal ileum from paucibacillary sheep.** (a) Ziehl-Neelsen stain ( $\times 250$ ) showing the absence of mycobacteria. (b) H&E stained low power ( $\times 250$ ) showing mixed inflammatory infiltrate into lamina propria comprising lymphocytes, eosinophils, macrophages and multinucleate giant cells. (c) H&E stained high power ( $\times 400$ ) showing multinucleate giant cells (large arrow) adjacent to a crypt. There is an associated proprial inflammatory reaction dominated by lymphocytes and eosinophils (small arrows).

## Discussion

The three major mycobacterial diseases of mammals – tuberculosis, leprosy and paratuberculosis affect different organ systems but share at least two important characteristics. Firstly, not all infected individuals become clinically affected and second, there are at least two pathological forms of each disease [2,25,26]. This is most obvious in human leprosy where, although there is a spectrum of disease, the majority of patients are at either end of that spectrum [27]. The tuberculoid form of the disease has lesions formed of infiltrating T cells and contain few bacteria; and the lepromatous form has lesions of infiltrating macrophages containing large numbers of bacteria [27,28]. The pathological picture of ruminant paratuberculosis seems to mimic human leprosy [29] although this is most true of the disease in sheep where the pathology can be differentiated into tuberculoid (paucibacillary), lepromatous (multibacillary) and asymptomatic (infected but no pathology) [1]. There is a difference between these two diseases however as the sheep tuberculoid form is an end stage disease [5] and it is not 'self-curing' as it is in leprosy [27]. There also seem to be differences between ovine and bovine paratuberculosis, as in cattle the pathological form seems to be related to the disease development [6,29], with early stage tuberculoid lesions developing into end-stage lepromatous disease. In addition, intermediate stages between these two extremes have also been reported [30,31]. Similar disease patterns are also observed in tuberculosis, but as with bovine paratuberculosis they seem to be more variable than leprosy [32].

Immunological responses to infectious disease challenge have a major bearing on the clinical manifestations of that infection and the clinical consequence for the host. This is most obvious in human leprosy [33,34] where the type 1 T cell cytokine pattern predominates in the self-curing tuberculoid patients in contrast to the type 2 pattern in malign lepromatous disease. The aim of this present study is to try and understand the relationship between the immunology and the different pathological changes that occur as a result of *Mycobacterium avium* subspecies *paratuberculosis* infection in sheep.

Despite the fact that there is a large variation in the levels of cytokine transcript expression, this study shows unambiguously that there is a relationship between the three pathological forms of sheep paratuberculosis and the immune response as represented by the cytokine transcript profiles within the target tissue. The large variation is probably due to the fact that these sheep are unrelated, of different breeds and are infected naturally rather than experimentally; in addition they carry an unquantified gastrointestinal worm burden that might influence ileal cytokine expression. We cannot measure levels of functional protein for all the cytokines within the ileum but

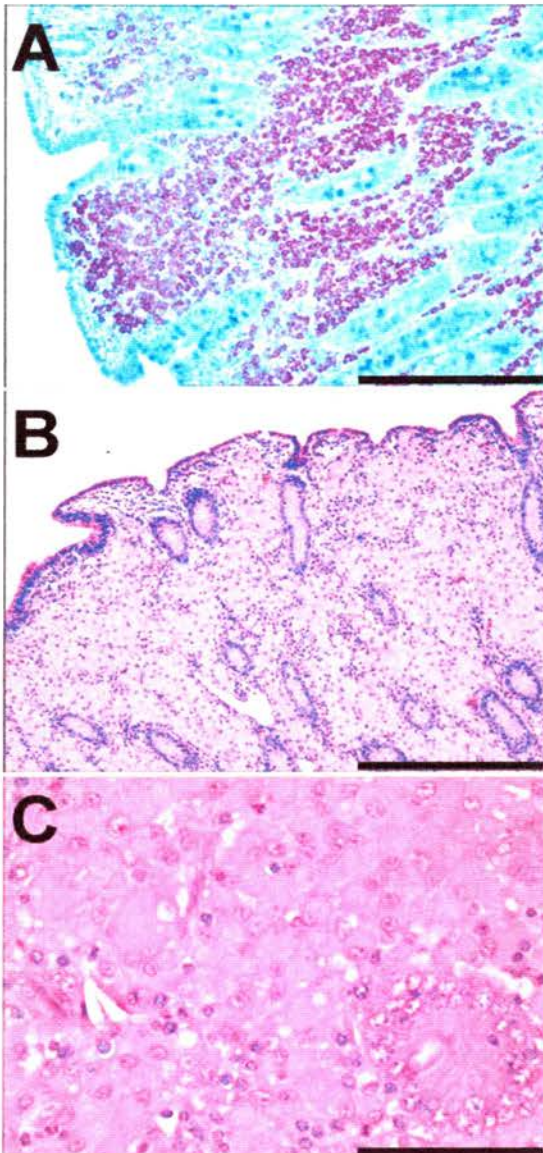


**Figure 3**  
**Histopathology of the terminal ileum from multi-bacillary sheep.** (a) Ziehl-Neelsen stain ( $\times 250$ ) showing the presence of many intracellular mycobacteria associated with the infiltrating macrophages. (b) H&E stained low power ( $\times 250$ ) showing infiltration of the lamina propria by sheets of epithelioid macrophages distending the propria and flattening the surface mucosa. (c) H&E stained high power ( $\times 400$ ) demonstrating the uniform population of epithelioid macrophages with abundant cytoplasm infiltrating around an intestinal crypt.

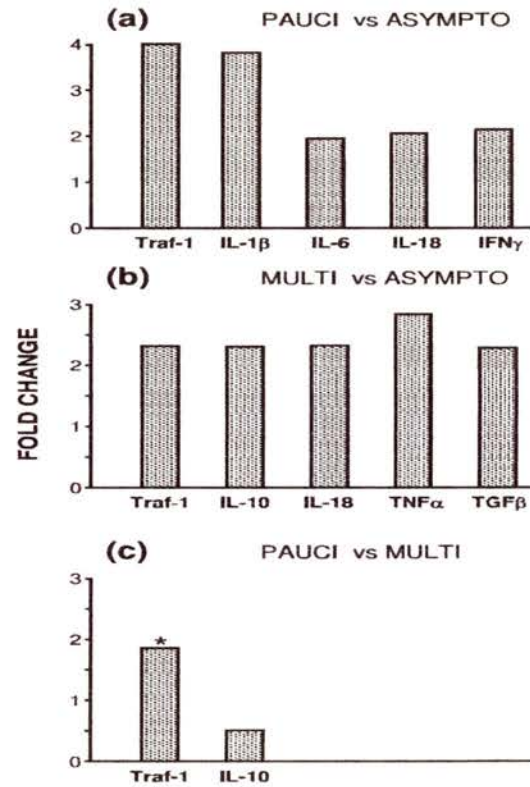


**Figure 4**  
**Statistically significant changes in genes between the three IS900+ groups.** (a) Comparison of paucibacillary and asymptomatic; (b) comparison of multibacillary and asymptomatic; (c) comparison of paucibacillary and multibacillary. Results are given as significant ( $p \leq 0.05$ ) fold-changes of mean copy-numbers relative to the mean copy-numbers of the comparative group. IL-3 was not included, as the copy number in the control samples was 0, thus fold change values could not be calculated. The data for TRAF-1, highlighted with \* in (c) excludes a single outlier in the ten data points;  $p = 0.062$  with the outlier;  $p \leq 0.02$  without the outlier.

assume that the relative quantities of cytokine protein and transcript are linked.

As has been shown with bovine paratuberculosis [19-21], the paucibacillary and multibacillary forms of the sheep disease are also associated with the polarization of the immune response. The comparison of each form of the disease with tissue from asymptomatic animals shows that IFN $\gamma$  is significantly increased in the paucibacillary lesions and IL-10 is raised in the multibacillary form. Furthermore, direct comparison of the diseased tissues shows that these two cytokines are reciprocally expressed,

**Table 1: Cytokine transcript levels in terminal ileum from sheep with paratuberculosis infected sheep and controls**

Gene	Multibacillary	Paucibacillary	Asymptomatic	Control
IL-1 $\alpha$	69 <sup>1</sup> $\pm$ 56	38 $\pm$ 14	51 $\pm$ 42	20 $\pm$ 8
IL-1 $\beta$	30839 $\pm$ 41353	16470 $\pm$ 8559	4176 $\pm$ 2557	8613 $\pm$ 6090
IL-3	29 $\pm$ 74	1 $\pm$ 3	87 $\pm$ 131	0 $\pm$ 0
IL-6	71778 $\pm$ 124310	11023 $\pm$ 2980	4996 $\pm$ 1698	5473 $\pm$ 7583
IL-8	1448098 $\pm$ 1453346	609805 $\pm$ 511880	480573 $\pm$ 601312	150388 $\pm$ 59472
IL-10	305964 $\pm$ 127868	174186 $\pm$ 82536	126941 $\pm$ 94659	240619 $\pm$ 185599
IL-12	7178 $\pm$ 7381	7589 $\pm$ 6467	4506 $\pm$ 5179	1615 $\pm$ 2436
IL-18	102838 $\pm$ 45161	84037 $\pm$ 34888	42352 $\pm$ 10066	126047 $\pm$ 41771
GM-CSF	2512 $\pm$ 1067	2973 $\pm$ 963	1786 $\pm$ 684	1986 $\pm$ 552
IFN $\gamma$	3354 $\pm$ 1063	5209 $\pm$ 2554	2529 $\pm$ 1620	1537 $\pm$ 427
TGF- $\beta$	50349 $\pm$ 30161	28007 $\pm$ 13809	21871 $\pm$ 11222	14519 $\pm$ 6032
TNF $\alpha$	21113 $\pm$ 13334	11681 $\pm$ 7914	7492 $\pm$ 4925	2770 $\pm$ 2120
TRAF-1	11504 $\pm$ 6076	20087 $\pm$ 10563	5018 $\pm$ 5134	3708 $\pm$ 1662

<sup>1</sup>Copy number  $\pm$  SD, normalized to SDHA and GAPDH

**Table 2: Breed, age and sex of sheep**

Disease Type	Sheep Breed	Age (years)	Sex
Multibacillary	Blackface $\times$ Bleu du Maine	4.5	F
Multibacillary	Blackface $\times$ Bleu du Maine	4.5	F
Multibacillary	Blackface	5	F
Multibacillary	Blackface	5	F
Multibacillary	Blackface	3	F
Multibacillary	Blackface	3	F
Multibacillary	Blackface	2	F
Multibacillary	Blackface	4	F
Multibacillary	Blackface	4	F
Multibacillary	Blackface	3	F
Paucibacillary	Blackface $\times$ Bleu du Maine	4.5	F
Paucibacillary	Texel	5.5	F
Paucibacillary	Blackface $\times$ Bleu du Maine $\times$ Lleyn $\times$ Roussin	2.5	F
Paucibacillary	Lleyn $\times$ Roussin	3.5	F
Paucibacillary	Blackface $\times$ Bleu du Maine	4.5	F
Paucibacillary	Blackface $\times$ Bleu du Maine	4.5	F
Paucibacillary	Bleu du Maine	4	F
Paucibacillary	Blackface $\times$ Bleu du Maine	6	F
Paucibacillary	Texel	2.5	F
Paucibacillary	Blackface	2.5	F
Asymptomatic	Blackface $\times$ Bleu du Maine	4.5	F
Asymptomatic	Blackface $\times$ Bleu du Maine	4.5	F
Asymptomatic	Blackface $\times$ Bleu du Maine	7	F
Asymptomatic	Blackface $\times$ Bleu du Maine	7	F
Asymptomatic	Texel	1	F
Asymptomatic	Blackface	2.5	F
Asymptomatic	Greyface	3	F
Asymptomatic	Greyface	3	F
Asymptomatic	Greyface	3	F
Asymptomatic	Greyface	3	F

The uninfected controls were: 6 Blackface (F) aged 4 years, 3 Texel (F) aged 4/5 years.

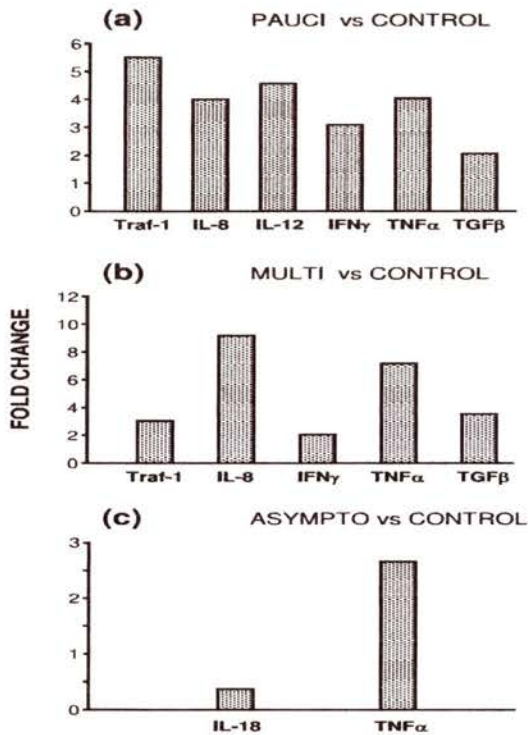


**Figure 5**  
**Statistically significant changes in genes between the three IS900+ groups and the uninfected control group.** (a) Comparison of paucibacillary and control; (b) comparison of multibacillary and control; (c) comparison of asymptomatic and control. Results are given as significant ( $p \leq 0.05$ ) fold-changes of mean copy-numbers relative to the mean copy-numbers of the comparative group.

although the increase (x1.55 fold) of IFN $\gamma$  in paucibacillary ileum is not quite significant ( $p = 0.057$ ). This confirms that in sheep paratuberculosis polarized type 1 and type 2 T cells are strongly associated to paucibacillary and multibacillary pathology respectively. The major biological function of IL-18 seems to be linked to inducing type 1 responses and stimulating IFN $\gamma$  production [35]. However, the pattern of IL-18 expression is not explained simply in terms of type 1 and type 2 responses as it is up-regulated in both disease forms. Perhaps the increased TGF $\beta$  level in the multibacillary ileum explains the low IFN $\gamma$  levels in that tissue [36].

Comparison of both disease forms to uninfected control samples shows up-regulation of TRAF-1, IL-8, IFN $\gamma$ , and TNF $\alpha$ , reflecting the high levels of inflammation present

in the affected tissues and agrees with the data in cattle [21,24]. TRAF-1 is anti-apoptotic and its up-regulation in both disease forms indicates that it may be associated with the accumulation of several different cell types in the lamina propria and not just macrophages [24]. Previous studies in stimulated PBMC from infected cattle have shown down-regulation of IL-12p35 in infected cattle compared to controls [21]. However, this study showed significant ( $p = 0.05$ ) up-regulation of IL-12p40 in paucibacillary samples ( $p = 0.06$  for multibacillary tissue). This may be explained by differences in the tissues tested or that IL-12p40 levels reflect IL-23 and not IL-12p70. IL-1 $\beta$  and IL-6 were also significantly raised in paucibacillary ileum compared to asymptomatic samples, the increase in multibacillary samples was large but without statistical significance ( $p = 0.12$ ). Both have been shown previously to be up-regulated in multibacillary disease [37], but as with IL-8 and TNF $\alpha$  they are also associated with general inflammation. Unlike other gastrointestinal inflammatory lesions [38], the expression of large quantities of pro-inflammatory cytokines in paratuberculosis is not reflected in the large scale infiltration of neutrophils. A possible explanation for this is the presence of increased levels of TGF $\beta$ , which has known anti-inflammatory and immunosuppressive functions [36]. IL-3 is absent from uninfected ileum but can be detected in both asymptomatic and multibacillary tissues; however, the low levels of transcripts present leave doubt about its biological relevance. Our data only partly fit with the 'Coussens' model of bovine paratuberculosis pathogenesis [39]. They are almost identical in relation to the T cell polarizing cytokines and most of the inflammatory mediators but contrasts in relation to IL-1 $\alpha$ . This cytokine is highly up-regulated in infected bovine tissue and the model hypothesises that the pathogenesis of paratuberculosis may be partly due to IL-1 $\alpha$  toxicity. However our data show that IL-1 $\alpha$  is virtually absent from sheep ileum. Apart from species differences a possible explanation for this discrepancy is that all the sheep paratuberculosis tissues originate from terminal disease states and not during the development of the pathology.

Of particular interest is the comparison between the infected, asymptomatic and the uninfected, control sheep. Unlike cattle, where asymptomatic animals are regarded as 'preclinical' and show histological lesions [19], asymptomatic sheep show completely normal ileal histology and their susceptibility to disease has been questioned [4]. The normality of the asymptomatic cases is largely confirmed by the fact that the majority of cytokines are expressed at 'normal' levels; however TNF $\alpha$  and IL-18 are exceptions, TNF $\alpha$  is significantly up-regulated and IL-18 is down-regulated in asymptomatic samples. The low levels of IL-18 are not matched by a similar down-regulation of IFN $\gamma$ .

**Table 3: Primer sequences used for real time RT-PCR**

Gene Accession number	Primer Sequence 5'-3'	Product size (bp)
IL-1 $\alpha$ GenBank: <a href="#">NM_174092</a>	F: TTGGTGCACATGGCAAGTG R: GCACAGTCAAGGCTATTTTCC	72
IL-1 $\beta$ GenBank: <a href="#">X56972</a>	F: CCTTGGGTATCAGGGACAA R: TGCGTATGGCTTTCTTTAGG	317
IL-3 GenBank: <a href="#">Z18897</a>	F: ACCTCCTTCTGCTCCTGCTT R: TATTCCCAAGTCCCATCTT	193
IL-6 GenBank: <a href="#">X68723</a>	F: TCCAGAACGAGTTTGAGG R: CATCCGAATAGCTCTCAG	236
IL-8 GenBank: <a href="#">X78306</a>	F: ATGAGTACAGAACTTCGA R: TCATGGATCTTGCTTCTC	222
IL-10 GenBank: <a href="#">U11421</a>	F: CTGTTGACCCAGTCTCTGCT R: ACCGCCTTTGCTTTGTTT	305
IL-12p40 GenBank: <a href="#">AF004024</a>	F: TCAGACCAGAGCAGTGAGGT R: GCAGGTGAAGTGTCCAGAAT	243
IL-18 GenBank: <a href="#">AJ401033</a>	F: GAGCACAGGCATAAAGATGG R: TGAACAGTCAGAATCAGGCATA	241
IFN $\gamma$ GenBank: <a href="#">X52640</a>	F: CTAAGGGTGGGCCTCTTTTC R: CATCCACCGGAATTTGAATC	55
TNF $\alpha$ GenBank: <a href="#">X56756</a>	F: GAATACCTGGACTATGCCGA R: CCTCACTTCCCACATCCCT	238
TGF $\beta$ GenBank: <a href="#">X76916</a>	F: GAACTGCTGTGTTCTGTCAGC R: GGTGTGCTGGTTGTACAGG	169
GM-CSF GenBank: <a href="#">X53561</a>	F: GATGGATGAAACAGTAGAAGTCG R: CAGCAGTCAAAGGGAATGAT	261
TRAF1 GenBank: <a href="#">XM_589090</a>	F: AGCAGAGGGTGTGGAGTTG R: CTGGGGAGAAGAGGCTGAC	186
GAPDH GenBank: <a href="#">AF030943</a>	F: GGTGATGCTGGTCTGAGTA R: TCATAAGTCCCTCCACGATG	265
SDHA GenBank: <a href="#">NM_174178</a>	F: ACCTGATGCTTTGTCTCTGC R: CCTGGATGGGCTTGGAGTAA	126

## Conclusion

In this study, we have quantified the expression levels of thirteen important immunoregulatory genes in the three forms of ovine paratuberculosis using real-time RT-PCR analyses. We have confirmed that the paucibacillary and multibacillary pathologies are linked to type 1 and type 2 T cell responses respectively. However, many other cytokines are differentially expressed and it is clear that these cytokines are part of a complex network and interact to form the final pathologies. It is also clear that asymptomatic animals are also responding to infection, although the data do not explain how the disease is controlled in these animals. The epidemiology of the disease would suggest a genetic susceptibility similar to that recognised for tuberculosis and leprosy, and these data suggest several likely candidates for future genetic analysis.

## Methods

All procedures involving animals was approved by the Home Office under the appropriate Animals (Scientific Procedures) Act 1986 Project Licence.

## Experimental animals/tissues

Animals with the clinical disease and asymptomatic animals were out bred sheep with naturally acquired MAP infection from one of three farms (Table 2). Individual sheep were delivered to the Moredun Research Institute based on clinical symptoms of Johne's disease. All sheep were euthanized and the diagnosis of Johne's disease was confirmed by histopathology of the terminal ileum and IS900 real-time PCR. Sheep from the same flocks with no clinical signs of Johne's disease but that were positive for IS900 were considered to be asymptomatic [4]. All control sheep tested negative for IS900. There were ten animals in each of the infected group and nine uninfected controls. Terminal ileum samples for histopathology were removed post-mortem and fixed in 10% formol-saline. Four  $\mu$ m sections from paraffin wax-embedded tissue were stained with haematoxylin and eosin or Ziehl-Neelsen (ZN). For RNA preparations, tissue blocks (~0.5 g) were placed in five volumes of in RNAlater (Ambion, Huntingdon, UK), which were then incubated overnight at 4°C and then stored at -80°C.

**IS900 quantitative PCR**

All RNA samples were tested for the presence of MAP by IS900 real-time RT-PCR for a MAP specific insertion sequence [40]. Primers and probes were as Eishi et al. [41], and the reactions were carried out in an ABI Prism 7000 real-time PCR machine. Each reaction contained 12.5 µl Platinum® Quantitative PCR SuperMix-UDG with ROX (Invitrogen; Paisley, UK), 50 nM each primer, 100 nM probe and 5 µl cDNA, made up to 25 µl with deionised water. The reactions were cycled as follows: 50°C for 2 minutes, 95°C for 10 minutes and 40 cycles of 95°C for 15 seconds, then 60°C for 1 minute.

**Isolation RNA Isolation and cDNA synthesis**

Tissue samples were thawed at room temperature, 250 mg wet weight of ileum tissue was shredded and then disrupted and homogenised in a buffer containing 4 M guanidine isothiocyanate using a ribolyser (Fast-Prep from Thermo-Hybrid, Runcorn, UK). Total RNA was extracted using a Qiagen RNeasy® Maxi Kit (Qiagen, Crawley, UK) and DNase treated using the Ambion DNase I kit (Ambion, Huntingdon, UK). Samples were eluted into 800 µl of nuclease-free water. The RNA was quantified by spectrophotometry, ethanol precipitation and resuspended in 300 µl of nuclease-free water. Samples were checked for genomic DNA contamination by GAPDH PCR.

For cDNA synthesis, 2.5 µg of RNA was diluted to a final volume of 16.25 µl in nuclease free water. 500 ng of Oligo (dT) (Promega, Southampton, UK) was added, and incubated for five minutes at 70°C, followed by five minutes on ice. To this 5 µl of 5× MMLV buffer, 1.25 µl of 100 mM dNTPs and 1 µl of MMLV RT enzyme (Promega) were added, and the mixture was incubated at 42°C for 60 minutes, followed by 15 minutes at 70°C to inactivate the enzyme. The cDNA was diluted four-fold in nuclease free water and stored at -20°C until used.

**Cloning of ovine cytokine gene fragments**

Primers (Table 3) were selected and designed using Primer3 [42] software. All selected primer sequences were then checked for possible cross-hybridization using the BLAST [43] and subjected to quality check using Net Primer [44]. The PCR mixture contained 2 µl of cDNA; 5 µl (10×) PCR buffer (Promega); 1 µl dNTP mix (Promega); 20 pmol of each primer (Sigma-Genosys, Haverhill, UK); 1 µl Taq polymerase (5 units) and nuclease free water was added to a final volume of 50 µl. Reactions were then cycled under the following conditions: 95°C for 2 mins 30 cycles of 30 s at 95°C, annealing at (see Table 1), 45 s; 60 s at 72°C, followed by a final extension at 72°C for 5 mins. PCR products were analysed by agarose gel electrophoresis, visualized by ethidium bromide/UV transillumination, purified using the QIAquick® system (Qiagen), cloned into pGEM T-Easy® (Promega) and sequenced.

mination, purified using the QIAquick® system (Qiagen), cloned into pGEM T-Easy® (Promega) and sequenced.

**Quantitative real-time PCR**

Two-step, quantitative real-time RT-PCR was carried out using a Rotor-Gene™ 3000 (Corbett Life Science, Cambridge, UK) using primers as in Table 3. Standard curves for each gene were generated using 10-fold serial dilution series of linearized plasmid DNA templates. Quantitative real-time PCR reactions were run in 20 µl containing 2 µl of FastStart Taq buffer, 200 µM dNTPs (Promega), 250 nM each primer, MgCl<sub>2</sub> to an optimum concentration, 0.7 µl of a 1/1000 dilution of SYBR green master mix, 0.75 U FastStart Taq DNA Polymerase (all Roche Diagnostics, Lewes, UK) and 2 µl of template cDNA, made up to 20 µl with deionised water. The cycling conditions for all genes were as follows: 5 minutes at 94°C, 45 cycles of 20 seconds at 94°C, 20 seconds at 60°C and 20 seconds at 72°C, followed by a melt curve starting at 65°C rising to 94°C at 0.3°C per second. Copy numbers were determined from the Ct values of each sample in comparison to the copy number values assigned from the plasmid DNA standard using Rotor-Gene analysis software (6.0.34). Data were normalized using glyceraldehyde-3-phosphate dehydrogenase (GAPDH) or succinate dehydrogenase (SDHA) housekeeping genes. A normalization factor was calculated taking into account the 75th percentile of the housekeeping gene copy numbers for each run. Results were compared pair wise using a 2-sample t test to determine statistical significance. Each sample was analysed in duplicate, n = 10 for each IS900+ sheep and n = 9 for the uninfected controls.

**Variability assay**

To determine the level of variability inherent in the real-time PCR reactions, a variability assay was carried out. A single sample was reverse transcribed in three simultaneous reactions. The cDNA produced was then amplified ten times each in an SDHA real-time PCR reaction. The resulting copy numbers were compared to give a value for the variability inherent within the reactions. The assay showed that the overall variability inherent to the method is 2.2 fold.

**Competing interests**

The authors declare that they have no competing interests.

**Authors' contributions**

JAS performed the real-time PCR experiments and was responsible for the draft manuscript preparation. CAW supervised JAS in the practical work; he performed the post-mortems and helped JAS with data analysis and draft manuscript preparation. SMR performed the histopathological diagnosis and analysis. JH was in overall control of

the project and was responsible for its design, coordination and funding; he produced the final manuscript.

## Acknowledgements

We would like to acknowledge Dr Anton Gossner, Dr Katie Matthews, Dr Tom McNeilly and Sofia Roupaka in the Centre for Infectious Diseases, University of Edinburgh, for supplying primers and cloned plasmids. This Project was funded by BBSRC Grant 15/S13964. JAS is funded by BBSRC/Genesis-Faraday CASE studentship and sponsored by Moredun Scientific Ltd. Midlothian, UK

## References

- Clarke CJ, Little D: **The pathology of ovine paratuberculosis: gross and histological changes in the intestine and other tissues.** *J Comp Pathol* 1996, **114**:419-437.
- Gonda MG, Chang YM, Shook GE, Collins MT, Kirkpatrick BW: **Effect of Mycobacterium paratuberculosis infection on production, reproduction, and health traits in US Holsteins.** *Prev Vet Med* 2007.
- van Roermund HJ, Bakker D, Willemsen PT, de Jong MC: **Horizontal transmission of Mycobacterium avium subsp. paratuberculosis in cattle in an experimental setting: Calves can transmit the infection to other calves.** *Vet Microbiol* 2007.
- Begara-McGorum I, Wildblood LA, Clarke CJ, Connor KM, Stevenson K, McInnes CJ, Sharp JM, Jones DG: **Early immunopathological events in experimental ovine paratuberculosis.** *Vet Immunol Immunopathol* 1998, **63**:265-287.
- Clarke CJ: **The pathology and pathogenesis of paratuberculosis in ruminants and other species.** *J Comp Pathol* 1997, **116**:217-261.
- Stabel JR: **Transitions in immune responses to Mycobacterium paratuberculosis.** *Vet Microbiol* 2000, **77**:465-473.
- Withers FW: **Incidence of the disease.** *The Veterinary Record* 1959, **71**:1150-1153.
- Cetinkaya B, Egan K, Harbour DA, Morgan KL: **An abattoir-based study of the prevalence of subclinical Johne's disease in adult cattle in south west England.** *Epidemiol Infect* 1996, **116**:373-379.
- Bleharski JR, Li H, Meinken C, Graeber TG, Ochoa MT, Yamamura M, Burdick A, Sarno EN, Wagner M, R-Illinghoff M, Rea TH, Colonna M, Stenger S, Bloom BR, Eisenberg D, Modlin RL: **Use of genetic profiling in leprosy to discriminate clinical forms of the disease.** *Science* 2003, **301**:1527-1530.
- Burrells C, Clarke CJ, Colston A, Kay JM, Porter J, Little D, Sharp JM: **A study of immunological responses of sheep clinically affected with paratuberculosis (Johne's disease). The relationship of blood, mesenteric lymph node and intestinal lymphocyte responses to gross and microscopic pathology.** *Vet Immunol Immunopathol* 1998, **66**:343-358.
- Burrells C, Clarke CJ, Colston A, Kay JM, Porter J, Little D, Sharp JM: **Interferon-gamma and interleukin-2 release by lymphocytes derived from the blood, mesenteric lymph nodes and intestines of normal sheep and those affected with paratuberculosis (Johne's disease).** *Vet Immunol Immunopathol* 1999, **68**:139-148.
- Alzuhri HM, Woodall CJ, Clarke CJ: **Increased intestinal TNF-alpha, IL-1 beta and IL-6 expression in ovine paratuberculosis.** *Vet Immunol Immunopathol* 1996, **49**:331-345.
- Carrigan MJ, Seaman JT: **The pathology of Johne's disease in sheep.** *Aust Vet J* 1990, **67**:47-50.
- Sweeney RW, Whitlock RH, Rosenberger AE: **Mycobacterium paratuberculosis isolated from fetuses of infected cows not manifesting signs of the disease.** *Am J Vet Res* 1992, **53**:477-480.
- Koets A, Rutten V, Hoek A, van Mil F, M'ller K, Bakker D, Gruys E, van Eden W: **Progressive bovine paratuberculosis is associated with local loss of CD4(+) T cells, increased frequency of gamma delta T cells, and related changes in T-cell function.** *Infect Immun* 2002, **70**:3856-3864.
- Yamamura M, Uyemura K, Deans RJ, Weinberg K, Rea TH, Bloom BR, Modlin RL: **Defining protective responses to pathogens: cytokine profiles in leprosy lesions.** *Science* 1991, **254**:277-279.
- Barnes PF, Lu S, Abrams JS, Wang E, Yamamura M, Modlin RL: **Cytokine production at the site of disease in human tuberculosis.** *Infect Immun* 1993, **61**:3482-3489.
- Mosmann TR, Coffman RL: **TH1 and TH2 cells: different patterns of lymphokine secretion lead to different functional properties.** *Annu Rev Immunol* 1989, **7**:145-173.
- Tanaka S, Sato M, Onitsuka T, Kamata H, Yokomizo Y: **Inflammatory cytokine gene expression in different types of granulomatous lesions during asymptomatic stages of bovine paratuberculosis.** *Vet Pathol* 2005, **42**:579-588.
- Langelaar MF, Weber CN, Overdijk MB, M'ller KE, Koets AP, Rutten VT: **Cytokine gene expression profiles of bovine dendritic cells after interaction with Mycobacterium avium ssp. paratuberculosis (M.a.p.), Escherichia coli (E. coli) or recombinant M.a.p. heat shock protein 70.** *Vet Immunol Immunopathol* 2005, **107**:153-161.
- Coussens PM, Verman N, Coussens MA, Eftman MD, McNulty AM: **Cytokine gene expression in peripheral blood mononuclear cells and tissues of cattle infected with Mycobacterium avium subsp. paratuberculosis: evidence for an inherent proinflammatory gene expression pattern.** *Infect Immun* 2004, **72**:1409-1422.
- Khalifeh MS, Stabel JR: **Upregulation of transforming growth factor-beta and interleukin-10 in cows with clinical Johne's disease.** *Vet Immunol Immunopathol* 2004, **99**:39-46.
- Lee H, Stabel JR, Kehrli ME: **Cytokine gene expression in ileal tissues of cattle infected with Mycobacterium paratuberculosis.** *Vet Immunol Immunopathol* 2001, **82**:73-85.
- Aho AD, McNulty AM, Coussens PM: **Enhanced expression of interleukin-1alpha and tumor necrosis factor receptor-associated protein 1 in ileal tissues of cattle infected with Mycobacterium avium subsp. paratuberculosis.** *Infect Immun* 2003, **71**:6479-6486.
- North RJ, Jung YJ: **Immunity to tuberculosis.** *Annu Rev Immunol* 2004, **22**:599-623.
- Fitness J, Tosh K, Hill AV: **Genetics of susceptibility to leprosy.** *Genes Immun* 2002, **3**:441-453.
- Rea TH, Modlin RL: **Immunopathology of leprosy skin lesions.** *Semin Dermatol* 1991, **10**:188-193.
- Myrvang B, Godal T, Ridley DS, Friland SS, Song YK: **Immune responsiveness to Mycobacterium leprae and other mycobacterial antigens throughout the clinical and histopathological spectrum of leprosy.** *Clin Exp Immunol* 1973, **14**:541-553.
- Cocito C, Gilot P, Coene M, de Kesel M, Poupard P, Vannuffel P: **Paratuberculosis.** *Clin Microbiol Rev* 1994, **7**:328-345.
- Kurade NP, Tripathi BN, Rajukumar K, Parihar NS: **Sequential development of histologic lesions and their relationship with bacterial isolation, fecal shedding, and immune responses during progressive stages of experimental infection of lambs with Mycobacterium avium subsp. paratuberculosis.** *Vet Pathol* 2004, **41**:378-387.
- Gonzales J, Geijo MV, Garcia-Pariente C, Verna A, Corpa JM, Reyes LE, Ferreras MC, Juste RA, Garcia MJF, Perez V: **Histopathological classification of lesions associated with natural paratuberculosis infection in cattle.** *J Comp Pathol* 2005, **133**:184-196.
- Flynn JL, Chan J: **Immunology of tuberculosis.** *Annu Rev Immunol* 2001, **19**:93-129.
- Libraty DH, Airan LE, Uyemura K, Jullien D, Spellberg B, Rea TH, Modlin RL: **Interferon-gamma differentially regulates interleukin-12 and interleukin-10 production in leprosy.** *J Clin Invest* 1997, **99**:336-341.
- Modlin RL: **Th1-Th2 paradigm: insights from leprosy.** *J Invest Dermatol* 1994, **102**:828-832.
- Dinarello CA: **IL-18: A TH1-inducing, proinflammatory cytokine and new member of the IL-1 family.** *J Allergy Clin Immunol* 1999, **103**:11-24.
- Becker C, Fantini MC, Neurath MF: **TGF-beta as a T cell regulator in colitis and colon cancer.** *Cytokine Growth Factor Rev* 2006, **17**:97-106.
- Alzuhri HM, Woodall CJ, Clarke CJ: **Increased intestinal TNF-alpha, IL-1[beta] and IL-6 expression in ovine paratuberculosis.** *Veterinary Immunology and Immunopathology* 1996, **49**:331-345.
- Elliott SN, Wallace JL: **Neutrophil-mediated gastrointestinal injury.** *Can J Gastroenterol* 1998, **12**:559-568.
- Coussens PM: **Model for immune responses to Mycobacterium avium subspecies paratuberculosis in cattle.** *Infect Immun* 2004, **72**:3089-3096.
- Green EP, Tizard ML, Moss MT, Thompson J, Winterbourne DJ, McFadden JJ, Hermon-Taylor J: **Sequence and characteristics of**

**IS900, an insertion element identified in a human Crohn's disease isolate of Mycobacterium paratuberculosis.** *Nucleic Acids Res* 1989, **17**:9063-9073.

41. Eishi Y, Suga M, Ishige I, Kobayashi D, Yamada T, Takemura T, Takizawa T, Koike M, Kudoh S, Costabel U, Guzman J, Rizzato G, Gambacorta M, du Bois R, Nicholson AG, Sharma OP, Ando M: **Quantitative analysis of mycobacterial and propionibacterial DNA in lymph nodes of Japanese and European patients with sarcoidosis.** *J Clin Microbiol* 2002, **40**:198-204.
42. **Primer3** 2007 [[http://frodo.wi.mit.edu/cgi-bin/primer3/primer3\\_www.cgi](http://frodo.wi.mit.edu/cgi-bin/primer3/primer3_www.cgi)].
43. **Blast** 2007 [[http://www.ncbi.nlm.nih.gov/blast/Blast.cgi?CMD=Web&PAGE\\_TYPE=BlastHome](http://www.ncbi.nlm.nih.gov/blast/Blast.cgi?CMD=Web&PAGE_TYPE=BlastHome)].
44. **Net Primer** 2007 [<http://www.premierbiosoft.com/netprimer/index.html>].

Publish with **BioMed Central** and every scientist can read your work free of charge

*"BioMed Central will be the most significant development for disseminating the results of biomedical research in our lifetime."*

Sir Paul Nurse, Cancer Research UK

Your research papers will be:

- available free of charge to the entire biomedical community
- peer reviewed and published immediately upon acceptance
- cited in PubMed and archived on PubMed Central
- yours — you keep the copyright

Submit your manuscript here:  
[http://www.biomedcentral.com/info/publishing\\_adv.asp](http://www.biomedcentral.com/info/publishing_adv.asp)

